Chemoselective Installation of Amine Bonds on Proteins Through Aza-Michael Ligation

Allyson M. Freedy,[‡] Maria J. Matos,[‡] Omar Boutureira,[‡] Francisco Corzana,[‡] Ana Guerreiro,[‡] Padma Akkapeddi, Víctor J. Somovilla, Tiago Rodrigues, Karl Nicholls, Bangwen Xie, Gonzalo Jiménez-Osés, Kevin M. Brindle, André A. Neves, & Gonçalo J. L. Bernardes*

[‡]These authors contributed equally to the work.

To whom correspondence should be addressed:

Email (G.J.L.B.): gb453@cam.ac.uk

Table of Contents

1. Synthesis of small molecule *N*-nucleophiles

Synthesis of compound 8a

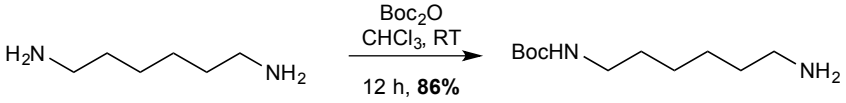

Boc_2O (1.00 g, 4.6 mmol) was dissolved in $CHCl_3$ (20 mL) and added dropwise to the 1,6-diaminehexane (2.66 g, 22.9 mmol), dissolved in $CHCl_3$ (10 mL). The reaction mixture was allowed to stir overnight at room temperature. The solution was concentrated and purified by flash column chromatography, eluting with 10% MeOH–1% Et_3N in $CHCl_3$, to give the desired compound **8a** as a yellow waxy solid (0.86 g, 86%). The spectroscopic data was identical to that reported in the literature.[1] ^{1}H NMR (400 MHz, $CDCl_3$): δ (ppm) 1.28–1.65 (m, 17H; $(CH_3)_3C$, $4CH_2$), 2.69 (t, *J* = 7.0 Hz, 2H; CH_2), 3.06–3.16 (m, 2H; CH_2), 4.61 (brs, 1H; N*H*Boc). HRMS ESI$^+$ (*m/z*): Calcd. for $C_{11}H_{25}N_2O_2^+$ [M + H]$^+$ 217.1916, found 217.1910.

Synthesis of compound 9a

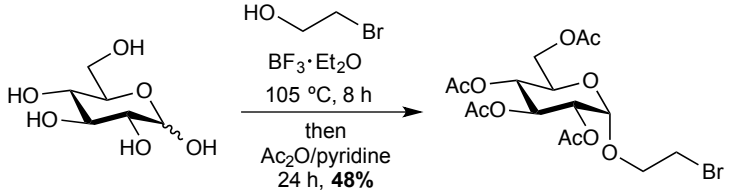

$BF_3{\cdot}Et_2O$ (145 µL, 1.1 mmol) was added dropwise to a suspension of D-glucose (1.45 g, 8.1 mmol) in $Br(CH_2)_2OH$ (19 mL) under N_2 and the resulting mixture heated to 105 ºC. After 8 h the resulting solution was cooled and the solvent removed. The residue was dissolved in 2:3 Ac_2O/pyridine (16 mL). After a further 24 h period the solvent was removed and the residue purified by column chromatography (EtOAc:hexane, 3:7) to give the desired 2-bromoethyl 2,3,4,6-tetra-*O*-acetyl-α-D-glucopyranoside (1.76 g, 48%) as a colourless oil that crystallized on standing to give a white solid. The spectroscopic data was identical to that reported in the literature.[2] ^{1}H NMR (400 MHz, $CDCl_3$): δ (ppm) 2.01 (s, 3H; Ac), 2.03 (s, 3H; Ac), 2.07 (s, 3H; Ac), 2.09 (s, 3H; Ac), 3.51 (t, *J* = 5.9 Hz, 2H; -CH_2Br), 3.83 (dt, *J* = 11.6 Hz, 5.8 Hz, 1H; -OCH_2-), 3.96 (dt, *J* = 11.6, 5.8 Hz, 1H; -OCH_2-), 4.10 (dd, J = 12.0, 2.2 Hz, 1H; H-6), 4.14 (ddd, *J* = 10.2, 4.4, 2.2, 1H; H-5), 4.24 (dd, *J*

= 12.0, 4.4 Hz, 1H; H-6), 4.84 (dd, *J* = 10.3, 3.8 Hz, 1H; H-2), 5.05 (t, *J* = 9.7 Hz, 1H; H-4), 5.14 (d, *J* = 3.8 Hz, 1H; H-1), 5.49 (dd, *J* = 10.3, 9.5 Hz, 1H; H-3). ^{13}C NMR (100 MHz, $CDCl_3$): δ (ppm) 20.6, 20.7 (4×Ac), 29.9 (-CH_2Br), 61.9 (C-6), 67.8 (-OCH2-), 68.5 (C-5), 68.8 (C-4), 70.0 (C-3), 70.8 (C-2) 96.0 (C-1), 169.6, 170.0, 170.2, 170.6 (4×Ac; *C*O_2). HRMS ESI$^+$ (*m/z*): Calcd. for $C_{16}H_{23}N_{10}BrNa^+$ $[M+Na]^+$ 477.0372, found 477.0381.

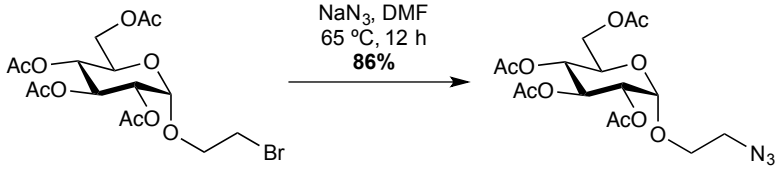

Sodium azide (0.27 g, 4.08 mmol) was added to a suspension of 2-bromoethyl 2,3,4,6-tetra-*O*-acetyl-α-D-glucopyranoside (0.93 g, 2.04 mmol) in DMF (8 mL). After 12 h at 65 °C, the mixture was concentrated *in vacuo*. The residue was purified by flash chromatography on silica gel (hexane/EtOAc 7:3) to give 2-azidoethyl 2,3,4,6-tetra-*O*-acetyl-α-D-glucopyranoside as a white solid (0.73 g, 86%). ^{1}H NMR (400 MHz, $CDCl_3$): δ (ppm) 2.03 (s, 3H, Ac), 2.05 (s, 3H, Ac), 2.09 (s, 3H, Ac), 2.11 (s, 3H, Ac), 3.38–3.47 (m, 1H, -$CH_2C\mathit{H}_2N_3$), 3.48–3.55 (m, 1H, -$CH_2C\mathit{H}_2N_3$), 3.62–3.70 (m, 1H, -$C\mathit{H}_2CH_2N_3$), 3.89 (ddd, *J* = 10.1, 6.2, 3.3Hz, 1H, -$C\mathit{H}_2CH_2N_3$), 4.04–4.16 (m, 2H, H-5, H-6), 4.22–4.31 (m, 1H, H-6), 4.91 (dd, *J* = 10.3, 3.8 Hz, 1H, H-2), 5.05–5.13 (m, 1H, H-4), 5.14 (d, *J* = 3.6 Hz, 1H, H-1), 5.52 (t, *J* = 9.8 Hz, 1H, H-3). ^{13}C NMR (100 MHz, $CDCl_3$): δ (ppm) 20.7 (4×Ac), 50.4 (-$CH_2C\mathit{H}_2N_3$), 61.9 (C-6), 67.4 (-$C\mathit{H}_2CH_2N_3$), 67.6 (C-5), 68.4 (C-4), 70. 0 (C-3), 70.6 (C-2), 96.0 (C1), 169.6, 170.0, 170.3, 170.6 (4×Ac; CO_2). HRMS ESI$^+$ (*m/z*): Calcd. for $C_{16}H_{23}O_{10}N_3Na^+$ $[M+Na]^+$ 440.1287, found 440.1273.

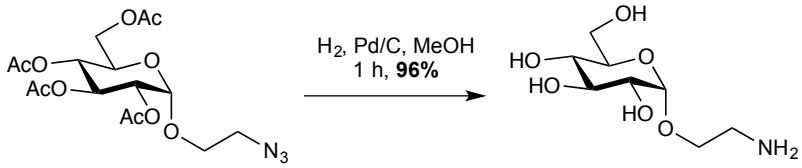

A suspension of 2-azidoethyl 2,3,4,6-tetra-*O*-acetyl-α-D-glucopyranoside (0.70 g, 1.6 mmol) and activated palladium on charcoal 10% Pd/C (0.12 g) in anhydrous MeOH (20 mL) was stirred under H_2. After 1 h, the reaction was stopped and the mixture was filtered. The filtrate was concentrated *in vacuo* and purified by column chromatography (CH_2Cl_2/MeOH/Et_3N, 9:1:0.1) to give 2-aminoethyl 2,3,4,6-tetra-*O*-acetyl-α-D-glucopyranoside **9a** (0.60 g, 96%) as a white fluffy solid. ^{1}H NMR (400 MHz, $CDCl_3$): δ

(ppm) 2.01 (s, 3H, Ac), 2.02 (s, 3H, Ac), 2.06 (s, 3H, Ac), 2.09 (s, 3H, Ac), 2.87–2.95 (m, 2H, -CH_2*C*H_2NH_2), 3.41–3.51 (m, 1H, H-6), 3.69–3.79 (m, 1H, H-6), 4.01–4.11 (m, 2H, H-5, -C*H*$_2CH_2NH_2$), 4.25 (dd, *J* = 12.2, 4.2 Hz, 1H, -C*H*$_2CH_2N_3$), 4.89 (dd, *J* = 10.2, 3.7 Hz, 1H, H-2), 5.03–5.10 (m, 2H, H-1, H-4), 5.48 (t, *J* = 9.8 Hz, 1H, H-3). ^{13}C NMR (100 MHz, $CDCl_3$): δ (ppm) 20.5, 20.6, 20.6, 20.7 (4×Ac), 39.1 (-CH_2*C*H_2N_3), 41.4 (-*C*$H_2CH_2N_3$), 61.8 (C-6), 67.2 (C-5), 68.5 (C-4), 70.1 (C-3), 70.7 (C-2), 95.9 (C-1), 169.5, 170.0, 170.1, 170.6 (4×Ac; CO_2). HRMS ESI$^+$ (*m/z*): Calcd. for $C_{16}H_{26}O_{10}N^+$ [M + H]$^+$ 392.1557, found 392.1542.

2. General procedure for aza-Michael addition on small molecules

Boc-Dha methyl ester[3] **1** (50 mg, 0.25 mmol) was dissolved in a 1:1 mixture of DMF and 50 mM sodium phosphate buffer at pH 8.0 (2 mL) and treated with the corresponding N-nucleophile **2a**–**9a** (0.4 mmol, 1.5 eq.). The mixture was stirred at 37 ºC for 4 h and then diluted with ether (150 mL) and water (75 mL). The organic layer was separated and the solvent removed. The reaction crude was purified by column chromatography (EtOAc:hexane, 9:1) to give the corresponding aza-Michael adduct.

Benzylamine 2a

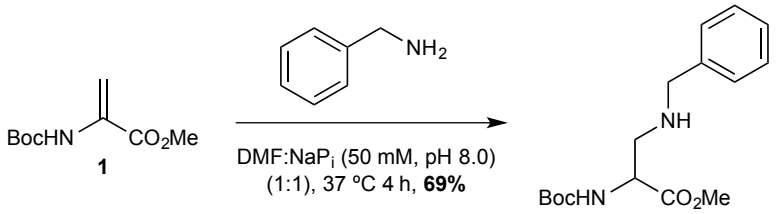

^{1}H NMR (400 MHz, $CDCl_3$): δ (ppm) 1.47 (s, 9H, Boc), 2.94–3.05 (m, 2H, Hβ), 3.74–3.85 (m, 5H, CO_2*Me*, PhC*H*$_2$-), 4.38–4.46 (m, 1H, Hα), 5.40–5.50 (m, 1H, N*H*Boc), 7.24–7.37 (m, 6H; NH-, Ph). ^{13}C NMR (100 MHz, $CDCl_3$): δ (ppm) 28.3 ((*C*H$_3$)$_3$C), 50.0 (Cβ), 52.4 (CO_2*Me*), 53.4 (Ph*C*H$_2$-), 53.6 (Cα), 80.0 ((CH$_3$)$_3$*C*), 127.1, 128.1, 128.4, 139.8 (Ph), 155.5 (NCO_2), 172.4 (*C*O_2Me). HRMS ESI$^+$ (*m/z*): Calcd. for $C_{16}H_{25}O_4N_2^+$ $[M + H]^+$ 309.1809, found 309.1796.

Imidazole 4a

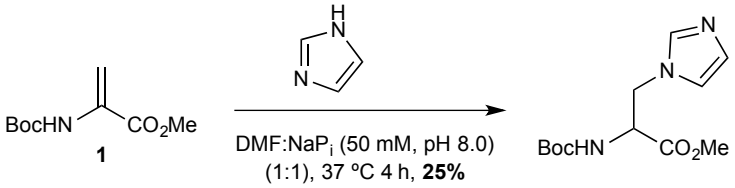

^{1}H NMR (400 MHz, $CDCl_3$): δ (ppm) 1.48 (s, 9H, Boc), 3.81 (s, 3H, CO_2Me), 4.41–4.46 (m, 2H, Hβ), 4.56–4.63 (m, 1H, Hα), 5.17–5.25 (m, 1H, N*H*Boc), 6.84, 7.07, 7.41 (s×3, imidazole). ^{13}C NMR (100 MHz, $CDCl_3$): δ (ppm) 28.2 ((*C*H$_3$)$_3$C), 47.9 (Cβ), 53.0 (CO_2*Me*), 54.5 (Cα), 80.8 ((CH$_3$)$_3$*C*), 119.3, 129.8, 137.7 (imidazole), 155.5 (NCO_2), 169.7 (*C*O_2Me). HRMS ESI$^+$ (*m/z*): Calcd. for $C_{12}H_{20}O_4N_3^+$ $[M + H]^+$ 270.1448, found 270.1438.

Cyclohexylmethylamine 6a

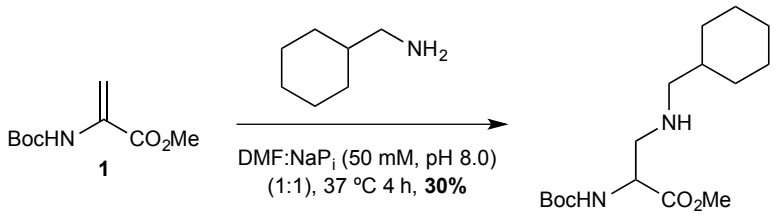

^{1}H NMR (300 MHz, $CDCl_3$): δ (ppm) 0.79–94 (m, 2H, Cy), 1.08–1.30 (m, 4H, Cy), 1.31–1.49 (m, 10H, Cy, (CH_3)$_3$C), 1.60–1.77 (m, 4H, Cy), 2.41 (dd, *J* = 6.7, 1.7Hz, 2H, Cy-CH_2), 2.86–3.01 (2H, Hβ), 3.74 (s, 3H; CO_2CH_3), 4.30–4.41 (m, 1H; Hα), 5.30–5.47 (brs, 1H, N*H*Boc); ^{13}C NMR (75 MHz, $CDCl_3$): δ (ppm) 26.0, 26.6, 31.3, 37.8 (Cy), 28.3 ((CH_3)$_3$C), 50.8 (Cβ), 52.3 (CO_2Me), 53.4 (Cα), 56.3 (CyCH_2); 79.9 ((CH_3)$_3$*C*), 155.6 (NCO_2), 172.6 (*C*O_2Me). HRMS ESI$^+$ (*m/z*): Calcd. for $C_{16}H_{31}O_4N_2^+$ [M + H]$^+$ 315.2284, found 315.2276.

4-Amino-TEMPO, free radical 7a

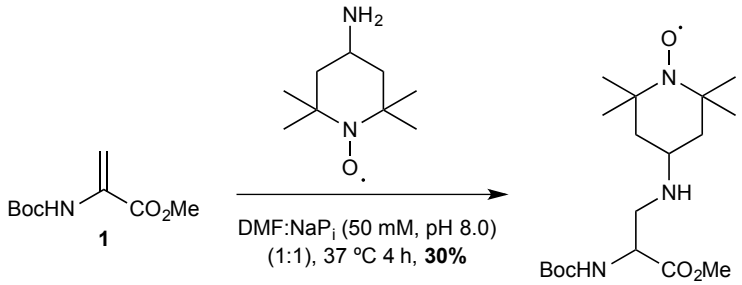

HRMS ESI$^+$ (*m/z*): Calcd. for $C_{18}H_{35}O_5N_3^+$ [M + H]$^+$ 373.2571, found 373.2576.

***N*-Boc-1,6-hexanediamine 8a**

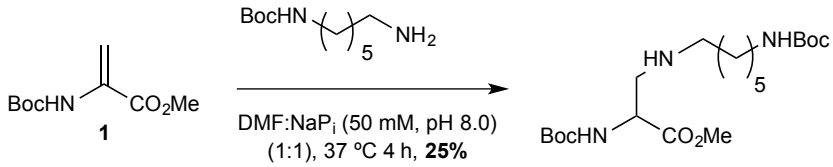

^{1}H NMR (400 MHz, $CDCl_3$): δ (ppm) 1.28–1.65 (m, 26H, 2Boc, 4CH_2), 2.68–2.79 (m, 2H, CH_2), 3.06–3.17 (m, 4H; CH_2, 2Hβ), 3.79 (s, 3H, CO_2Me), 4.42–4.52 (m, 1H; Hα), 4.53–4.62, (m, 1H, NH), 5.72–5.82 (m, 1H, N*H*Boc). ^{13}C NMR (100 MHz, $CDCl_3$): δ (ppm) 26.4, 26.5, 28.3, 28.4 ((CH_3)$_3$C, 4CH_2), 40.4 (CH_2), 49.0 (CH_2), 49.8 (Cβ), 52.6 (Cα, CO_2Me), 80.8 ((CH_3)$_3$*C*), 155.5 (NCO_2), 171.6 (*C*O_2Me). HRMS ESI$^+$ (*m/z*): Calcd. for $C_{20}H_{40}O_6N_3^+$ [M + H]$^+$ 418.2912, found 418.2903.

2-Aminoethyl 2,3,4,6-tetra-*O*-acetyl-α-D-glucopyranoside 9a

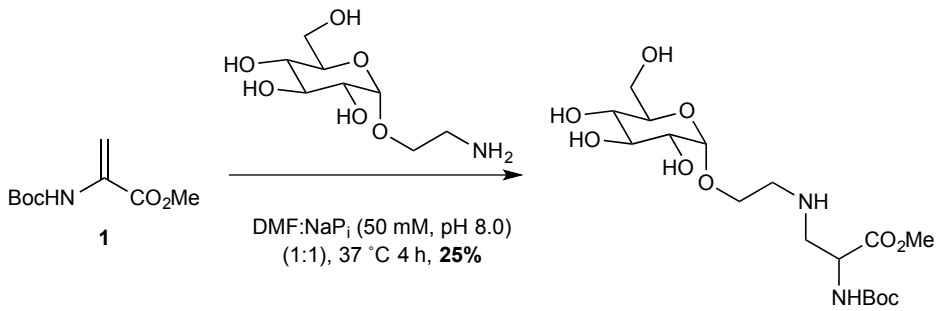

^{1}H NMR (400 MHz, $CDCl_3$): δ (ppm) 1.45 (s, 9H, Boc), 2.01 (s, 3H, Ac), 2.03 (s, 3H, Ac), 2.08 (s, 3H, Ac), 2.10 (s, 3H, Ac), 2.80–2.85 (m, 2H, -OCH_2CH_2NH-), 2.90–3.01 (m, 1H, Hβ), 3.06 (td, *J* = 16.5, 14.4, 4.8 Hz, 1H, Hβ), 3.47–3.54 (m, 1H, -OCH_2CH_2NH-), 3.75–3.81 (m, 4H, -OCH_2CH_2NH-, CO_2Me), 4.01–4.06 (m, 1H, H-5), 4.07–4.11 (m, 1H, H-6), 4.27 (dt, *J* = 12.4, 4.7 Hz, 1H, H-6), 3.35–4.42 (m, 1H, Hα), 4.89 (ddd, *J* = 10.3, 3.8, 1.8 Hz, 1H, H-2), 5.03–5.08 (m, 2H; H-4, H-1), 5.45 (ddd, *J* = 10.3, 9.3, 6.8 Hz, 1H, H-3). ^{13}C NMR (100 MHz, $CDCl_3$): δ (ppm) 20.6, 20.7, (4×Ac), 28.3 ($(CH_3)_3C$), 48.5 (-OCH_2CH_2NH-), 50.6 (Cβ), 52.4 (CO_2Me), 53.5 (Cα), 61.9 (C-6), 67.2 (C-5), 68.0 (-OCH_2CH_2NH-), 68.6 (C-4), 70.1 (C-3), 70.7 (C-2), 80.0 ($(CH_3)_3C$), 95.9 (C-1), 155.6 (NCO_2), 169.6, 170.1, 170.2, 170.7, (4×Ac; CO_2), 172.3 (CO_2Me). HRMS ESI$^+$ (*m/z*): Calcd. for $C_{25}H_{41}O_{14}N_2^+$ $[M + H]^+$ 593.2563, found 593.2544.

3. Chemoselectivity of the aza-Michael addition to Dha

The chemoselectivity of the aza-Michael addition was studied with histamine **5a** and using the general protocol aforementioned. The reaction proceeded with a conversion of 60%, giving a mixture of the two possible adducts in a ratio 1.7:1, in favour of the product resulting from the attack of the primary amine.

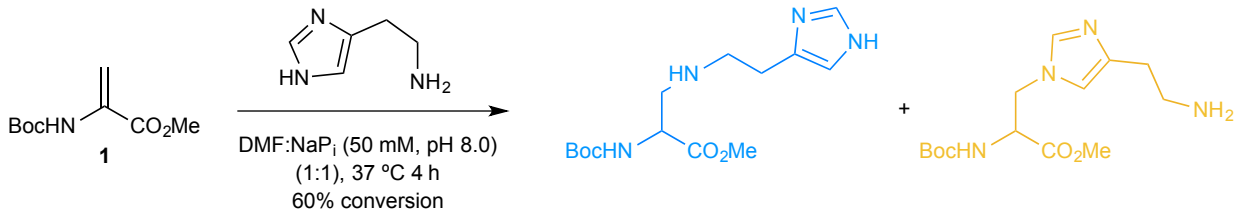

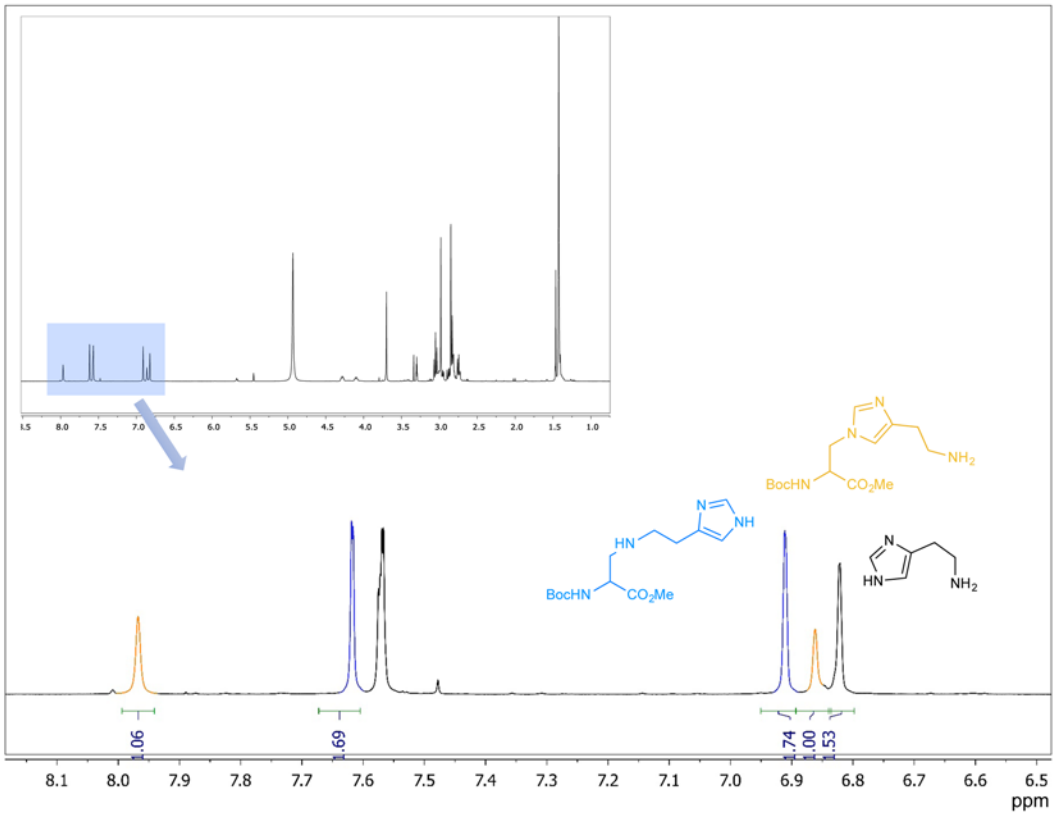

Figure S1. ^{1}H NMR of the crude reaction, showing the chemoselectivity of the aza-Michael addition of histamine **5a** to compound **1**.

4. Stereoselectivity of aza-Michael addition to a Dha-dipeptide S1

Treatment of dipeptide Boc-Ala-Dha methyl ester **S1**[3] with benzylamine **2a** was successfully accomplished in 40% yield after column chromatography and employing the standard conditions previously mentioned. As can be inferred from the ^{1}H NMR, the reaction afforded a mixture 1:1 of the corresponding diastereomers **S2**.

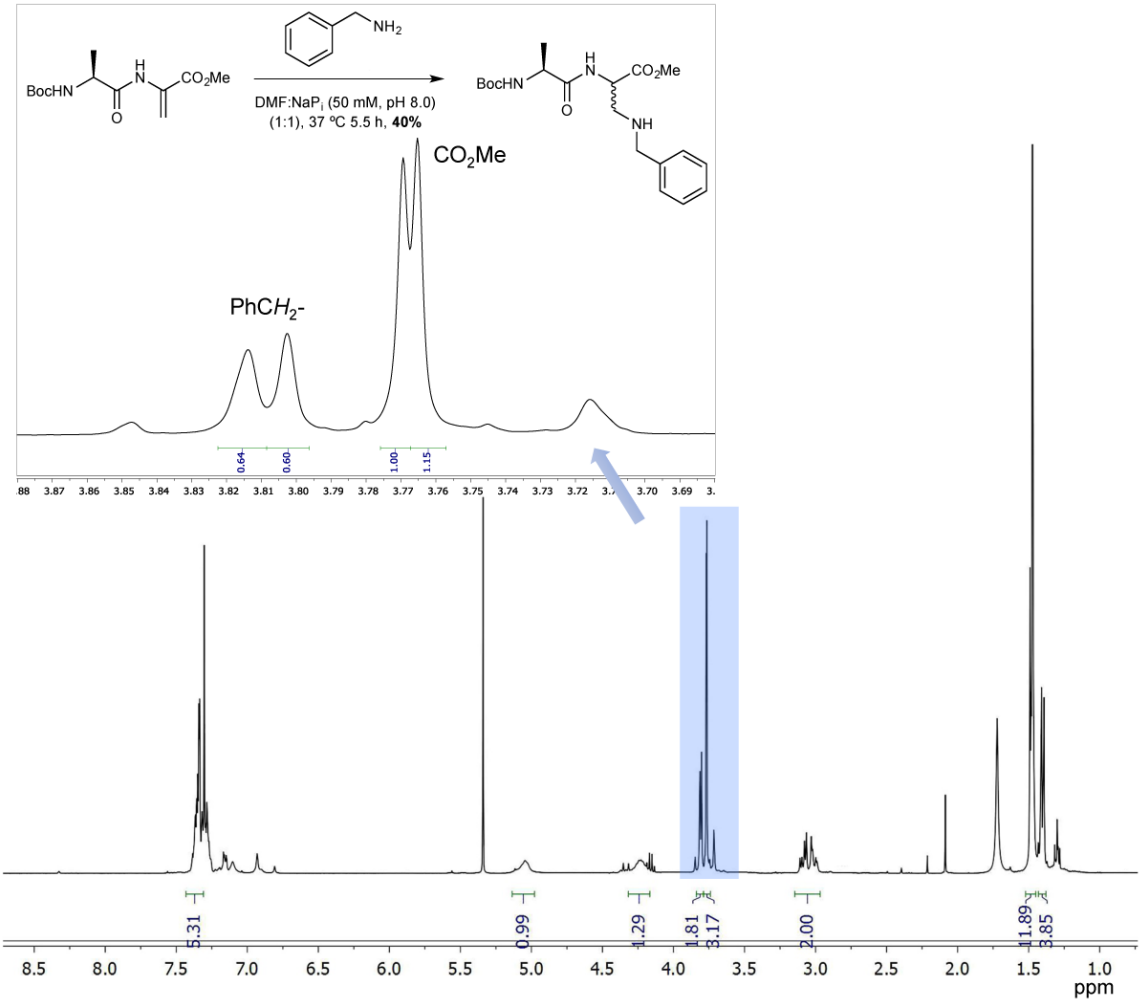

Figure S2. ^{1}H NMR showing the two possible diastereomers generated after the aza-Michael addition of **2a** to dipeptide Boc-Ala-Dha methyl ester **S1**.

5. ^{1}H NMR pH stability studies

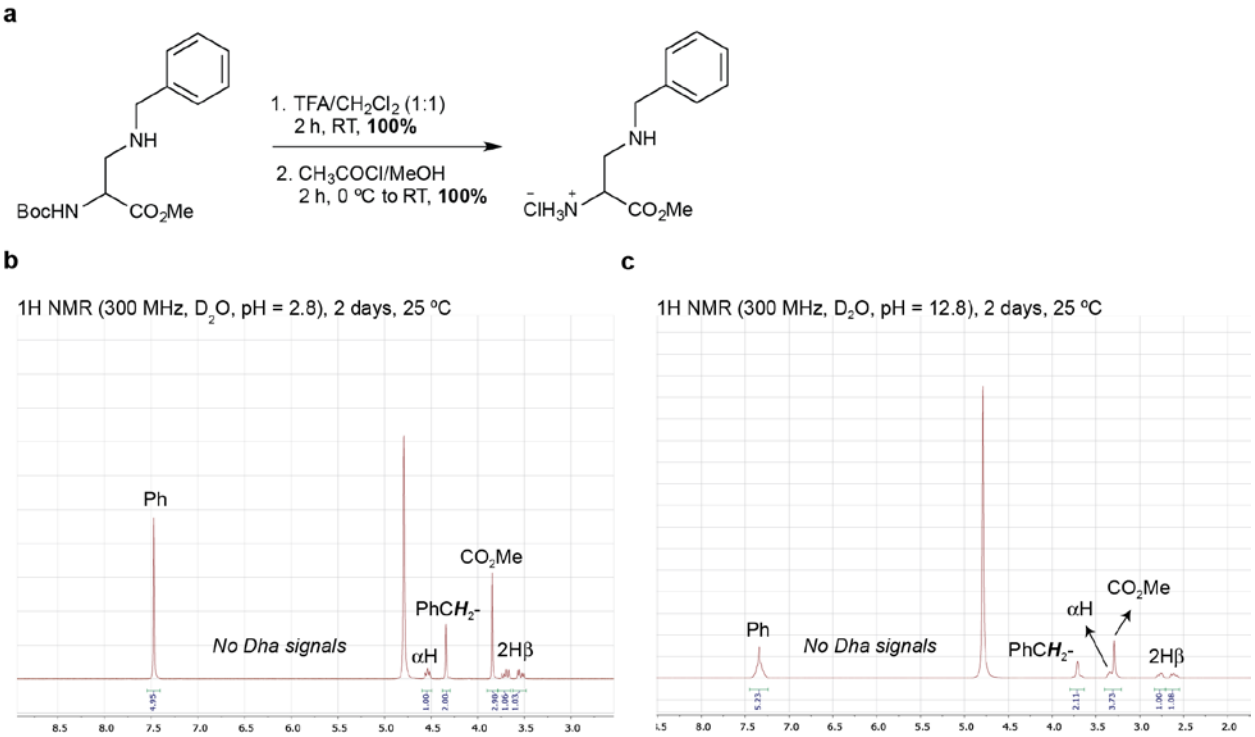

Figure S3. The product of the aza-Michael addition of benzylamine **2a** with **1** was incubated at various pH levels, ranging from 2.8–12.8. Representative ^{1}H NMR spectra are shown for pH 2.8 and 12.8.

6. Kinetics studies

To a solution of compound **1** in DMF/sodium phosphate buffer (50 mM, pH 8.0) (1:1) was added a significant excess of benzylamine **2a** or imidazole **4a** at 37 ºC. Reaction progress was monitored by ^{1}H NMR and through integration of the signal of the Boc group in the starting material. NMR peak heights of the starting material relative to the residual solvent peaks were converted to concentrations at various time points. Data obtained for initial time points was fitted by a single-phase exponential decay model using Origin 9 (Origin Lab Corporation) to obtain pseudo first-order rate constants at different concentrations of **2a** or **4a**. These rate constants at various N-nucleophile concentrations were fitted by linear regression to determine the second order rate constant according a literature procedure.[4]

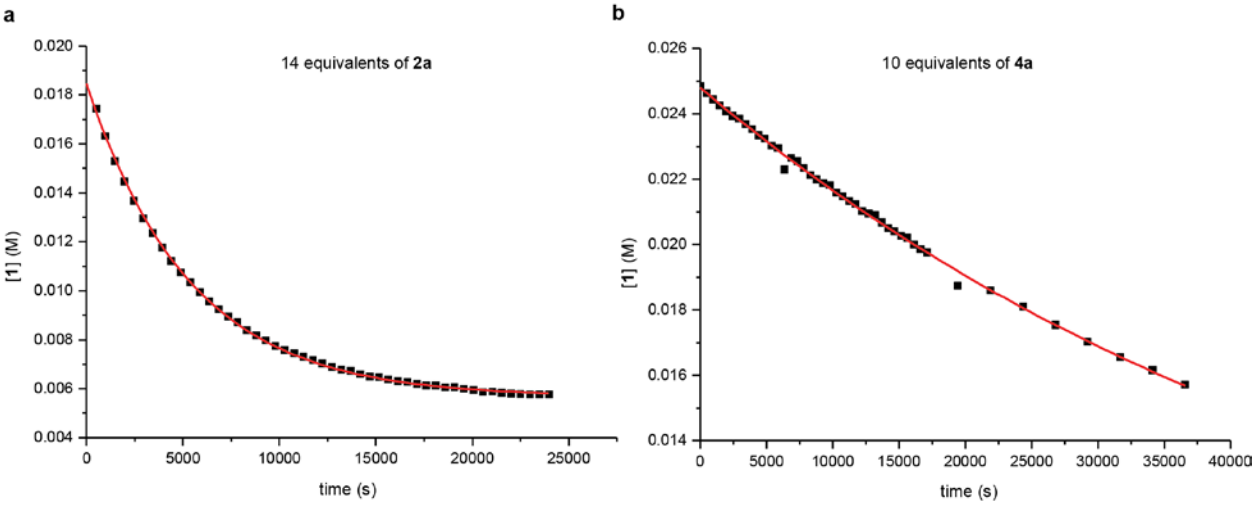

Figure S4. a, Kinetics study of the reaction of Boc-Dha methyl ester **1** with benzylamine **2a**. **b**, Kinetics study of the reaction of Boc-Dha methyl ester **1** with imidazole **4a**.

7. DFT calculations

All geometry optimizations were carried out using the M06-2X hybrid functional[5] and 6-311+G(2d,p) basis set using ultrafine integration grids. Full geometry optimizations and transition structure (TS) searches were carried out with the Gaussian 09 package.[6] The possibility of different conformations was taken into account for all structures. Frequency analyses were carried out at the same level used in the geometry optimizations, and the nature of the stationary points was determined in each case according to the appropriate number of negative eigenvalues of the Hessian matrix. The quasiharmonic approximation reported by Trular *et al.*[7] was used to replace the harmonic oscillator approximation for the calculation of the vibrational contribution to enthalpy and entropy. Scaled frequencies were not considered. Mass-weighted intrinsic reaction coordinate (IRC) calculations were carried out by using the Gonzalez and Schlegel scheme[8] in order to ensure that the TSs indeed connected the appropriate reactants and products. Bulk solvent effects were considered implicitly during geometry optimization through the IEFPCM polarizable continuum model[9] as implemented in Gaussian 09. The standard state conversion ($\Delta G^{o\prime} = \Delta G^{o} - 1.89$ kcal mol^{-1} for A + B$\rightarrow$ C reactions at 298.15 K)[10] was used to convert free energy from gas phase at 1 atm to solution phase at 1 M. The internally stored parameters for water were used. Gibbs free energies (ΔG) were used for the discussion on the relative stabilities of the considered structures. Cartesian coordinates, electronic energies, entropies, enthalpies, Gibbs free energies, and lowest frequencies of the different conformations of the low energy conformations are available in Table S1.

Table S1. Energies, enthalpies, free energies, and entropies of the lowest energy structures calculated at the PCM(water)/M06-2X/6-311+G(2d,p) level. The minimum energy transition states for **2** and **4** are labelled as $\mathbf{2^{‡}}$ and $\mathbf{4^{‡}}$, respectively, as shown in Figure 1d of the manuscript. All calculated structures (higher energy conformers) can be obtained from the authors upon request.

Compound	E_0	E_0+ZPE	H	S	G	Lowest freq.
	(Hartree)[a]	(Hartree)[a]	(Hartree)[a]	(cal mol^{-1} K^{-1})[b]	(Hartree)[a]	(cm^{-1})
Ac-Dha-NHMe	–494.587054	–494.423430	–494.411005	107.3	–494.460241	36.6
Benzylamine (**2a**)	–326.865563	–326.718554	–326.710393	85.3	–326.749773	29.1
Imidazole (**4a**)	–226.204829	–226.132666	–226.128058	64.9	–226.158881	586.2
$\mathbf{2^{‡}}$	–821.430202	–821.117445	–821.097167	154.0	–821.162925	–309.7
$\mathbf{4^{‡}}$	–720.764867	–720.527608	–720.510831	133.2	–720.569681	–339.4

[a] 1 Hartree = 627.51 kcal mol^{-1}. [b] Thermal corrections at 298.15 K.

Cartesian coordinates of the structures calculated at the PCM(water)/M06-2X/6-311+G(2d,p) level. The minimum energy transition states for **2** and **4** are labelled as $\mathbf{2^{‡}}$ and $\mathbf{4^{‡}}$, respectively, as shown in Figure 1 of the manuscript. All calculated structures (higher energy conformers) can be obtained from the authors upon request.

Structure Ac-Dha-NHMe

N	-0.877642	-0.237039	-0.345739
C	0.059903	0.796044	-0.163087
C	-0.227150	2.079706	0.025446
C	1.505152	0.365375	-0.134135
H	-1.241310	2.445143	0.037391
O	2.410080	1.144074	-0.401025
H	0.593188	2.765187	0.183990
H	-0.589757	-1.013475	-0.924746
N	1.728915	-0.919744	0.199933
C	3.085177	-1.421296	0.330403
H	3.631073	-1.245362	-0.594901
H	3.043678	-2.489327	0.525134
H	3.612673	-0.923054	1.145317
C	-2.181300	-0.241535	0.080327
O	-2.662476	0.659056	0.741157
C	-2.976510	-1.447374	-0.350767
H	-3.407020	-1.245227	-1.333486
H	-2.362507	-2.343788	-0.421467
H	-3.785534	-1.604622	0.357423
H	0.974150	-1.458555	0.595819

Structure **2a**

C	1.944170	-0.000168	-0.556756
H	2.223711	0.878836	-1.140251
H	2.223672	-0.879453	-1.139845
N	2.750891	0.000107	0.671965
C	0.450927	-0.000085	-0.322864
C	-0.246109	-1.199348	-0.185766
C	-0.245981	1.199271	-0.185870
C	-1.608698	-1.202106	0.087321
H	0.284247	-2.139391	-0.297339
C	-1.608564	1.202202	0.087216
H	0.284479	2.139246	-0.297526
C	-2.293217	0.000089	0.225615
H	-2.137527	-2.141969	0.187836
H	-2.137296	2.142128	0.187649
H	-3.355535	0.000158	0.435240
H	2.501351	-0.809260	1.233778
H	2.501488	0.809827	1.233329

Structure $\mathbf{2^{‡}}$

N	2.505734	-0.934576	-0.510558
C	1.893999	0.098716	0.263450
C	0.831209	-0.187855	1.107457
C	2.318513	1.463387	0.082410
H	0.699348	-1.217745	1.422497
O	1.730748	2.430712	0.601439
H	0.599468	0.554013	1.862893
H	2.306440	-0.990588	-1.500233
N	3.404175	1.77630	-0.726455
C	4.012769	2.989684	-0.802888
H	3.275878	3.724238	-1.124274
H	4.817638	2.958949	-1.534237
H	4.419207	3.313965	0.158968
C	3.261889	-1.935221	0.007131
O	3.532180	-2.025122	1.198181
C	3.748575	-2.967724	-0.982439

H	3.229845	-3.906754	-0.785588
H	3.580602	-2.680605	-2.018845
H	4.812135	-3.131808	-0.816626
H	3.978885	0.877997	-0.940244
C	-1.994022	-0.331559	1.153850
H	-1.865454	-1.345711	1.534204
H	-1.921439	0.357710	1.996170
N	-0.850225	-0.052801	0.267807
C	-3.324389	-0.188108	0.460572
C	-3.968957	1.046394	0.420757
C	-3.904726	-1.278625	-0.183526
C	-5.172698	1.190641	-0.257220
H	-3.527344	1.897626	0.927582
C	-5.108623	-1.136898	-0.862004
H	-3.412460	-2.244600	-0.149312
C	-5.743875	0.098887	-0.900954
H	-5.667111	2.153704	-0.279248
H	-5.553000	-1.991719	-1.356192
H	-6.683680	0.209635	-1.426999
H	-0.875940	0.899140	-0.092349
H	-0.832211	-0.684262	-0.530247

Structure **4a**

N	0.131444	-1.221174	-0.000081
C	-0.987375	-0.534050	-0.000237
C	1.136588	-0.280505	0.000074
H	-1.985130	-0.942786	-0.000321
C	0.607300	0.978283	-0.000148
H	2.177243	-0.560712	0.000131
H	-1.450588	1.524910	0.000557
H	1.057739	1.955134	-0.000150
N	-0.751207	0.798473	0.000317

Structure **4‡**

N	1.218748	-0.912502	-0.454996
C	0.579563	0.044731	0.392512
C	-0.467874	-0.346064	1.219130
C	0.975507	1.426372	0.324367
H	-0.542641	-1.397066	1.473102
O	0.386382	2.337787	0.935356
H	-0.728209	0.335108	2.018868
H	1.002610	-0.919227	-1.442809
N	2.042963	1.730326	-0.484122
C	2.637253	3.050802	-0.439285
H	1.897711	3.804307	-0.706582
H	3.451099	3.090952	-1.160263
H	3.028182	3.295126	0.552123
C	2.012751	-1.918257	-0.009140
O	2.302827	-2.071565	1.170918
C	2.519779	-2.871296	-1.066022
H	2.054749	-3.844664	-0.905829
H	2.307164	-2.538899	-2.080444
H	3.594870	-2.989175	-0.938916
H	2.629380	0.962082	-0.769488
N	-2.111160	-0.259913	0.375908
C	-2.237619	0.358253	-0.773180
C	-3.351512	-0.710118	0.752163
H	-1.433048	0.825839	-1.318545
C	-4.246447	-0.349146	-0.209478
H	-3.508993	-1.253067	1.668529
H	-3.887962	0.728139	-2.011081
H	-5.306229	-0.508235	-0.300786
N	-3.522089	0.323138	-1.161715

8. Synthesis of aminomethylbenzoic acid derivatives

Synthesis of aminomethylbenzoic acid-PEG 25

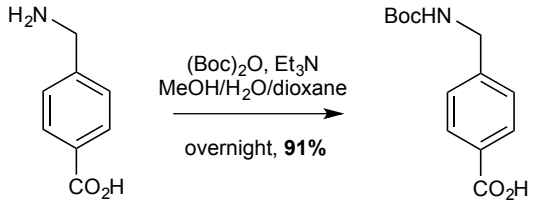

4-Aminomethylbenzoic acid (0.5 g, 3.31 mmol) and ditert-butyl-dicarbonate (0.87 g, 3.97 mmol) were added to a round bottom flask and dissolved in 12 mL of a mixture of methanol/water/dioxane. Trimethylamine (0.74 mL, 5.29 mmol) was then added and the mixture was left stirring overnight. The solvents were partially evaporated *in vacuo*, the crude was re-dissolved in water (20 mL) and then extract with ether (15 mL). The aqueous layer was then acidified with 10% citric acid and extracted with ethyl acetate (15 mL) to yield 0.76 g (91%) of *N*-Boc-aminomethylbenzoic acid as a white solid. ^{1}H NMR (400 MHz, $CDCl_3$): δ (ppm) 1.44 (s, 9H), 4.40 (s, 2H) 7.39 (d, *J* = 8.4 Hz, 2H), 8.08 (d, *J* = 8.0 Hz, 2H).^{13}C NMR (400 MHz, $CDCl_3$) 28.59, 44.59, 127.45, 128.56, 130.76, 135.37, 171.41 HRMS ESI$^+$ (*m/z*): Calcd. for $C_{13}H_{17}NO_4Na^+$ $[M+Na]^+$ 274.1050, found 274.1045.

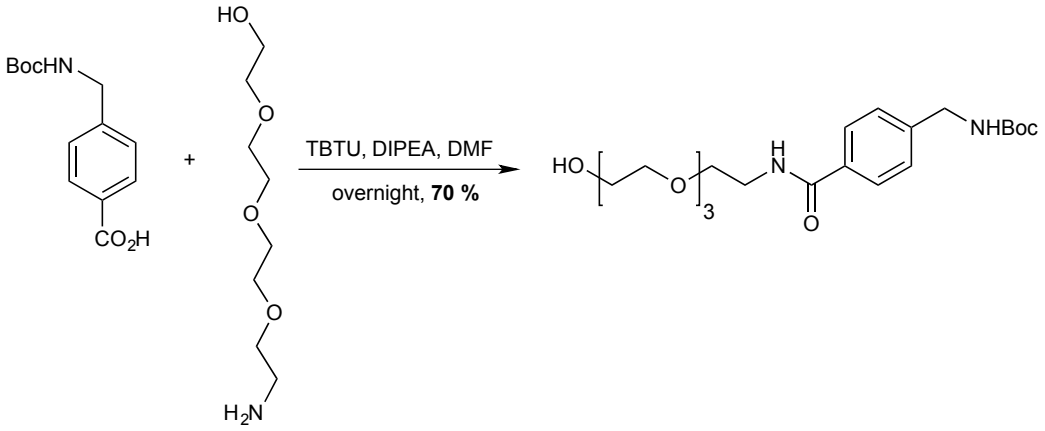

To a solution of *N*-Boc-aminomethylbenzoic acid (15 mg, 0.06 mmol) in DMF (5 mL), 4Å molecular sieves, TBTU (27 mg, 0.07 mmol) as a coupling reagent and DIPEA (0.04 mL, 0.24 mmol) as a base were added. After 30 min stirring vigorously, Boc-PEG-amine (n=4) (14 mg, 0.07 mmol) was poured onto the solution. The mixture was left stirring overnight. Afterwards, the crude was filtered through a pad of Celite® and purified by flash column

chromatography (hexane/EtOAc, 4:6). Finally, 18 mg of the desired compound was obtained in 70% yield as a white solid. ^{1}H NMR (400 MHz, CD_3OD): δ (ppm) 1.47 (s, 9H, C($\underline{C}H_3)_3$), 3.45–3.77 (m, 16H, PEG), 4.30 (s, 1H, Ar-CH_2), 7.38 (d, J = 8.1 Hz, 2H, $CH_{2\text{-}Ar}$), 7.81 (d, J = 8.1 Hz, 2H, $CH_{2\text{-}Ar}$). ^{13}C NMR (101 MHz, CD_3OD): δ (ppm) 27.3 C($CH_3)_3$, 39.5 (PEG), 43.3 ($CH_{2\text{-}Ar}$), 60.8, 69.2, 69.9, 69.9, 70.1, 70.2, 72.2 (PEG), 78.9 ($C(CH_3)_3$), 126.7, 127.1, 132.9, 143.7 (Ar), 168.7 (CO). HRMS (ESI) (*m/z*): Calcd. for $C_{21}H_{34}N_2O_7Na^+$ $[M+Na]^+$ 449.2258, found 449.2248.

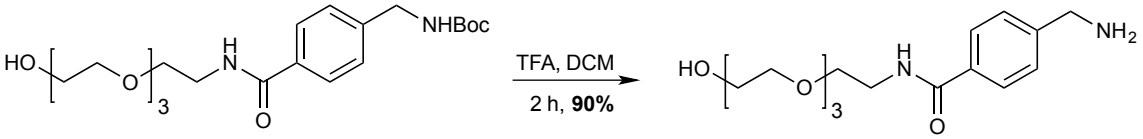

The previously synthesised compound was dissolved in 2 mL of a mixture of DCM and TFA 1:1, and was left to stir for 2 h. The reaction mixture was then dried *in vacuo* and the crude purified by flash column chromatography (DCM/MeOH, 95:5) to afford compound **25** as a white solid in 90% yield. ^{1}H NMR (400 MHz, CD_3OD): δ (ppm) 3.5–3.6 (m, 1H, PEG), 3.6–3.7 (m, 13H, PEG), 3.7–3.8 (m, 1H, PEG), 4.2 (s, 2H, Ar-CH_2), 4.5–4.5 (m, 1H, PEG), 7.6 (d, J = 8.0 Hz, 2H, $CH_{2\text{-}Ar}$), 7.9 (d, J = 8.0 Hz, 2H, $CH_{2\text{-}Ar}$). ^{13}C NMR (101 MHz, CD_3OD): δ (ppm) 39.6 PEG, 42.4 (Ar-CH_2), 60.8, 66.9, 67.9, 69.1, 69.9, 70.1, 72.2, (7$CH_{2\text{-}PEG}$), 127.7, 127.7, 128.6, 128.7, 134.9, 136.5, 6Ar, 168.0 (CO). HRMS (ESI) (*m/z*): Calcd. for $C_{16}H_{27}N_2O_5^+$ $[M+H]^+$ 327.1297, found 327.1290. Calcd. for $C_{16}H_{26}N_2O_5Na^+$ $[M+Na]^+$ 349.1734, found 349.1739.

Synthesis of aminomethylbenzoic acid-fluorescein 26

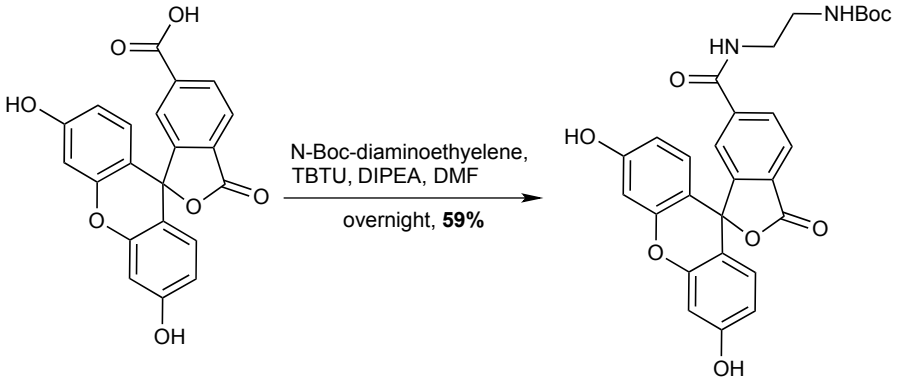

To a solution of 5(6)-carboxyfluorescein (0.5 g, 1.33 mmol) in dry acetonitrile (20 mL), 4Å molecular sieves, TBTU (0.51 g, 1.59 mmol) as a coupling reagent and DIPEA (0.69 mL, 1.59 mmol) as a base were added. After stirring vigorously for 30 min, *N*-Boc-ethylenediamine (0.26 g, 1.59 mmol) was poured onto the solution and the mixture was stirred overnight. Afterwards, the crude was filtered through a pad of Celite® and purified by flash column chromatography (DCM/MeOH, 95:5). Finally, 0.41 g of the desired compound was obtained in 59% yield as an orange solid.

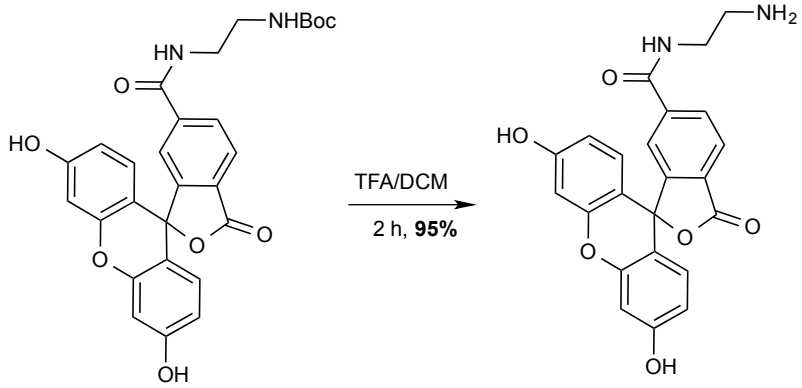

The previously synthesised compound was dissolved in 6 mL of a mixture of DCM and TFA 1:1, and was left to stir for 2 h. Then the reaction mixture was dried *in vacuo* to obtain an orange solid in 95% yield. HRMS ESI$^+$ (*m/z*): Calcd. for $C_{23}H_{19}N_2O_6^+$ [M+H]$^+$ 419.1238, found 419.1220.

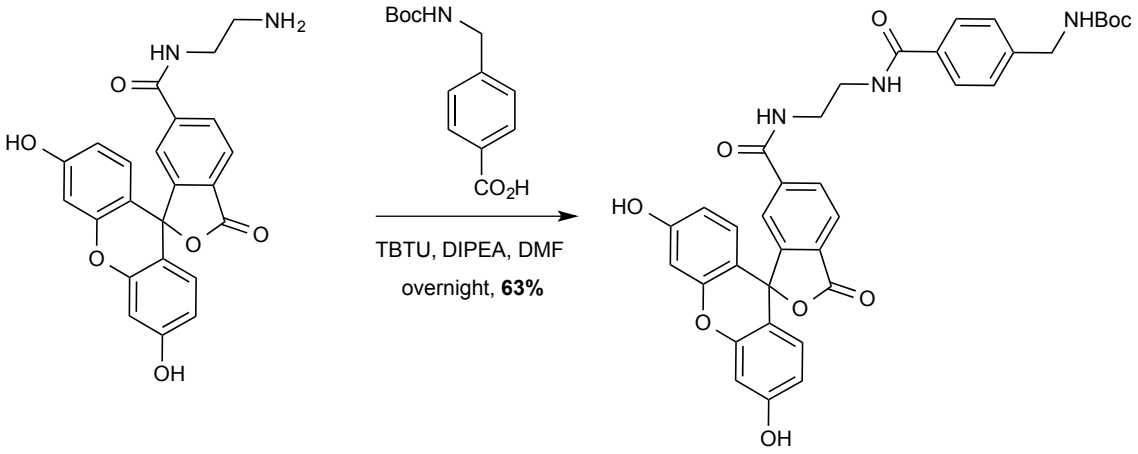

To a solution of *N*-Boc-aminomethylbenzoic acid (75 mg, 0.30 mmol) in DMF (10 mL), 4Å molecular sieves, TBTU (115 mg, 0.36 mmol) as a coupling reagent and DIPEA (0.21 mL, 1.19 mmol) as a base were added. After 30 min of vigorous stirring, fluorescein-amine (150 mg, 0.36 mmol) was poured onto the solution. The mixture was left to stir overnight. Afterwards, the crude was filtered through a pad of Celite® and purified by flash column chromatography by using a mixture of DCM and methanol (95:5). Finally, 188 mg of the desired compound was obtained in 63% yield as an orange solid. ^{1}H NMR (500 MHz, CD_3OD) δ 1.46 (d, *J* = 2.3 Hz, 18H, $C(CH_3)_3$-5/6-isomer), 3.53 (s, 4H, NHCH_2-5/6-isomer), 3.66 (s, 4H, NHCH_2-5/6-isomer), 4.24–4.31 (m, 4H, Ar-CH_2-5/6-isomer), 6.52 (t, *J* = 2.1 Hz, 2H, CH_{Ar} -5/6-isomer), 6.53 (t, *J* = 2.1 Hz, 2H, CH_{Ar} -5/6-isomer), 6.54–6.61 (m, 4H, CH_{Ar} -5/6-isomer), 6.68 (d, *J* = 2.4 Hz, 2H, CH_{Ar} -5/6-isomer), 6.70 (d, *J* = 2.4 Hz, 2H, CH_{Ar} -5/6-isomer), 7.24–7.31 (m, 3H, CH_{Ar}-5/6-isomer), 7.32–7.39 (m, 4H, CH_{Ar} -5/6-isomer), 7.57–7.61 (m, 1H, CH_{Ar}), 7.63 (d, *J* = 7.9 Hz, 2H, CH_{Ar} -5/6-isomer), 7.79 (d, *J* = 8.0 Hz, 2H, CH_{Ar} -5/6-isomer), 7.97 (d, *J* = 8.0 Hz, 2H, CH_{Ar} -5/6-isomer), 8.05 (d, *J* = 8.1 Hz, 1H, CH_{Ar}), 8.09 (dd, *J* = 8.0, 1.5 Hz, 1H, CH_{Ar}), 8.17 (dd, *J* = 8.1, 1.7 Hz, 1H, CH_{Ar}), 8.42 (d, *J* = 1.5 Hz, 1H, CH_{Ar}) ppm. ^{13}C NMR (126 MHz, CD_3OD) δ 27.4 C(CH_3)$_3$, 39.1 , 39.3 , 39.7 , 39.7 4NHCH_2, 43.3, 43.4 2Ar-CH_2, 102.2 Ar, 112.4 Ar, 112.4 Ar, 122.7 Ar, 123.6 Ar, 124.3 Ar, 124.8 Ar, 126.6 Ar, 126.7 Ar, 126.7 Ar, 127.0 Ar, 127.1 Ar, 128.7 Ar, 128.9 Ar, 128.9 Ar, 129.5 Ar, 132.7 Ar, 132.8 Ar, 134.0 Ar, 136.4 Ar, 140.9 Ar, 143.5 Ar, 143.6 Ar, 144.9 Ar, 152.7 Ar, 157.2 Ar, 160.1 Ar, 167.3 Ar, 167.4 CO, 169.0 CO, 169.1 CO, 169.2 CO ppm. HRMS ESI$^+$ (*m/z*): Calcd. for $C_{36}H_{33}N_3O_9^+$ $[M+H]^+$ 652.2301, found 652.2282.

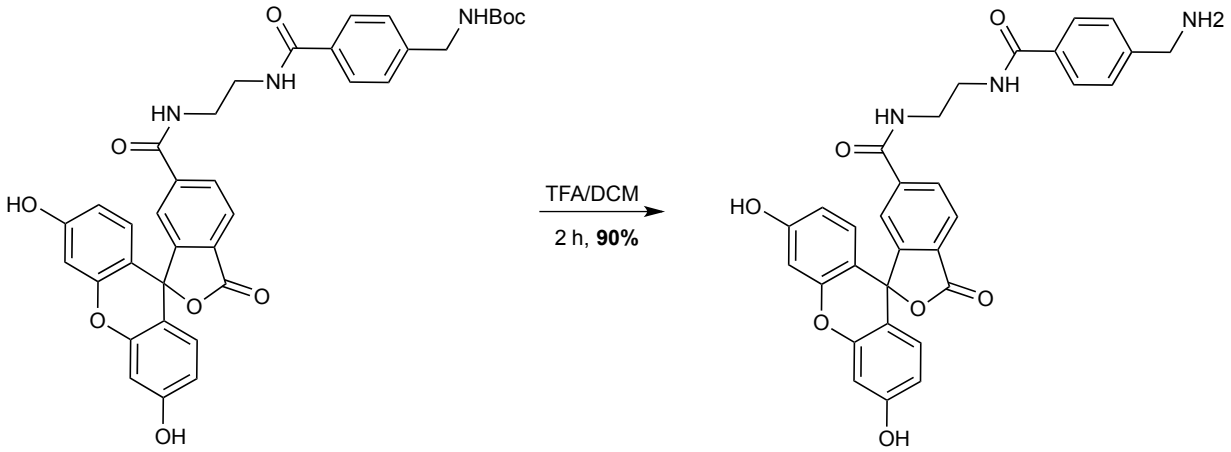

The previously synthesised compound was dissolved in 4 mL of a mixture of DCM and TFA 1:1, and was left to stir for 2 h. The reaction mixture was then dried *in vacuo* and the crude purified by flash column chromatography (DCM/MeOH, 95:5) to give derivative **26** as an orange solid in 90% yield. HRMS ESI$^+$ (*m/z*): Calcd. for $C_{31}H_{26}N_3O_7^+$ $[M+H]^+$ 552.1765, found 552.1758.

9. General method for LC–MS

Liquid chromatography-mass spectrometry (LC–MS) was performed on a Xevo G2-S TOF mass spectrometer coupled to an Acquity UPLC system using an Acquity UPLC BEH300 C4 column (1.7 μm, 2.1 × 50 mm). Solvents A, a water with 0.1% formic acid and B, 71% acetonitrile, 29% water and 0.075% formic acid were used as the mobile phase at a flow rate of 0.2 mL min^{-1}. The gradient was programmed as follows: 72% A to 100% B after 25 min then 100% B for 2 min and after that 72% A for 18 min. The electrospray source was operated with a capillary voltage of 2.0 kV and a cone voltage of 40 V. Nitrogen was used as the desolvation gas at a total flow of 850 L h^{-1}. Total mass spectra were reconstructed from the ion series using the MaxEnt algorithm preinstalled on MassLynx software (v. 4.1 from Waters) according to the manufacturer's instructions. To obtain the ion series described, the major peak(s) of the chromatogram were selected for integration and further analysis.

10. Protein reactions

Protein conjugation analysis by LC–MS

A typical analysis of a conjugation reaction by LC–MS is described below. The total ion chromatogram, combined ion series and deconvoluted spectra are shown for the product of the reaction of C2Am-Dha95 with benzylamine **2a**. Identical analyses were carried out for all the conjugation reactions performed in this work.

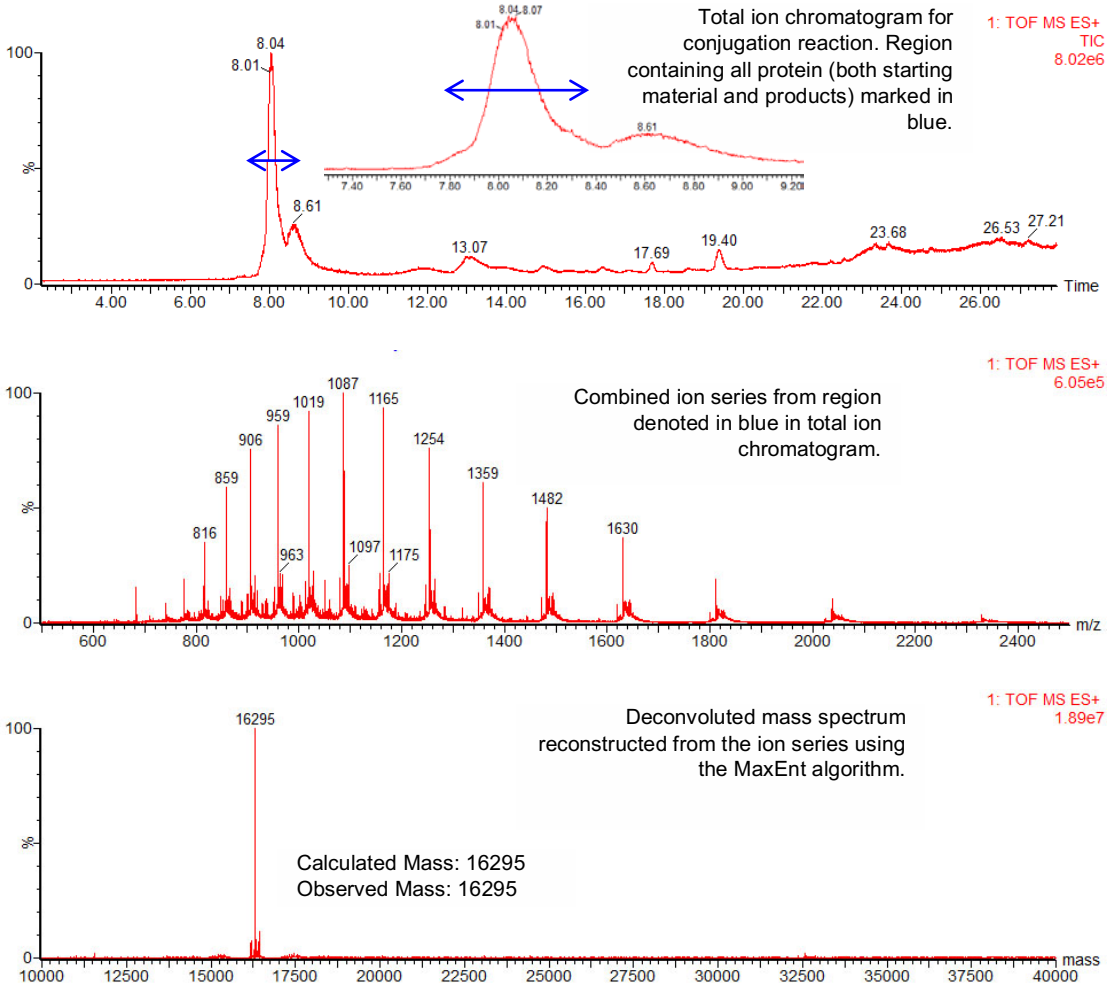

Figure S5. LC–MS analysis of the conjugation reaction of C2Am-Dha95 with benzylamine **2a**.

C2Am-Cys95

C2Am-Cys95 sequence[11] (modified residue in bold and underlined):

GSPGISGGGGGILDSMVEKLGKLQYSLDYDFQNNQLLVGIIQAAELPALDMGGTSDPY
VKVFLLPDKKKKFETKVHRKTLNPVFNEQFTFKVPY**C**ELGGKTLVMAVYDFDRFSKHDI
IGEFKVPMNTV DFGHVTEEWR DLQSAEK

Isotopically Averaged Molecular Weight = 16222.5283 Da

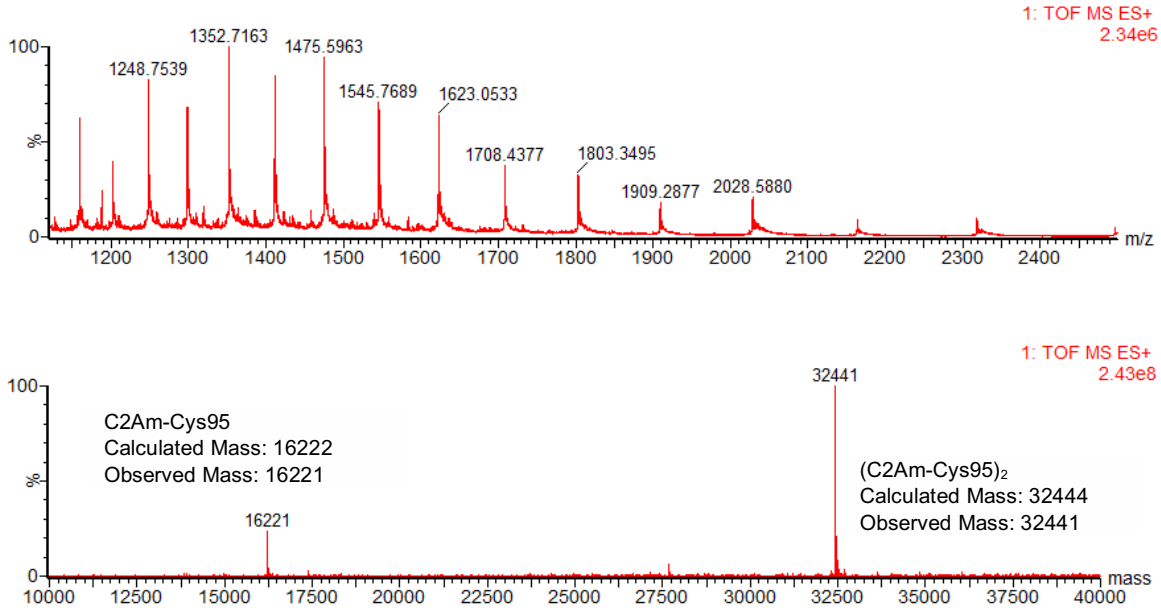

Figure S6. ESI–MS spectrum of non-reduced C2Am-Cys95.

Control: Disulfide reduction using DTT

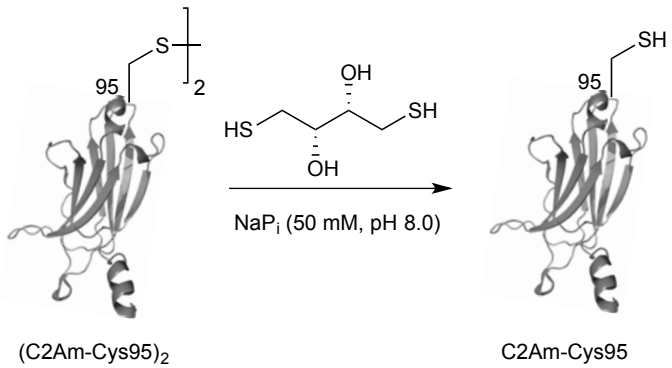

A 500 µL aliquot of C2Am-Cys95 (30.8 µM, 15.4 nmol) was transferred to a 0.5 mL eppendorf tube. D/L-Dithiothreitol (DTT) (30.8 mM, 15.4 µmol) was added as a solid at

room temperature and the resulting mixture vortexed for 30 seconds. After 15 min of additional shaking, a 10 µL aliquot was analysed directly by LC–MS and full reduction of the disulfide (calculated mass, 16222; observed mass, 16222) was observed. Small molecules were removed from the reaction mixture by loading the sample onto a Zeba Spin Desalting Column previously equilibrated with 50 mM sodium phosphate buffer at pH 8.0. The sample was eluted *via* centrifugation (2 min, 1500xg). The protein solution was then flash frozen with liquid nitrogen and stored at –20 ºC.

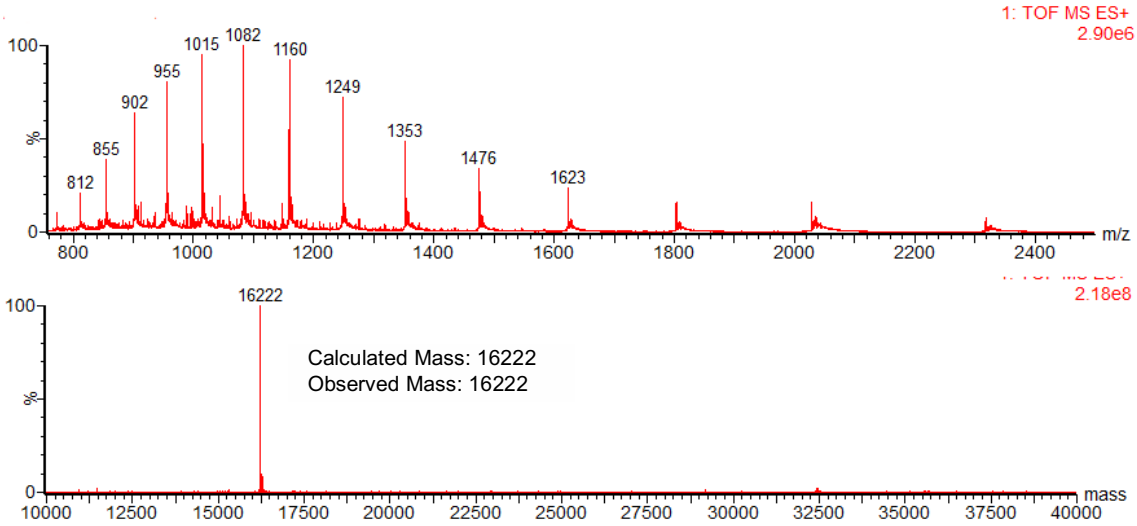

Figure S7. ESI–MS of the reaction of C2Am-Cys95 with DTT after 15 min.

Control: Ellman's reaction with C2Am-Cys95

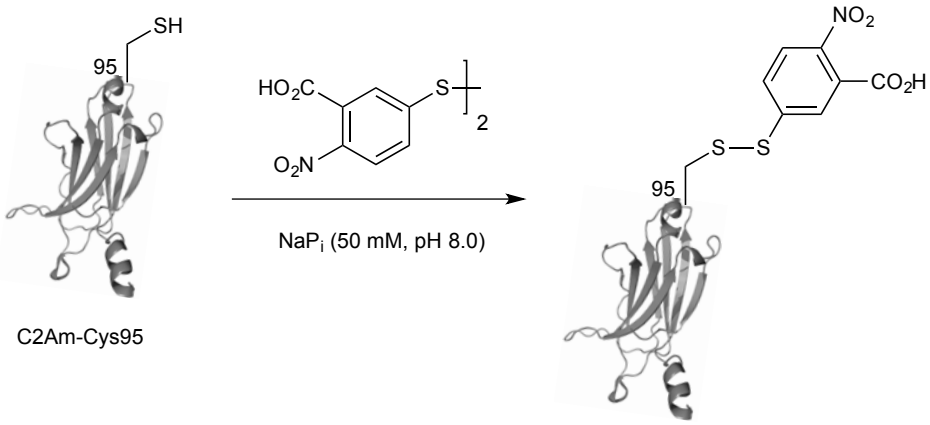

A 50 µL aliquot of C2Am-Cys95 (61.6 µM, 3.10 nmol) was transferred to a 0.5 mL eppendorf tube. Ellman's reagent (30.8 mM, 15.4 µmol) was added as a solid at room temperature and the resulting mixture vortexed for 30 seconds. After 30 min of additional shaking, a 3 µL aliquot was analysed by LC–MS (3 µL aliquot diluted by 7 µL of 50 mM sodium phosphate buffer at pH 8.0) and full conversion to the expected product (calculated mass, 16420; observed mass, 16419) was observed. The protein sample was flash frozen with liquid nitrogen and stored at –20 ºC.

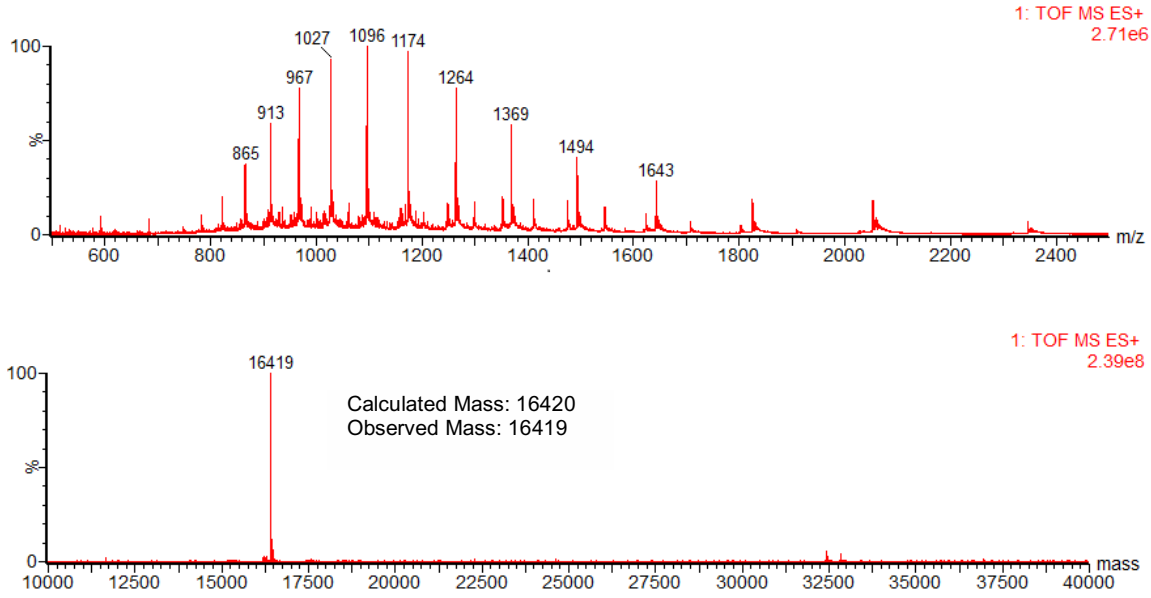

Figure S8. ESI–MS of the reaction of C2Am-Cys95 with Ellman's reagent after 30 min.

Synthesis of C2Am-Dha95

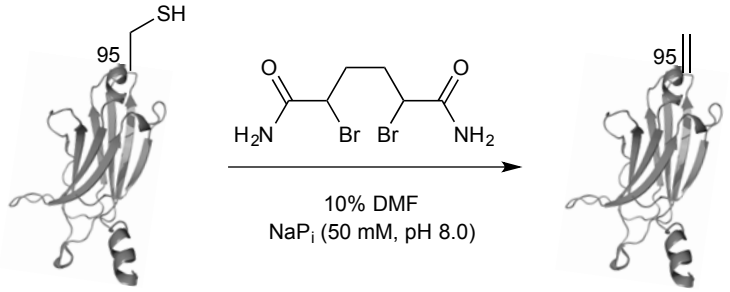

C2Am-Cys95 C2Am-Dha95

To a 450 µL aliquot of reduced C2Am-Cys95 (61.6 µM, 27.7 nmol), a freshly prepared solution of α,α′-di-bromo-adipyl(bis)amide[3] (45 µL of 92.4. mM solution, 41.6 µmol) in DMF was added and the resulting mixture was vortexed for 30 seconds and then was shaken at room temperature. After 2 h, the mixture was shaken at 37 ºC for an additional hour. The reaction progress was monitored by LC–MS with time points taken after 2 and 3 h. Time points were taken by aliquoting 2.5 µL of the reaction mixture and diluting it with 8 µL of 50 mM sodium phosphate buffer at pH 8.0. 10 µL of this diluted sample was injected. Full conversion to C2Am-Dha95 (calculated mass, 16188; observed mass, 16187) was observed after 3 h; 2 h at room temperature and 1 h at 37 ºC. Small molecules were removed from the reaction mixture by loading the sample onto a Zeba Spin Desalting Column previously equilibrated with 50 mM sodium phosphate buffer at pH 8.0. The sample was eluted *via* centrifugation (2 min, 1500xg). The protein solution was then flash frozen with liquid nitrogen and stored at –20 ºC.

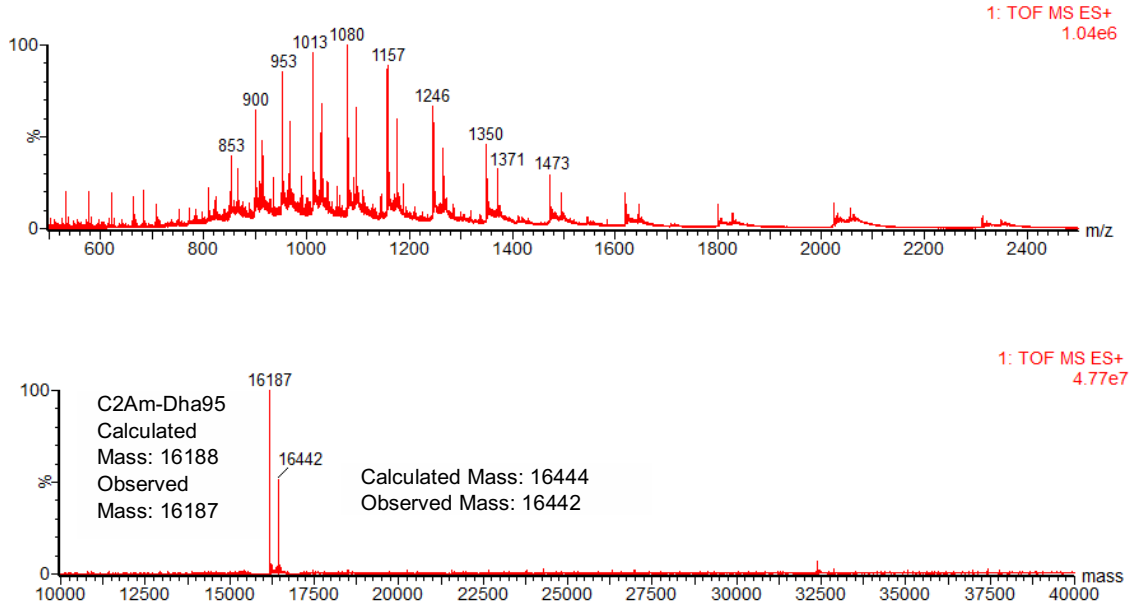

Figure S9. ESI–MS of the reaction of C2Am-Cys95 with α,α′-di-bromo-adipyl(bis)amide (92.4 mM) after 2 h at room temperature.

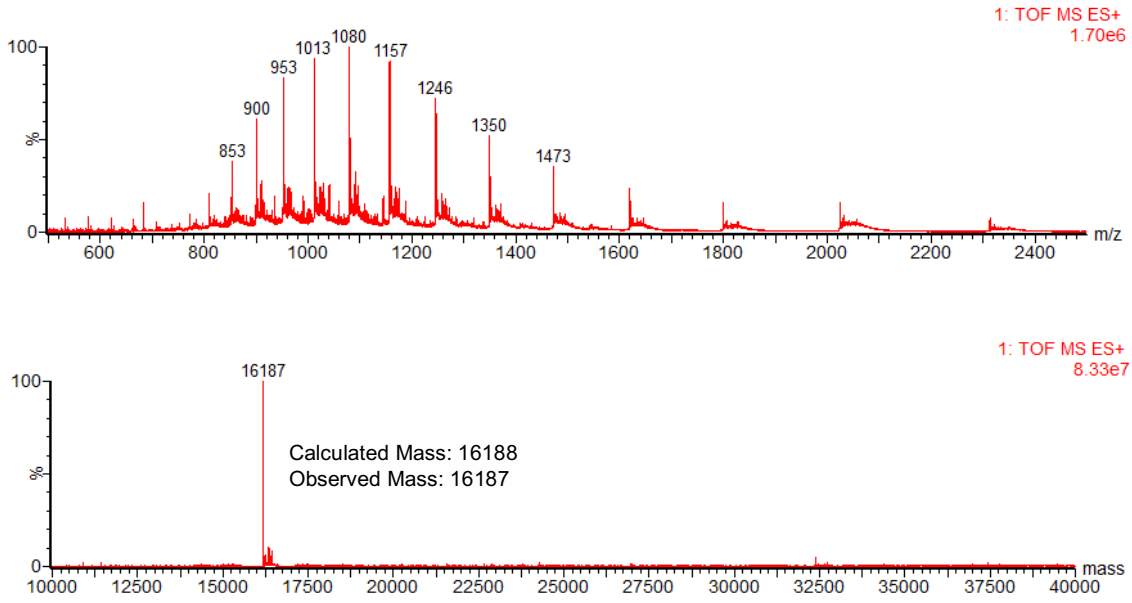

Figure S10. ESI–MS of the reaction of C2Am-Cys95 with α,α′-di-bromo-adipyl(bis)amide (92.4 mM) after 2 h at room temperature and 1 h at 37 ºC.

Circular Dichroism analysis of chemically mutated C2Am-Dha

Circular Dichroism (CD) spectroscopy was used to analyse protein secondary structure in solution. Samples were concentrated to 100 nM in NaPi buffer (50 mM, pH 8.0). CD measurements were recorded using a Chirascan spectrophotometer equipped with a Quantum TC125 temperature control unit (20 ºC). The data were acquired in a 0.1 cm path length with a response time of 1 s, a per-point acquisition delay of 5 ms and a pre- and post-scan delay of 190 nm to 260 nm, and the spectrum from a blank sample containing only buffer was subtracted from the averaged data.

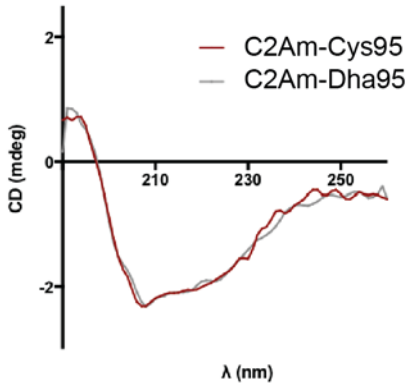

Control: β-mercaptoethanol addition to C2Am-Dha95

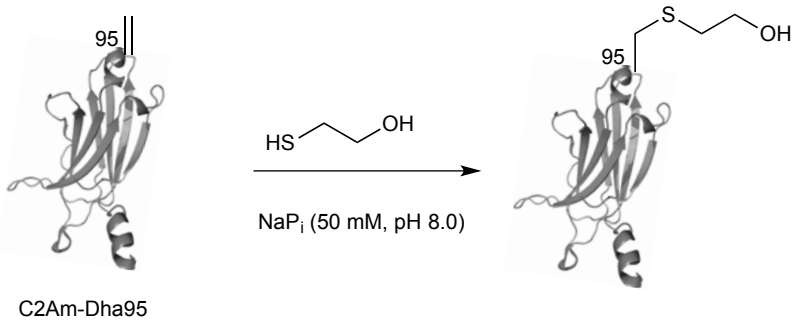

C2Am-Dha95

A 5 µL aliquot of C2Am-Dha95 (41.7 µM, 208.2 nmol) in 50 mM sodium phosphate buffer at pH 8.0 was thawed. β-Mercaptoethanol (1 µL) was added at room temperature and the resulting mixture was vortexed for 30 seconds. After 15 min of additional shaking at room temperature, a 2.5 µL aliquot was analysed by LC–MS (2.5 µL aliquot diluted by 8 µL of 50 mM sodium phosphate buffer at pH 8.0) and complete conversion to the expected product was observed (calculated mass, 16266; observed mass, 16265).

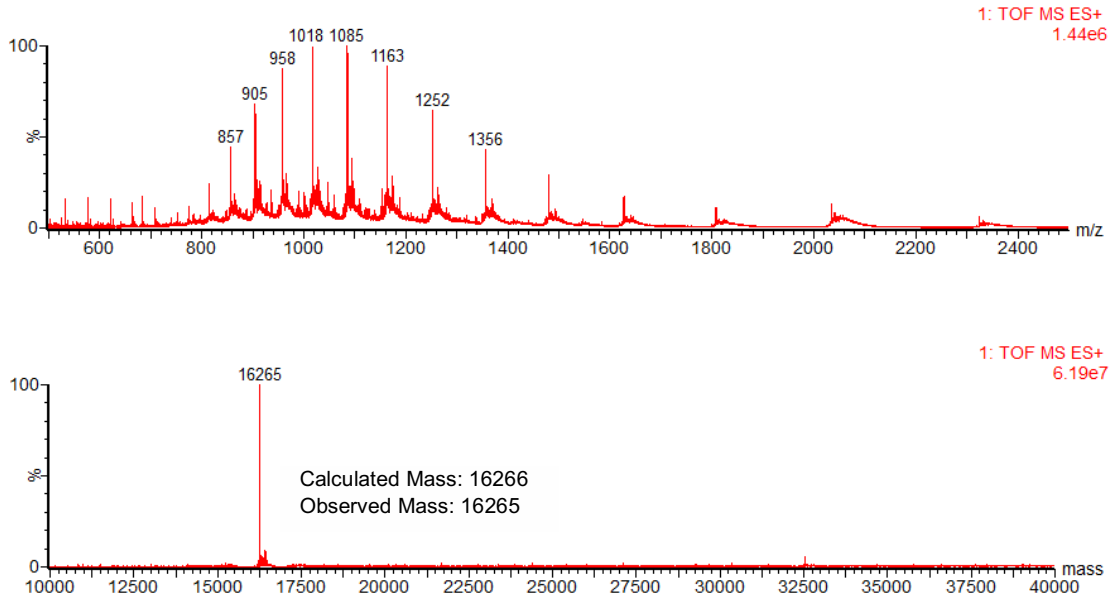

Figure S11. ESI–MS of the reaction of C2Am-Dha95 with β-mercaptoethanol after 15 min at room temperature.

Addition of benzylamine 2 to C2Am-Dha95

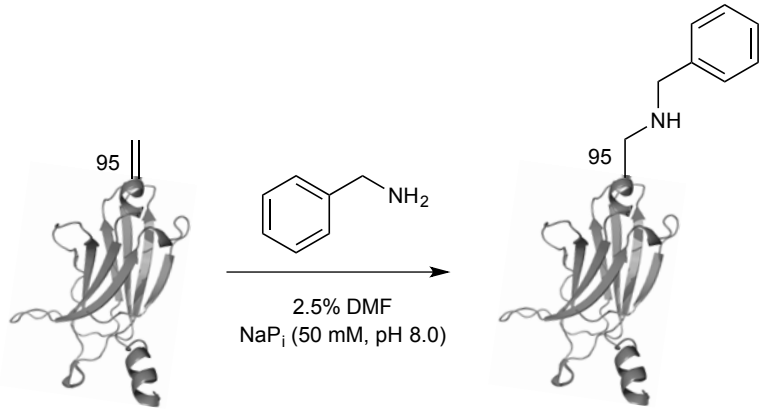

An 80 µL aliquot of C2Am-Dha95 (6.09 µM, 487 pmol) in 50 mM sodium phosphate buffer at pH 8.0 was thawed. Benzylamine **2a** (0.097 µL in 2 µL of DMF, 0.896 µmol) was added at room temperature and the resulting mixture vortexed for 30 seconds. The reaction progress was monitored by LC–MS with time points taken after 1 and 3 h. Time points were taken by aliquoting 5 µL of the reaction mixture and diluting it with 6 µL of 50 mM sodium phosphate buffer at pH 8.0. 10 µL of this diluted sample was injected. 90% conversion to the expected product was observed after 1 h, with complete conversion observed after 3 h (calculated mass, 16295, observed mass, 16294).

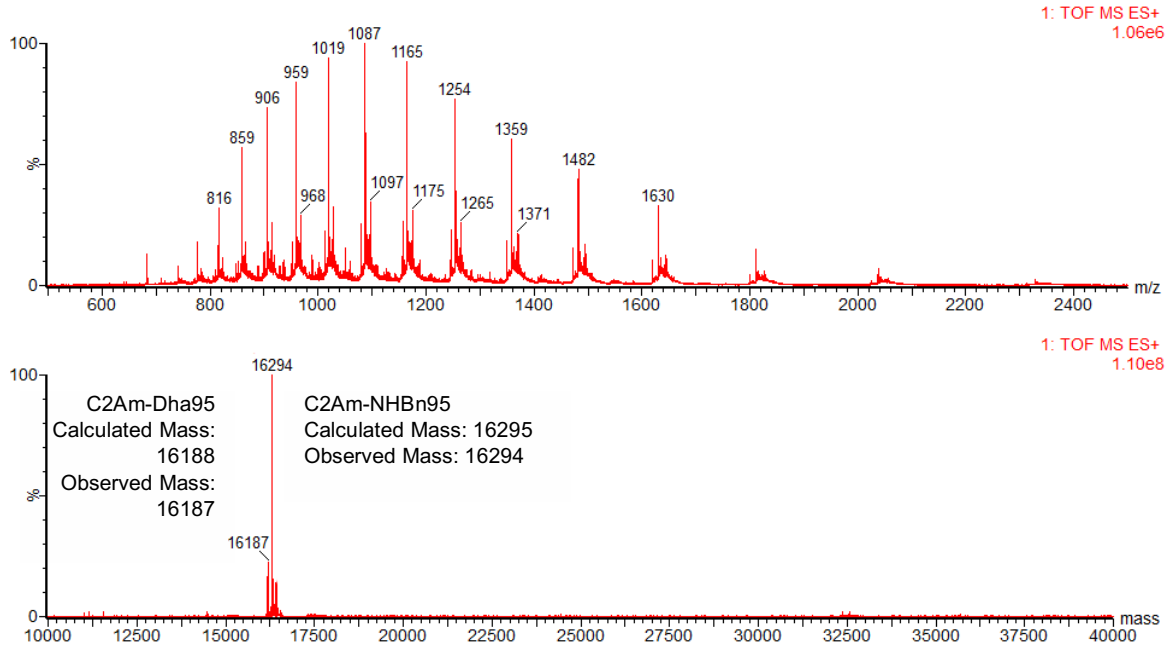

Figure S12. ESI–MS spectrum of the reaction of C2Am-Dha95 with benzylamine **2a** (11.2 mM) after 1 h at room temperature.

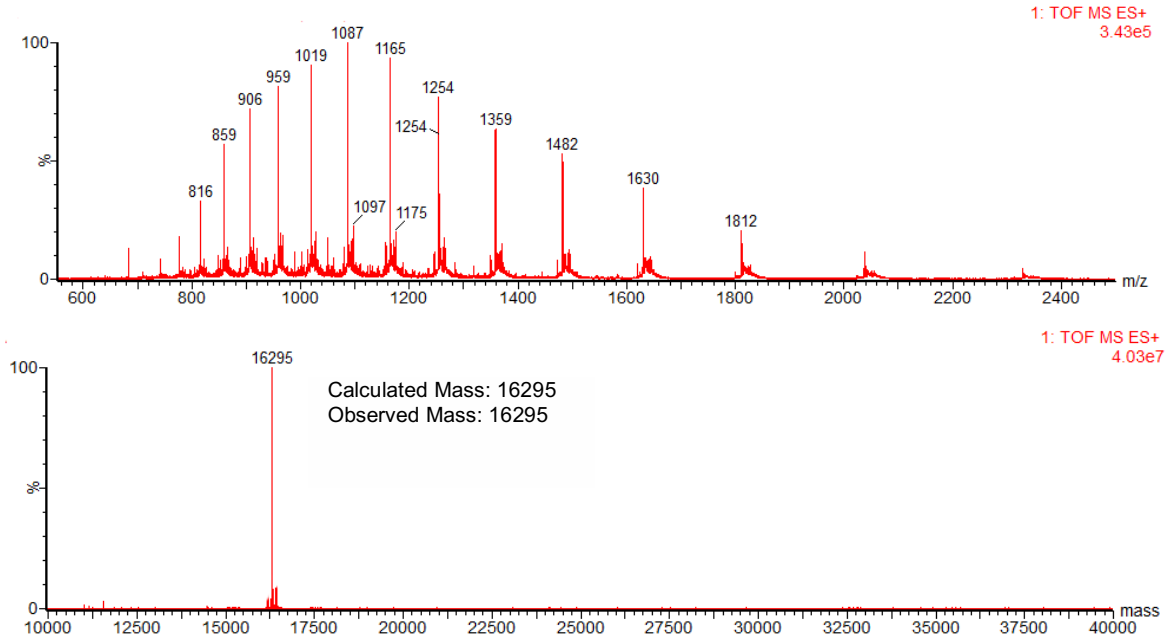

Figure S13. ESI–MS of the reaction of C2Am-Dha95 with benzylamine **2a** (11.2 mM) after 3 h at room temperature.

Expression of Annexin-V-Cys315

Plasmid Preparation

The plasmid pET12a-PAPI (Addgene) contains the gene of human Annexin-V. The plasmid was amplified in Max efficiency *E. coli* DH5α competent cells (Invitrogen). Transformation of *E. coli* DH5α was achieved by incubation of 50 µL bacteria and 1 µL DNA for 30 min on ice and heat shock for 45 seconds at 42 °C. Bacteria were then incubated for 45 min at 37°C in 200 µL 2xYT medium and plated on agar plates containing ampicillin for selection. Inoculation of 4 mL LB medium with ampicillin (100 µg/mL) over night with a single colony was starting point for a mini prep. A kit for plasmid preparation (PureLink®, Invitrogen) was used and corresponding protocol was followed.

Annexin-V-Cys315 Expression

E. coli C41(DE3) pLysS strain (Lucigen) was used for Annexin-V expression. Transformation protocol was identical to the one described. One day prior to expression, 100 mL LB medium were inoculated with one colony of transformed *E. coli* C41(DE3) pLysS and incubated over night at 37 °C and 180 rpm. Aliquots of the overnight culture were stored in a 15% glycerol LB media at –20 °C. The expression followed the procedure described by Tait *et al*.[12]

20 mL of the overnight culture were used to inoculate 400 mL of LB medium containing ampicillin (100 µg mL^{-1}). Bacteria were grown to OD600 0.6 (37 °C, 180 rpm) whereupon expression was induced by 1 mM IPTG (Invitrogen). Expression of Annexin-V was allowed for 4 h until cell culture was harvested by centrifugation at 4 °C and 7500 g for 10 min. Supernatant was inactivated and discarded and the cells were re-suspended in 50 mM Tris HCl (pH 7.2) containing 1 mM β-mercaptoethanol and 10 mM $CaCl_2$. After, cells were lysed using a sonicator (Sonics Vibra-Cell, pulse on 30 s, pulse off 40 s, 2.5 min) and cell fragments were spun down at 4 °C and 17000 g for 45 min. Supernatant was kept until the presence of the protein was confirmed. Cell fragments were then re-suspended in 50 mM Tris HCl (pH 7.2) containing 1 mM β-mercaptoethanol and 20 mM EDTA and spun down at 4 °C and 17000 g for 20 min. The supernatant was collected

and dialysed against 1 L of 20 mM Tris HCl (pH 8.0) containing 1 mM β-mercaptoethanol overnight. The following day, the protein in solution was treated with 1 mM PMSF, 2 µL mL^{-1} aprotinin and 10 µL mL^{-1} leupeptin and 10 U mL^{-1} benzonase nuclease in presence of 5 mM $MgCl_2$. Furthermore, the protein was dialysed against 3 changes of 20 mM Tris HCl (pH 8.0) at 4 °C.

Annexin-V-Cys315 Purification and Characterization

The purification was performed based on a protocol published by Coxon *et al*.[13] The protein was purified with FPLC (AKTA basic, GE Healthcare) and a size exclusion column (SepFast GF-HS M 16/60, Generon). The mobile phase was 20 mM Tris HCl (pH 8.0), flow rate 1 mL min^{-1} and fractions of 2 mL were collected and analysed by SDS-PAGE. A second round of purification was done with an anion exchange column (HighRes15 Q, Generon). The column was equilibrated with 20 mM Tris HCl (pH 8.0) at a flow rate of 1 mL min^{-1}. After loading the concentrated protein sample, the column was washed with 3 column volumes with the same buffer. A buffer gradient of 0%–100% 1 M NaCl in 20 mM Tris HCl eluted the protein and fractions of 1 mL were collected. The fractions were analysed by SDS-PAGE and combined.

For qualitative characterization of the purified protein, SDS-PAGE using 4–12% Tris-Bis gels (Life Technologies) in a MOPS running buffer (Life Technologies), 200 V, 55 min was done with a known concentration of BSA to estimate protein concentration. The protein was analysed by LC–MS (Waters Xevo G2-S, Nanoelectrospray ionization). Protein concentration was determined with a UV spectrometer at wavelength 280 nm, a known extinction coefficient ε=23380 M^{-1} cm^{-1} and the use of Beer-Lambert law.

Annexin-V-Cys315 sequence (modified residue in bold and underlined)

AQVLRGTVTDFPGFDERADAETLRKAMKGLGTDEESILTLLTSRSNAQRQEISAAFKTL
FGRDLLDDLKSELTGKFEKLIVALMKPSRLYDAYELKHALKGAGTNEKVLTEIIASRTPE
ELRAIKQVYEEEYGSSLEDDVVGDTSGYYQRMLVVLLQANRDPDAGIDEAQVEQDAQ
ALFQAGELKWGTDEEKFITIFGTRSVSHLRKVFDKYMTISGFQIEETIDRETSGNLEQLL
LAVVKSIRSIPAYLAETLYYAMKGAGTDDHTLIRVMVSRSEIDLFNIRKEFRKNFATSLYS
MIKGDTSGDYKKALLLL**C**GEDD

Isotopically Averaged Molecular Weight = 35805.58 Da (N-terminal Met cleaved)

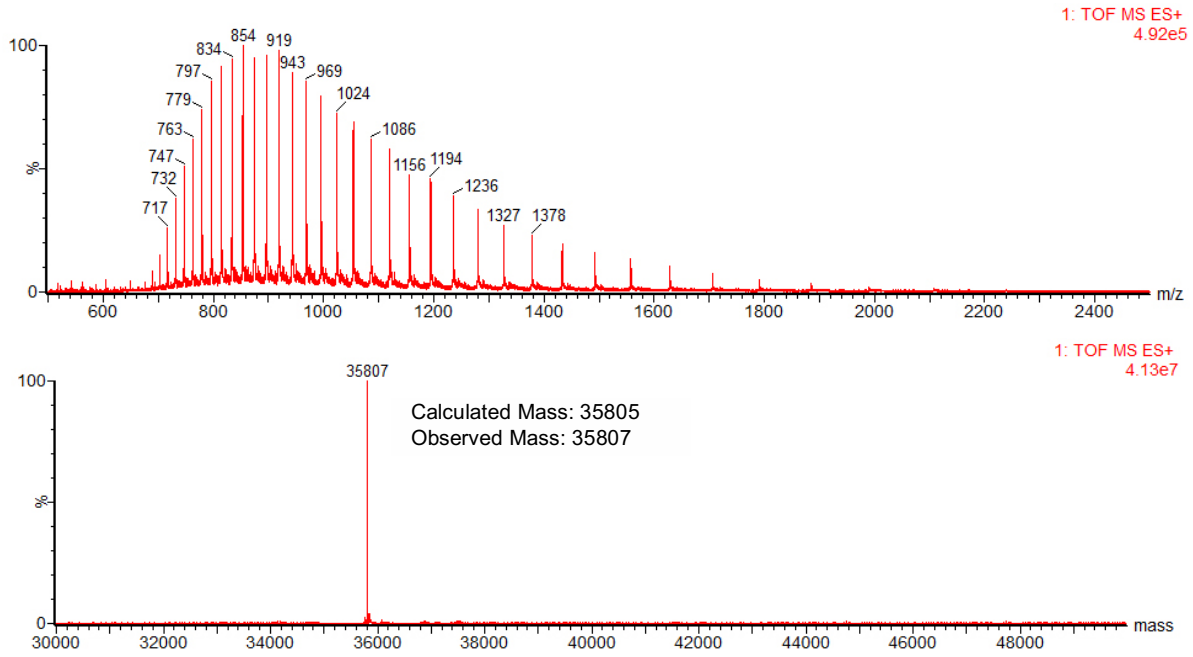

Figure S14. ESI–MS of Annexin-V-Cys315.

Benzylamine 2a addition to Annexin-V-Dha315

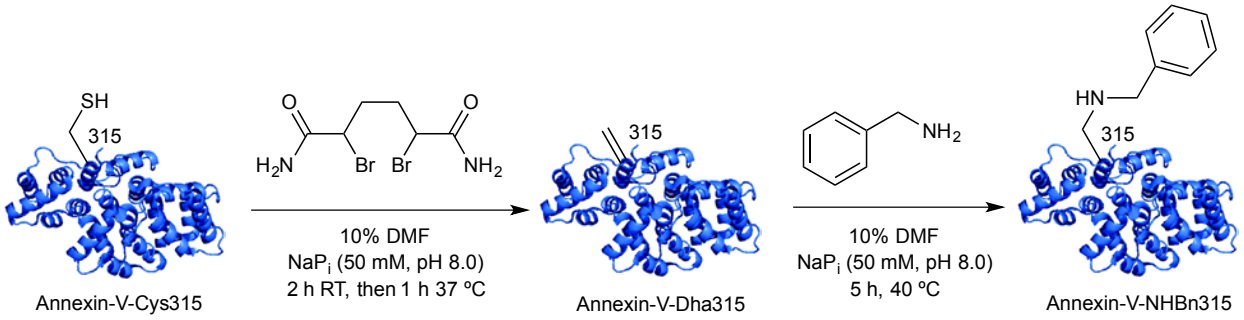

To a 500 µL aliquot of reduced Annexin-V-Cys315 (27.8 µM, 13.9 nmol) a freshly prepared solution of α,α′-di-bromo-adipyl(bis)amide[3] in DMF (50 µL of 140.0 mM solution, 7.0 µmol) was added and the resulting mixture vortexed for 30 seconds and then shaken. The reaction progress was monitored by LC–MS. Time points were taken by aliquoting 2.5 µL of the reaction mixture and diluting it with 8 µL of 50 mM sodium phosphate buffer at pH 8.0. 10 µL of this diluted sample was injected. Full conversion to Annexin-V-Dha315 (calculated mass, 35772; observed mass, 35773) was observed after 3 h; 2 h at room temperature and 1 h at 37 ºC. Small molecules were removed from the reaction mixture by loading the sample onto a Zeba Spin Desalting Column previously equilibrated with 50 mM sodium phosphate buffer at pH 8.0. The sample was eluted *via* centrifugation (2 min, 1500xg). The protein solution was then flash frozen with liquid nitrogen and stored at –20 ºC.

A 20 µL aliquot of Annexin-V-Dha315 (14.9 µM, 0.299 µmol) in 50 mM sodium phosphate buffer at pH 8.0 was thawed. Benzylamine **2a** (0.35 µL dissolved in 2 µL of DMF, 3.3 µmol) was added and the resulting mixture vortexed for 30 seconds. The reaction was then shaken for 5 h at 40 ºC. Time points were taken by aliquoting 5 µL of the reaction mixture and diluting it with 5µL of 50 mM sodium phosphate buffer at pH 8.0. 10 µL of this diluted sample was injected. >95% conversion to the Annexin-V-NHBn315 adduct was observed after 5 h (calculated mass, 35879, observed mass, 35878).

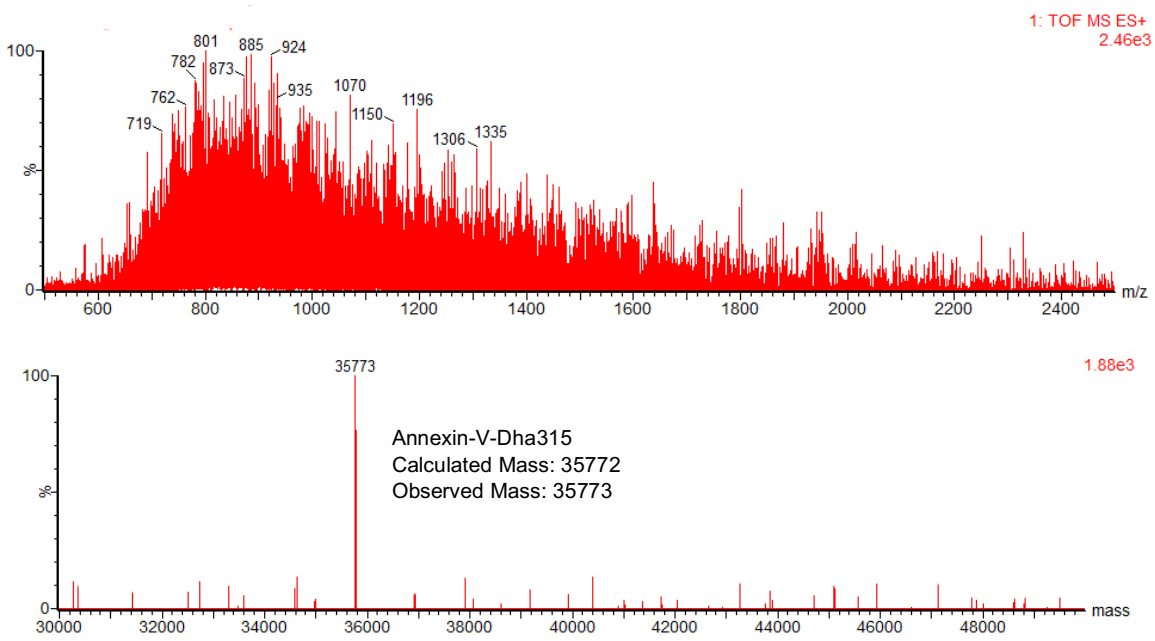

Figure S15. ESI–MS of the reaction of Annexin-V-Cys315 with α,α′-di-bromo-adipyl(bis)amide (14 mM) after 3 h; 2 h at room temperature and 1 h at 37 ºC.

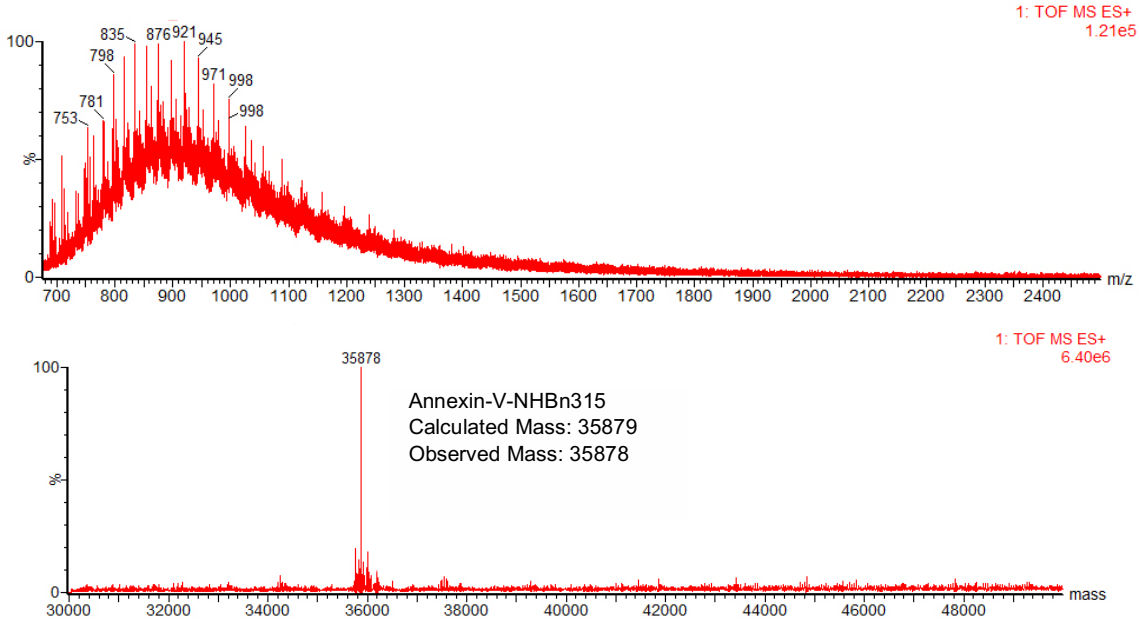

Figure S16. ESI–MS of the reaction of Annexin-V-Dha315 with benzylamine (165.7 mM) after 5 h at 40 ºC.

Scope of N-nucleophile additions to C2Am-Dha95

4-Hydroxybenzylamine (6.8 mM & 26.8 mM & 34.1 mM)

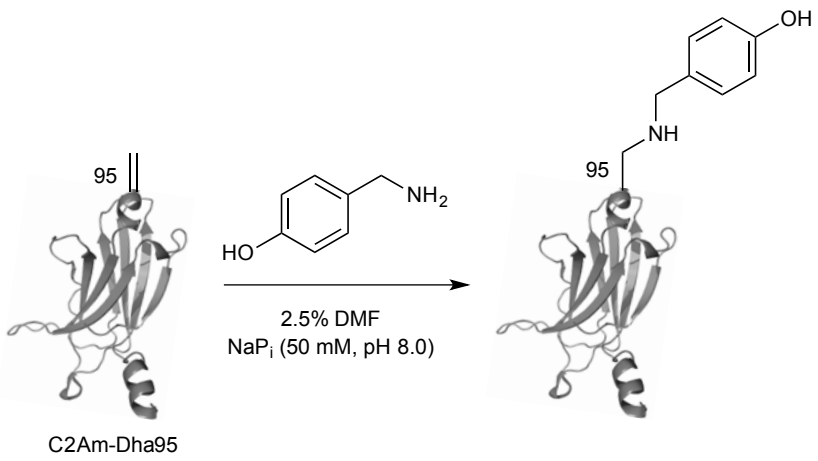

C2Am-Dha95

A 40 µL aliquot of C2Am-Dha95 (6.09 µM, 244 pmol) in 50 mM sodium phosphate buffer at pH 8.0 was thawed. 4-Hydroxybenzylamine (0.03 µL dissolved in 1 µL of DMF, 278 nmol) was added at room temperature and the resulting mixture vortexed for 30 seconds. Time points were taken by aliquoting 5 µL of the reaction mixture and diluting it with 5 µL of 50 mM sodium phosphate buffer at pH 8.0. 10 µL of this diluted sample was injected for LC–MS analysis. 40% conversion was observed after 3 h (calculated mass, 16311, observed mass, 16312).

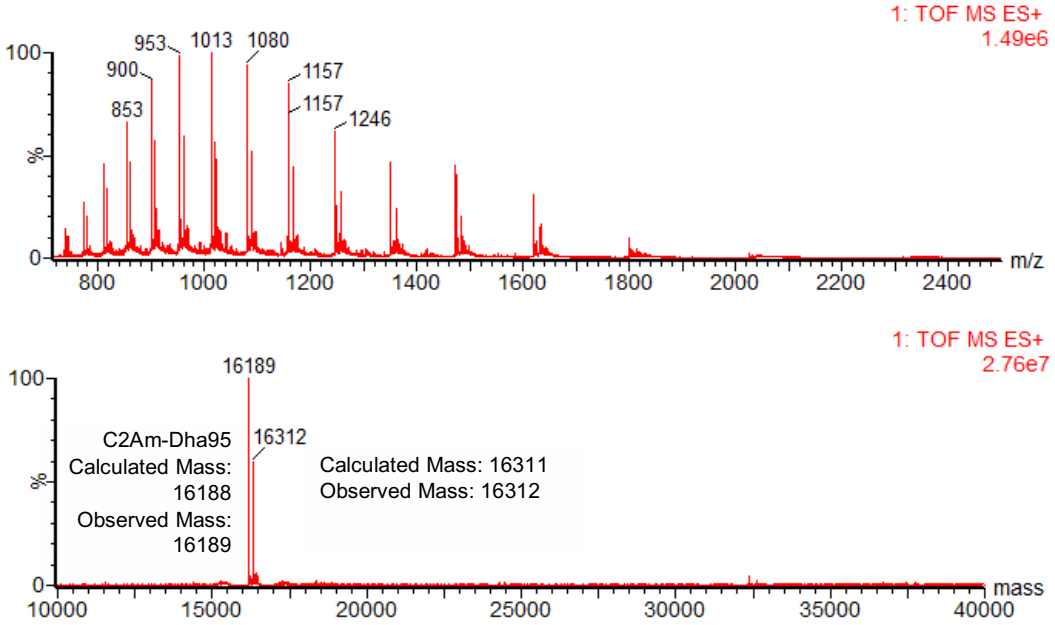

Figure S17. ESI–MS of the reaction of C2Am-Dha95 with 4-hydroxybenzylamine (6.8 mM) after 3 h at 37 ºC.

A 40 µL aliquot of C2Am-Dha95 (6.09 µM, 244 pmol) in 50 mM sodium phosphate buffer at pH 8.0 was thawed. 4-Hydroxybenzylamine (0.12 µL dissolved in 1 µL of DMF, 1.1 µmol) was added at 37 ºC and the resulting mixture vortexed for 30 seconds. Time points were taken by aliquoting 5 µL of the reaction mixture and diluting it with 5 µL of 50 mM sodium phosphate buffer at pH 8.0. 10 µL of this diluted sample was injected for LC–MS analysis. 70% conversion was observed after incubating for 3 h at 37 ºC (calculated mass, 16311, observed mass, 16312).

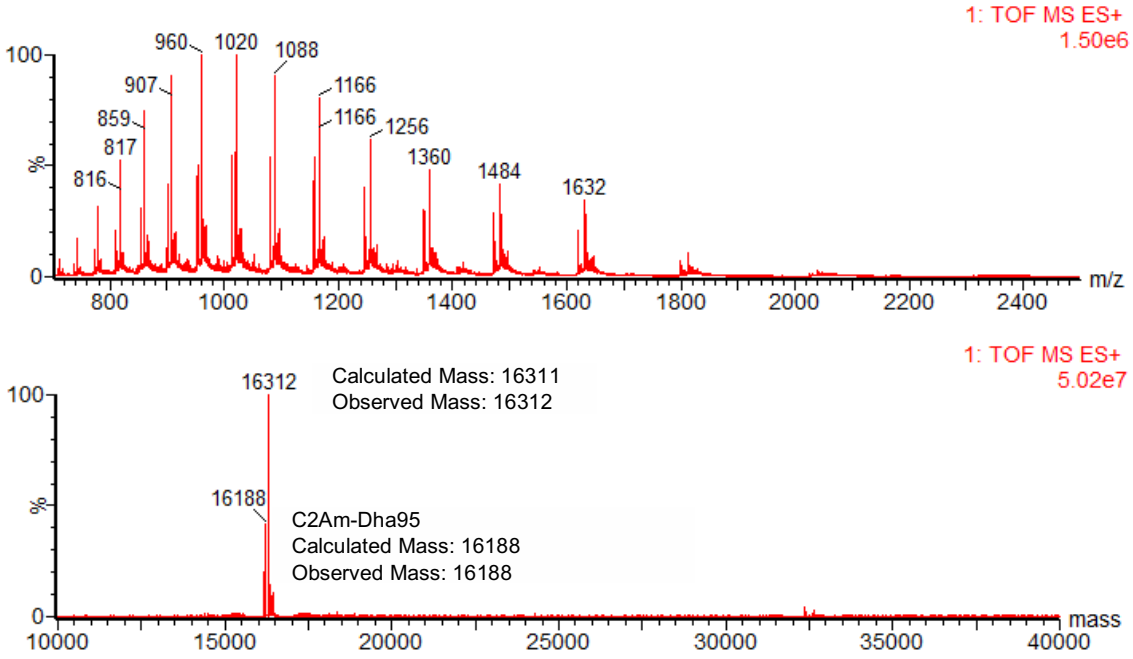

Figure S18. ESI–MS of the reaction of C2Am-Dha95 with 4-hydroxybenzylamine (26.8 mM) after 3 h at 37 ºC.

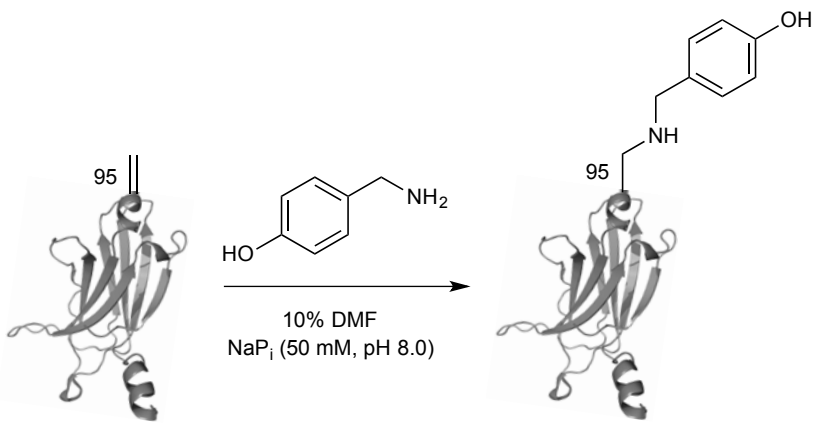

C2Am-Dha95

A 40 µL aliquot of C2Am-Dha95 (6.09 µM, 244 pmol) in 50 mM sodium phosphate buffer at pH 8.0 was thawed. 4-Hydroxybenzylamine (0.15 µL dissolved in 4 µL of DMF, 1.4 µmol) was added at 37 ºC and the resulting mixture vortexed for 30 seconds. Time points were taken by aliquoting 5 µL of the reaction mixture and diluting it with 5 µL of 50 mM sodium phosphate buffer at pH 8.0. 10 µL of this diluted sample was injected for LC–MS analysis. Full conversion was observed after incubating for 24 h at 37 ºC (calculated mass, 16311, observed mass, 16311).

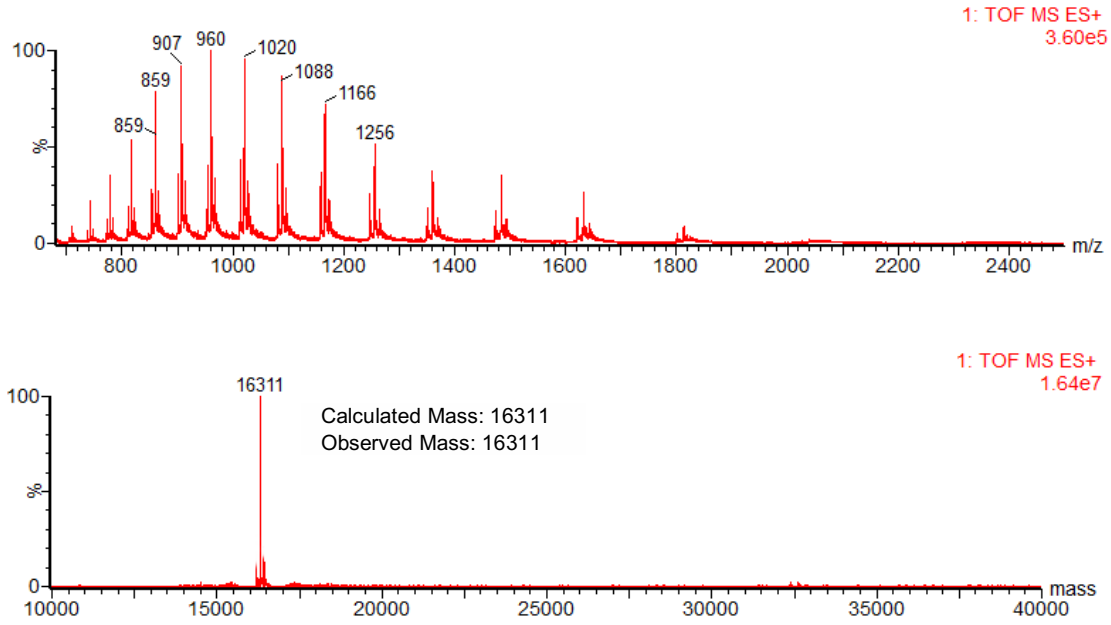

Figure S19. ESI–MS of the reaction of C2Am-Dha95 with 4-hydroxybenzylamine (34.1 mM) after 24 h at 37 ºC.

4-(Aminomethyl)benzoic acid

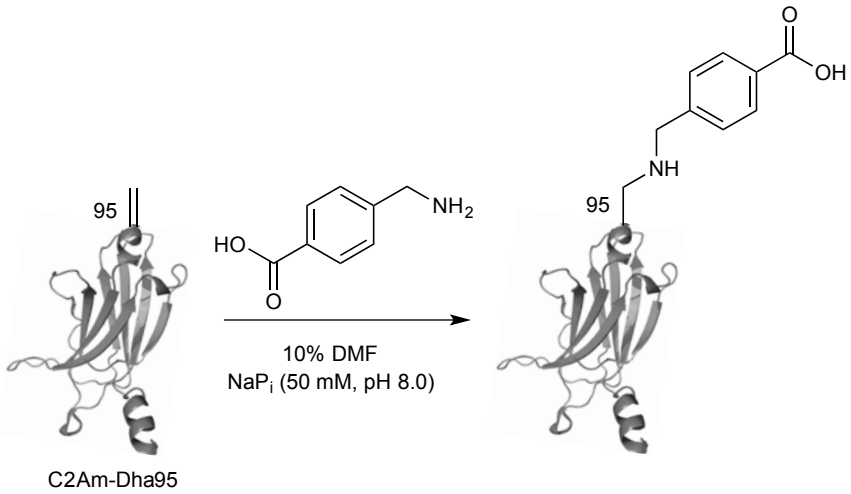

C2Am-Dha95

A 40 µL aliquot of C2Am-Dha95 (6.09 µM, 244 pmol) in 50 mM sodium phosphate buffer at pH 8.0 was thawed. 4-(Aminomethyl)benzoic acid (0.36 mg dissolved in 4 µL of DMF, 2.4 µmol) was added at 37 ºC and the resulting mixture vortexed for 30 seconds. Time points were taken by aliquoting 5 µL of the reaction mixture and diluting it with 5 µL of 50 mM sodium phosphate buffer at pH 8.0. 10 µL of this diluted sample was injected for LC–MS analysis. Full conversion was observed after incubating for 48 h at 37 ºC (calculated mass, 16339, observed mass, 16340).

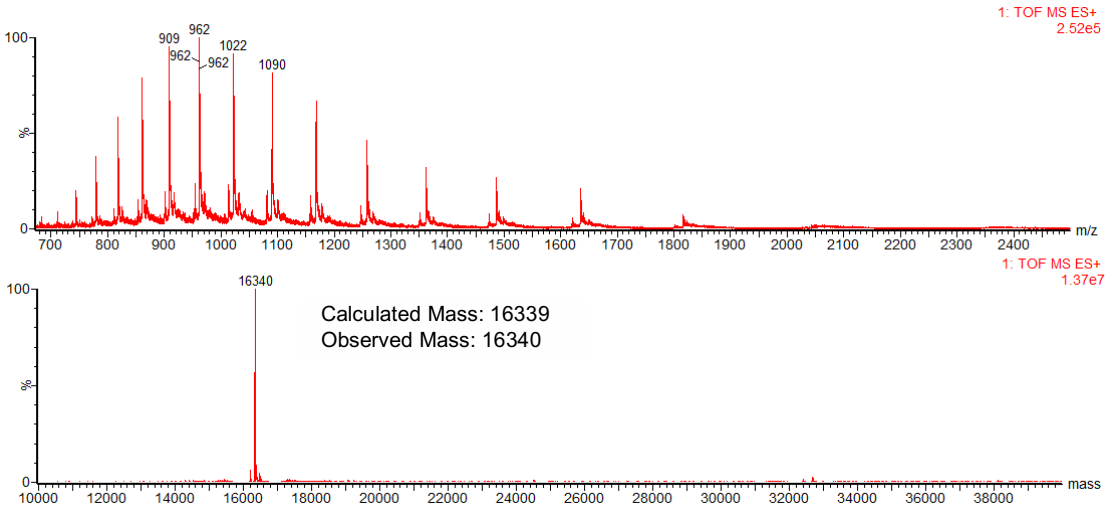

Figure S20. ESI–MS of the reaction of C2Am-Dha95 with 4-(aminomethyl)benzoic acid (58.5 mM) after 48 h at 37 ºC.

4-Bromobenzylamine

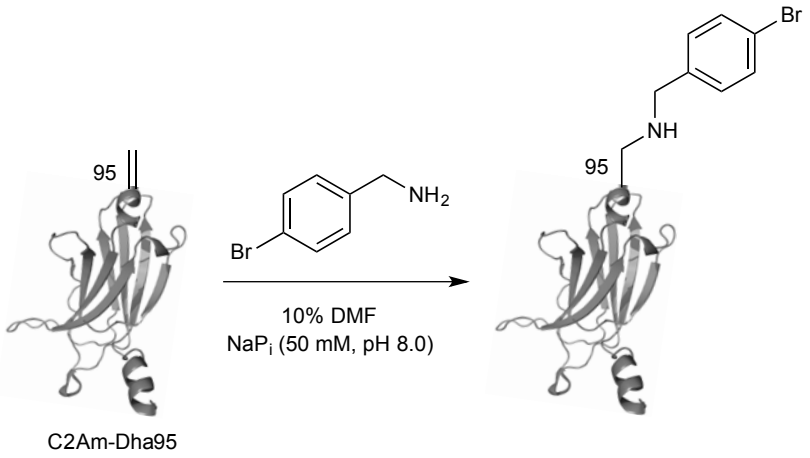

C2Am-Dha95

A 40 µL aliquot of C2Am-Dha95 (6.09 µM, 244 pmol) in 50 mM sodium phosphate buffer at pH 8.0 was thawed. 4-Bromobenzylamine (0.45 mg dissolved in 4 µL of DMF, 2.4 µmol) was added at 37 ºC and the resulting mixture vortexed for 30 seconds. Time points were taken by aliquoting 5 µL of the reaction mixture and diluting it with 5 µL of 50 mM sodium phosphate buffer at pH 8.0. 10 µL of this diluted sample was injected for LC–MS analysis. 65% conversion was observed after incubating for 24 h at 37 ºC (calculated mass, 16373, observed mass, 16374).

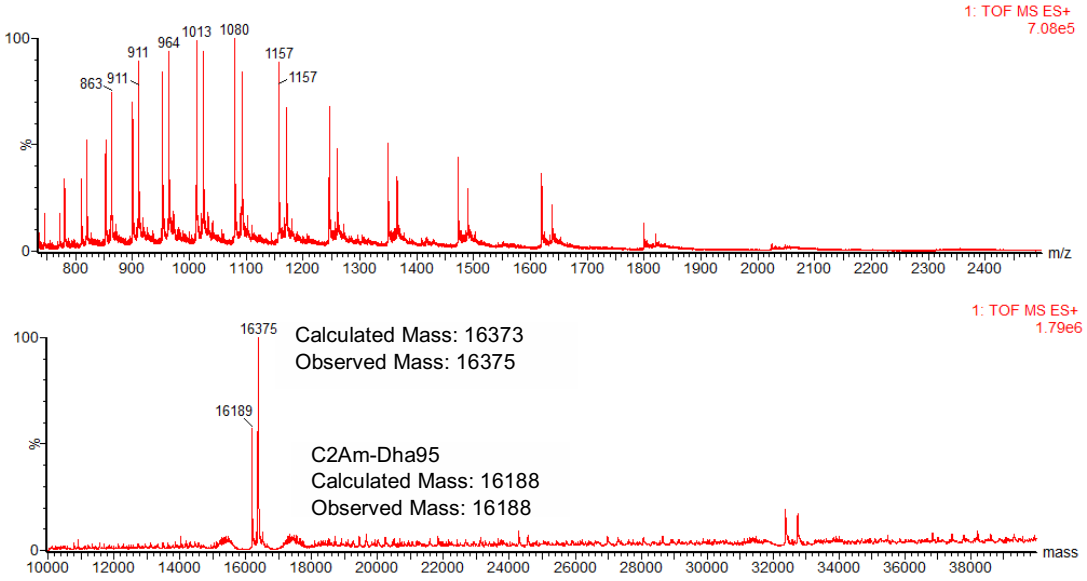

Figure S21. ESI–MS of the reaction of C2Am-Dha95 with 4-bromobenzylamine (58.5 mM) after 24 h at 37 ºC.

2-Phenylethylamine

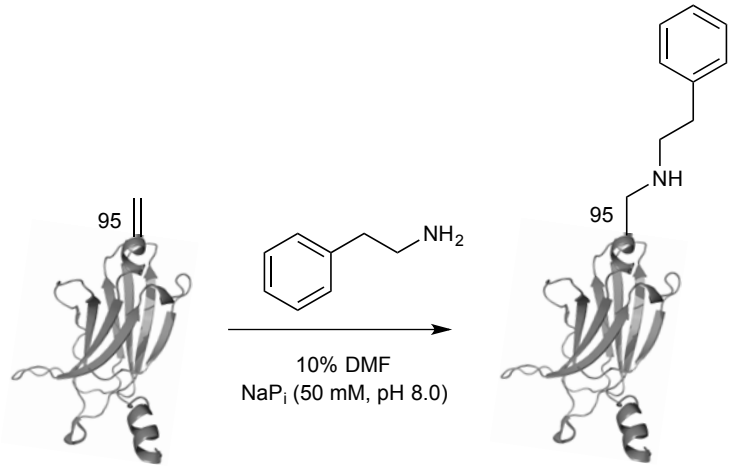

C2Am-Dha95

A 40 µL aliquot of C2Am-Dha95 (6.09 µM, 244 pmol) in 50 mM sodium phosphate buffer at pH 8.0 was thawed. 2-Phenylethylamine (0.3 µL dissolved in 4 µL of DMF, 2.4 µmol) was added at 37 ºC and the resulting mixture vortexed for 30 seconds. The reaction progress was monitored by LC–MS with a time point taken after 48 h. Time points were taken by aliquoting 5 µL of the reaction mixture and diluting it with 5 µL of 50 mM sodium phosphate buffer at pH 8.0. 10 µL of this diluted sample was injected for LC–MS analysis. 70% conversion was observed after 48 h (calculated mass, 16309, observed mass, 16311).

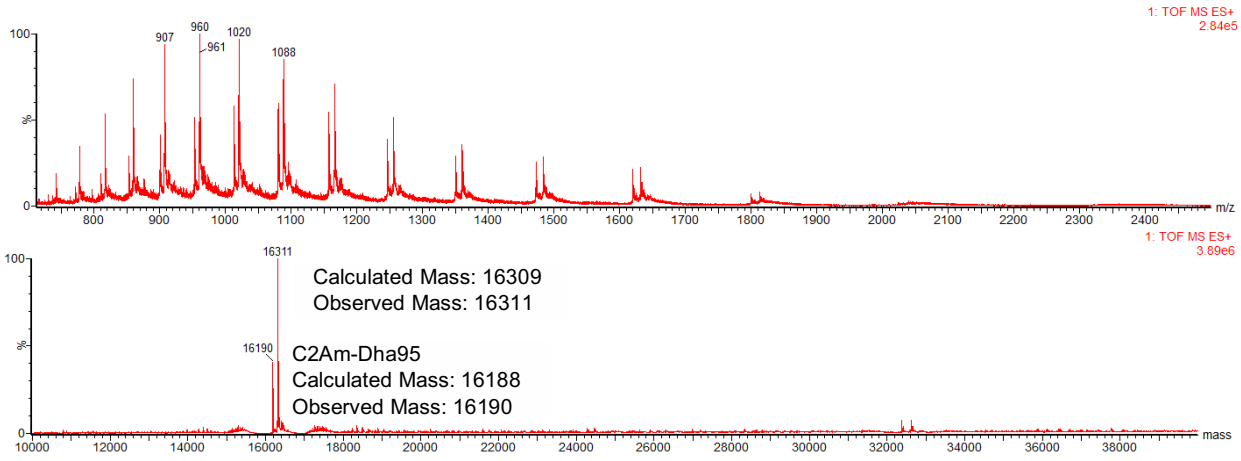

Figure S22. ESI–MS of the reaction of C2Am-Dha95 with 2-phenylethylamine (60.8 mM) after 48 h at 37 ºC.

Cyclohexylmethylamine

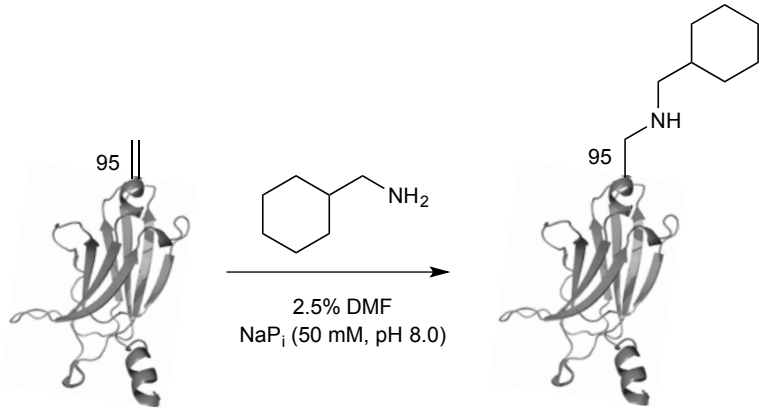

C2Am-Dha95

A 40 µL aliquot of C2Am-Dha95 (6.09 µM, 244 pmol) in 50 mM sodium phosphate buffer at pH 8.0 was thawed. Cyclohexylmethylamine (0.02 µL dissolved in 1µL of DMF, 0.219 µmol) was added at room temperature and the resulting mixture vortexed for 30 seconds. The reaction progress was monitored by LC–MS with time points taken after 1, 2 and 3 h. Time points were taken by aliquoting 2.5 µL of the reaction mixture and diluting it with 8 µL of 50 mM sodium phosphate buffer at pH 8.0. 10 µL of this diluted sample was injected for LC–MS analysis. 67% conversion to the expected product was observed after 1 h, >95% conversion after 2 h and full conversion observed after 3 h (calculated mass, 16301, observed mass, 16301).

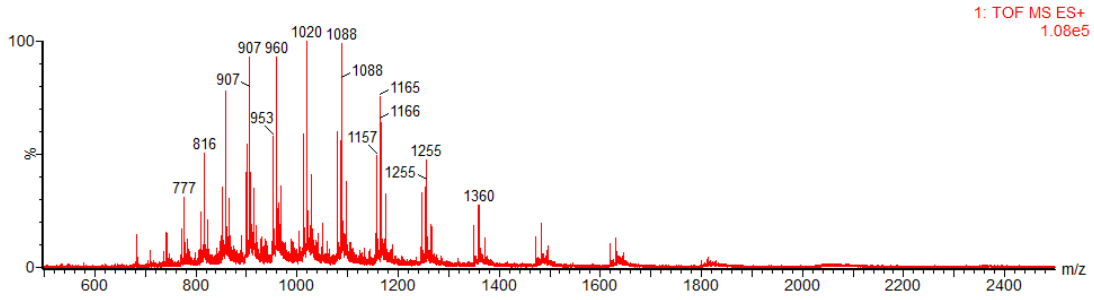

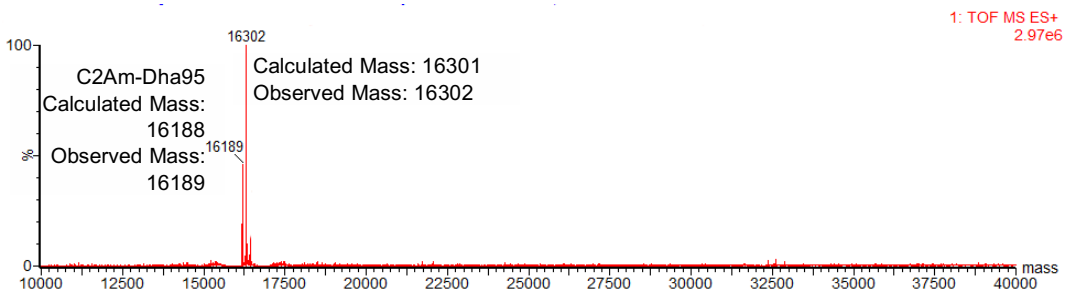

Figure S23. ESI–MS of the reaction of C2Am-Dha95 with cyclohexylmethylamine (5.5 mM) after 1 h at room temperature.

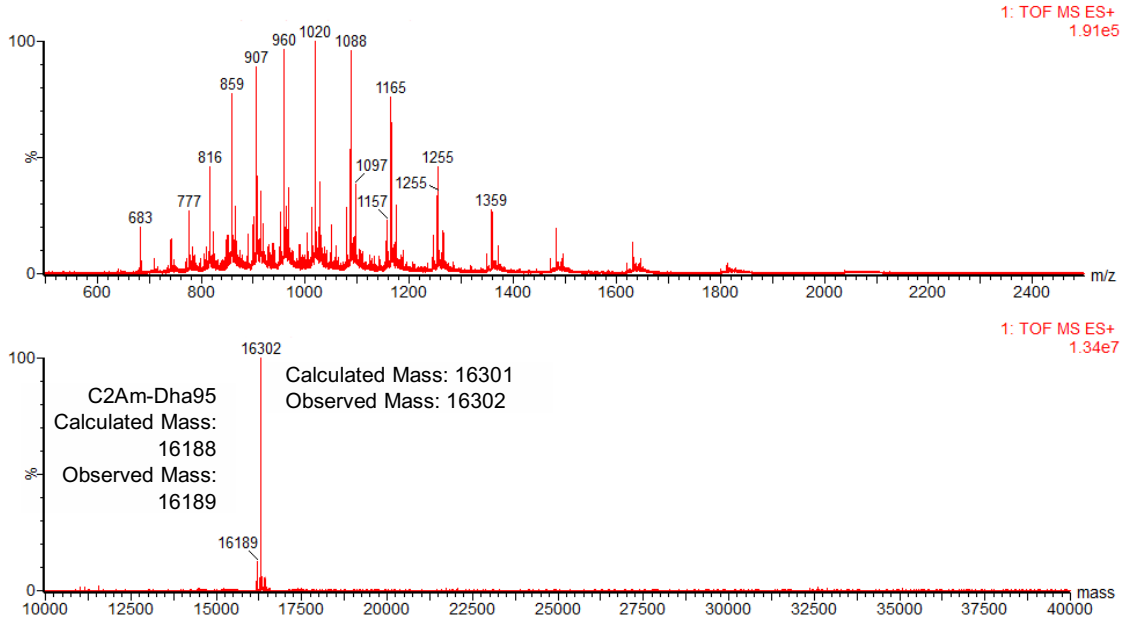

Figure S24. ESI–MS of the reaction of C2Am-Dha95 with cyclohexylmethylamine (5.5 mM) after 2 h at room temperature.

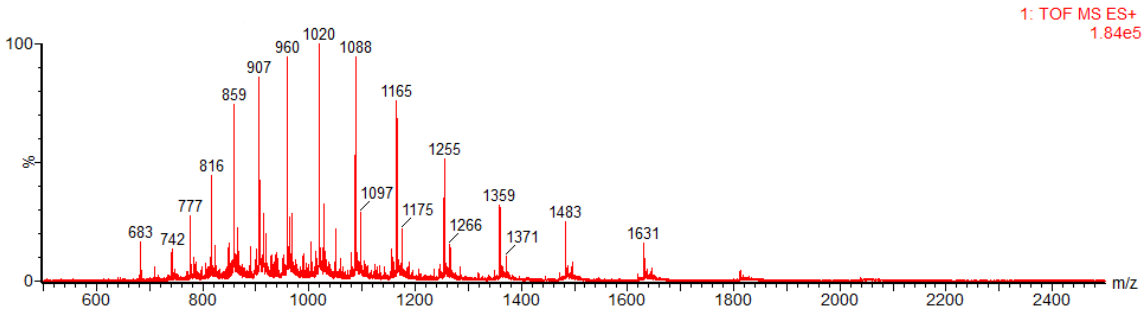

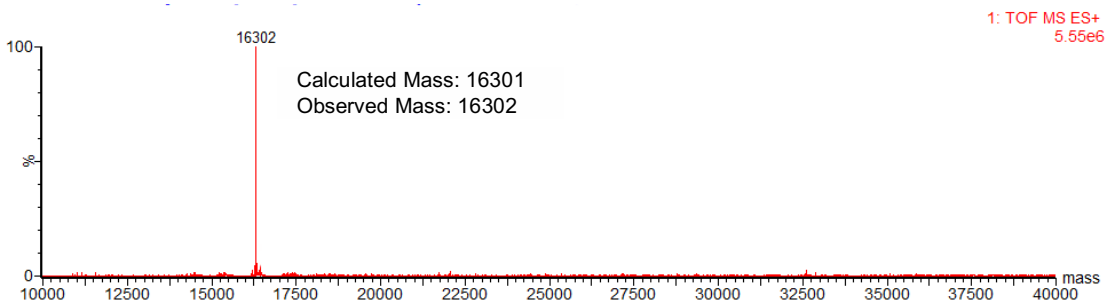

Figure S25. ESI–MS of the reaction of C2Am-Dha95 with cyclohexylmethylamine (5.5 mM) after 3 h at room temperature.

4-(Aminomethyl)cyclohexanecarboxylic acid

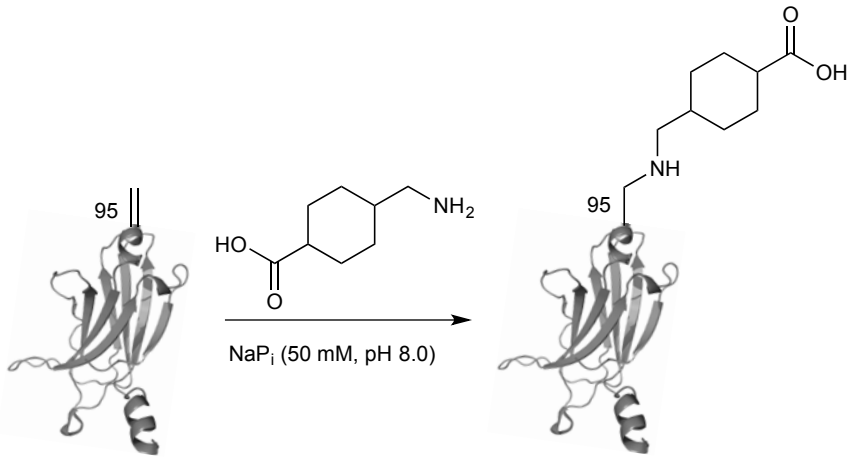

C2Am-Dha95

A 40 µL aliquot of C2Am-Dha95 (6.09 µM, 244 pmol) in 50 mM sodium phosphate buffer at pH 8.0 was thawed. 4-(Aminomethyl)cyclohexanecarboxylic Acid (0.35 mg dissolved in 35 µL of sodium phosphate buffer at pH 8.0, 2.2 µM) was added at 37 ºC and the resulting mixture vortexed for 30 seconds. Time points were taken by aliquoting 5 µL of the reaction mixture and diluting it with 5 µL of 50 mM sodium phosphate buffer at pH 8.0. 10 µL of this diluted sample was injected for LC–MS analysis. Complete conversion was observed after 24 h (calculated mass, 16345, observed mass, 16346).

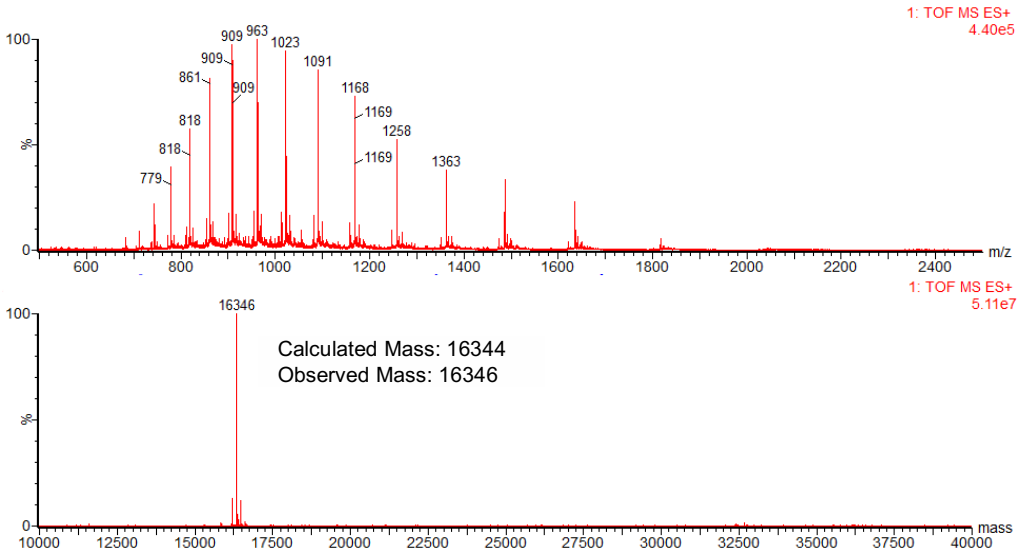

Figure S26. ESI–MS spectrum of the reaction of C2Am-Dha95 with 4-(aminomethyl)cyclohexanecarboxylic acid (29.6 mM) after 24 h at 37 ºC

Imidazole

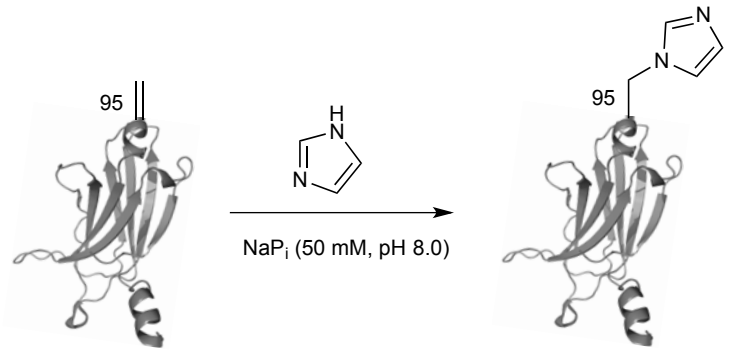

C2Am-Dha95

A 25 µL aliquot of C2Am-Dha95 (6.09 µM, 244 pmol) in 50 mM sodium phosphate buffer at pH 8.0 was thawed. Imidazole (0.23 mg, 3.45 µmol) was added at room temperature and the resulting mixture vortexed for 30 seconds. After additional mixing overnight at 37 ºC, a 2.5 µL aliquot of the reaction mixture was analysed by LC–MS (2.5 µL aliquot diluted by 8 µL of 50 mM sodium phosphate buffer at pH 8.0). 90% conversion to the expected adduct was observed after 16 h (expected mass, 16256, observed mass, 16257).

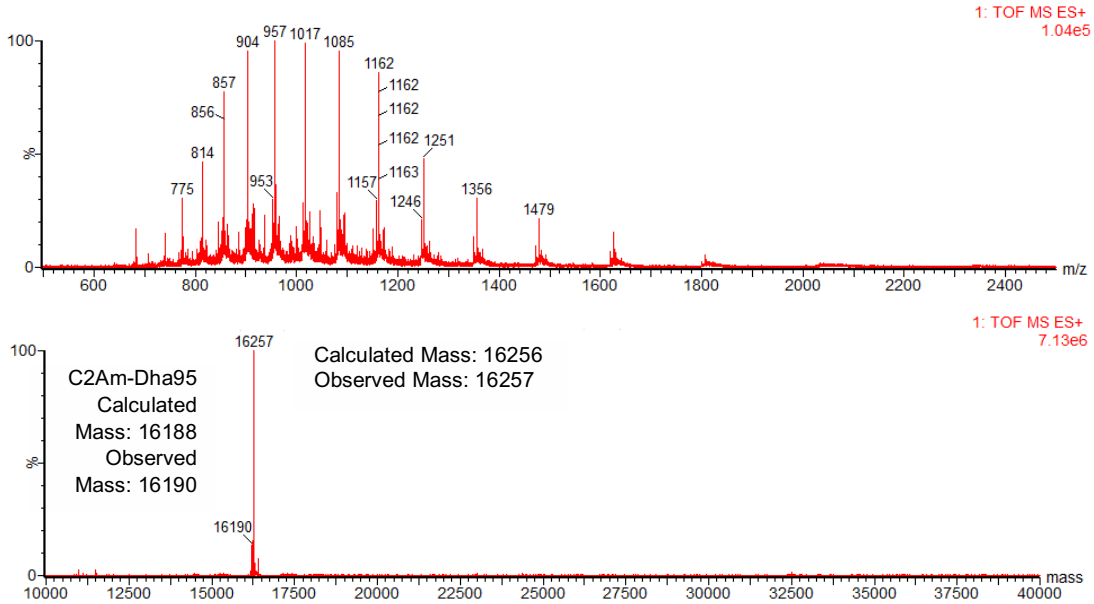

Figure S27. ESI–MS of the reaction of C2Am-Dha95 with imidazole (138 mM) after 16 h at 37 ºC.

Histamine

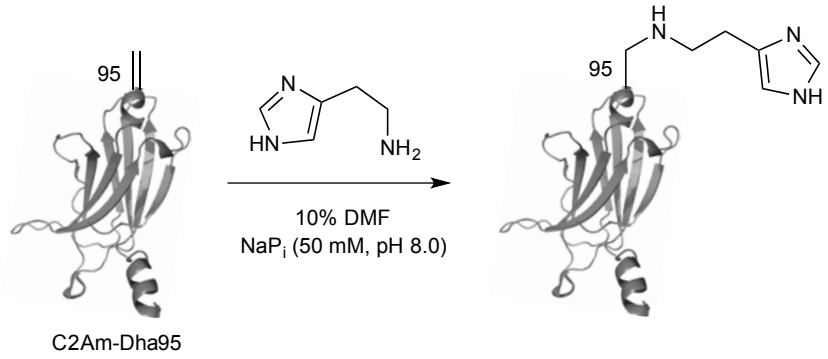

C2Am-Dha95

A 40 µL aliquot of C2Am-Dha95 (6.09 µM, 244 pmol) in 50 mM sodium phosphate buffer at pH 8.0 was thawed. Histamine (0.27 mg dissolved in 4 µL of DMF, 2.4 µmol) was added at 37 ºC and the resulting mixture vortexed for 30 seconds. The reaction progress was monitored by LC–MS with a time point taken after 24 h. Time points were taken by aliquoting 5 µL of the reaction mixture and diluting it with 5 µL of 50 mM sodium phosphate buffer at pH 8.0. 10 µL of this diluted sample was injected for LC–MS analysis. Full conversion was observed after 24 h (calculated mass, 16299, observed mass, 16300).

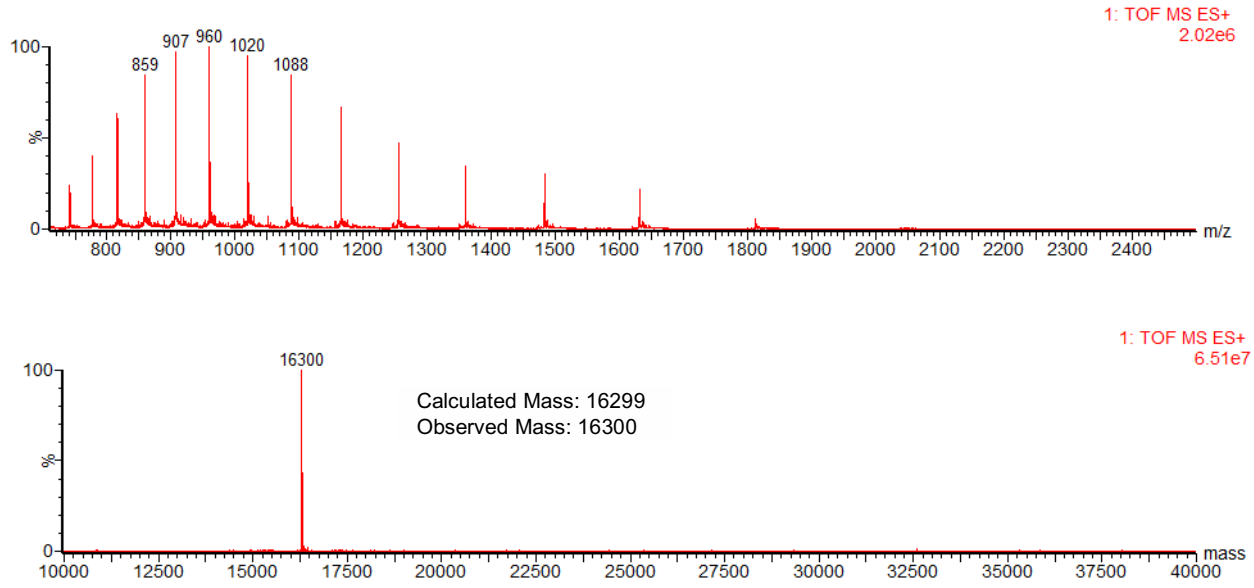

Figure S28. ESI–MS of the reaction of C2Am-Dha95 with histamine (60.8 mM) after 24 h at 37 ºC.

Cyclopentylamine

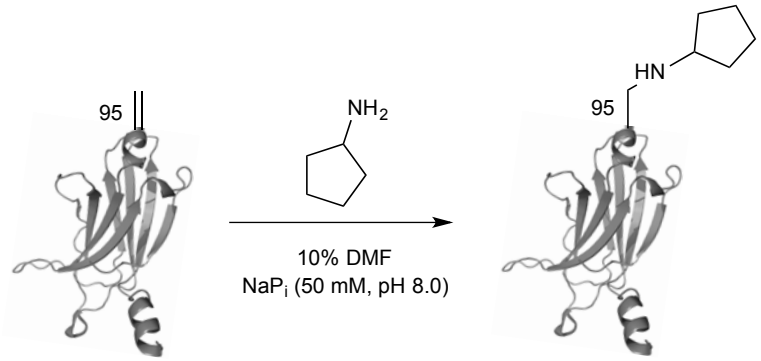

C2Am-Dha95

A 40 µL aliquot of C2Am-Dha95 (6.09 µM, 244 pmol) in 50 mM sodium phosphate buffer at pH 8.0 was thawed. Cyclopentylamine (0.24 µL dissolved in 4 µL of DMF, 2.4 µmol) was added at 37 ºC and the resulting mixture vortexed for 30 seconds. The reaction progress was monitored by LC–MS with a time point taken after 24 h. Time points were taken by aliquoting 5 µL of the reaction mixture and diluting it with 5 µL of 50 mM sodium phosphate buffer at pH 8.0. 10 µL of this diluted sample was injected for LC–MS analysis. 20% conversion was observed after 24 h (calculated mass, 16273, observed mass, 16274).

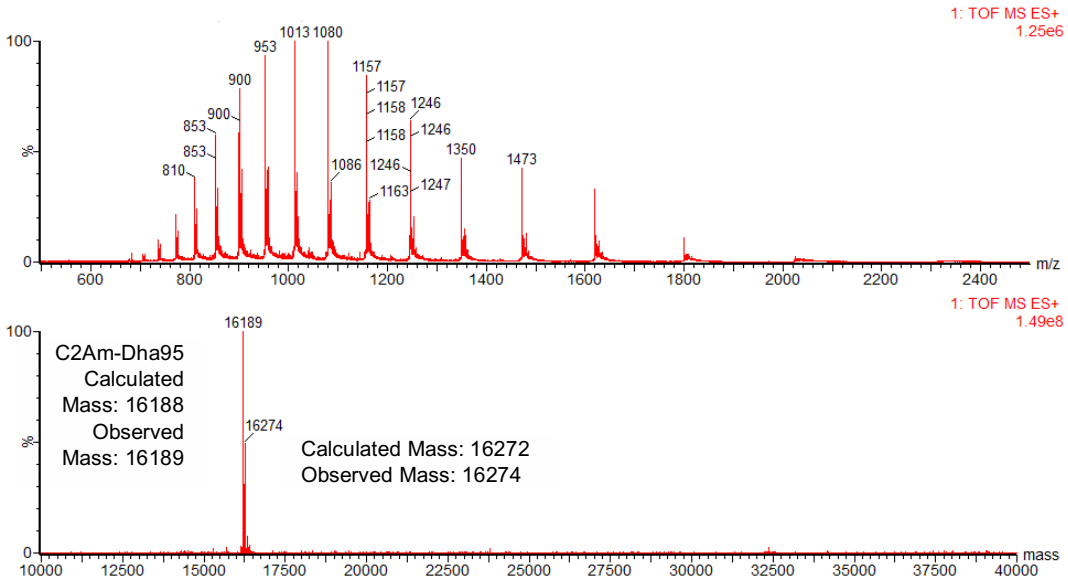

Figure S29. ESI–MS of the reaction of C2Am-Dha95 with cyclopentylamine (60.9 mM) after 24 h at 37 ºC.

Allyl amine

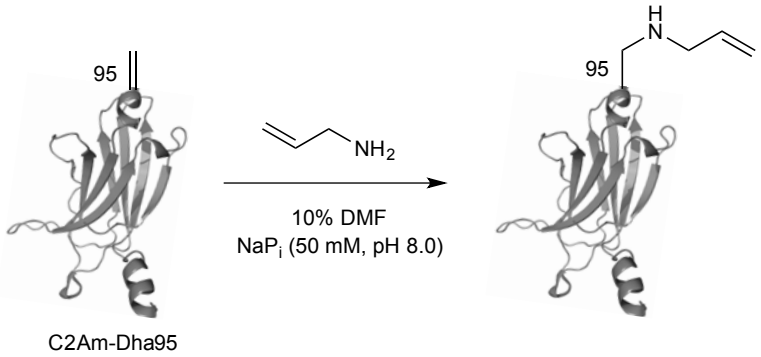

C2Am-Dha95

A 40 µL aliquot of C2Am-Dha95 (6.09 µM, 244 pmol) in 50 mM sodium phosphate buffer at pH 8.0 was thawed. Allyl amine (0.18 µL dissolved in 4 µL of DMF, 2.0 µmol) was added at 37 ºC and the resulting mixture vortexed for 30 seconds. The reaction progress was monitored by LC–MS with a time point taken after 24 h. Time points were taken by aliquoting 5 µL of the reaction mixture and diluting it with 5 µL of 50 mM sodium phosphate buffer at pH 8.0. 10 µL of this diluted sample was injected for LC–MS analysis. 40% conversion was observed after 24 h (calculated mass, 16245, observed mass, 16246).

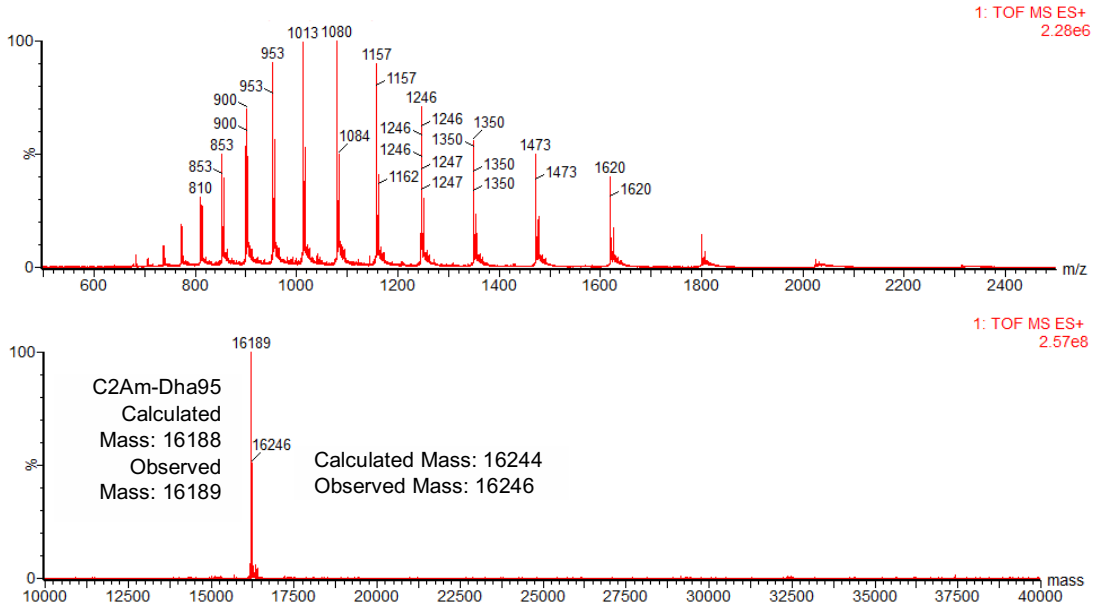

Figure S30. ESI–MS of the reaction of C2Am-Dha95 with allyl amine (50.1 mM) after 24 h at 37 ºC.

Propargyl amine

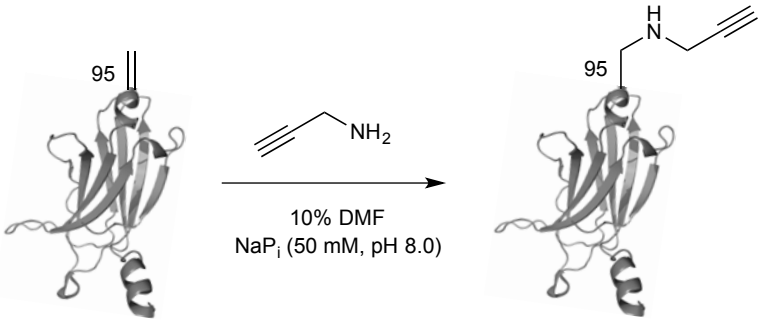

C2Am-Dha95

A 40 µL aliquot of C2Am-Dha95 (6.09 µM, 244 pmol) in 50 mM sodium phosphate buffer at pH 8.0 was thawed. Propargyl amine (0.016 µL dissolved in 4 µL of DMF, 243 µmol) was added at 37 ºC and the resulting mixture vortexed for 30 seconds. The reaction progress was monitored by LC–MS with a time point taken after 24 h. Time points were taken by aliquoting 5 µL of the reaction mixture and diluting it with 5 µL of 50 mM sodium phosphate buffer at pH 8.0. 10 µL of this diluted sample was injected for LC–MS analysis. 50% conversion was observed after 24 h (calculated mass, 16243, observed mass, 16244).

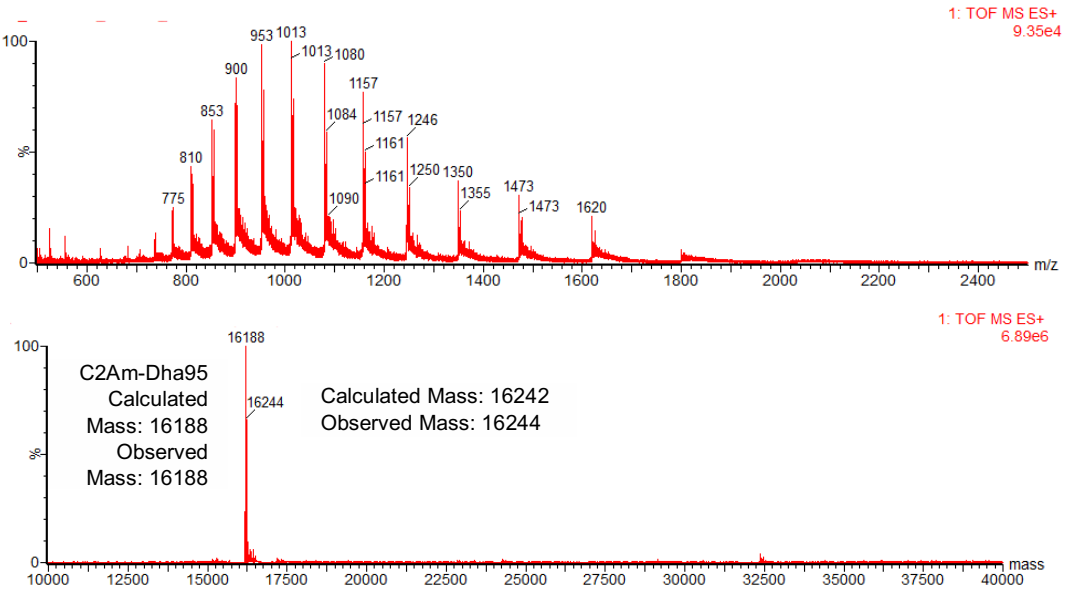

Figure S31. ESI–MS of the reaction of C2Am-Dha95 with propargyl amine (6.08 mM) after 24 h at 37 ºC.

Ethanolamine

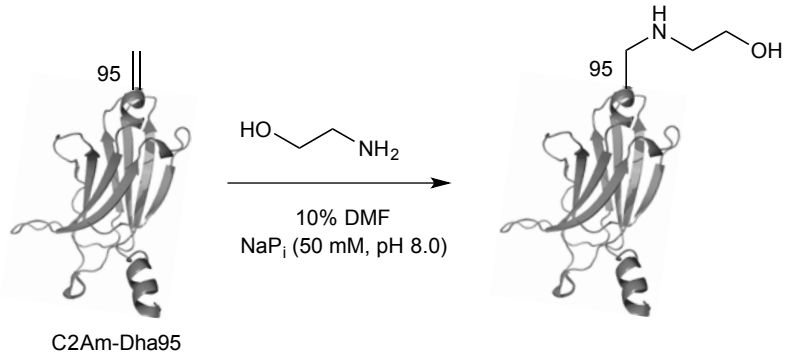

C2Am-Dha95

A 40 µL aliquot of C2Am-Dha95 (6.09 µM, 244 pmol) in 50 mM sodium phosphate buffer at pH 8.0 was thawed. Ethanolamine (0.147 µL dissolved in 4 µL of DMF, 2.4 µmol) was added at 37 ºC and the resulting mixture vortexed for 30 seconds. The reaction progress was monitored by LC–MS with a time point taken after 24 h. Time points were taken by aliquoting 5 µL of the reaction mixture and diluting it with 5 µL of 50 mM sodium phosphate buffer at pH 8.0. 10 µL of this diluted sample was injected for LC–MS analysis. 50% conversion was observed after 24 h (calculated mass, 16249, observed mass, 16250).

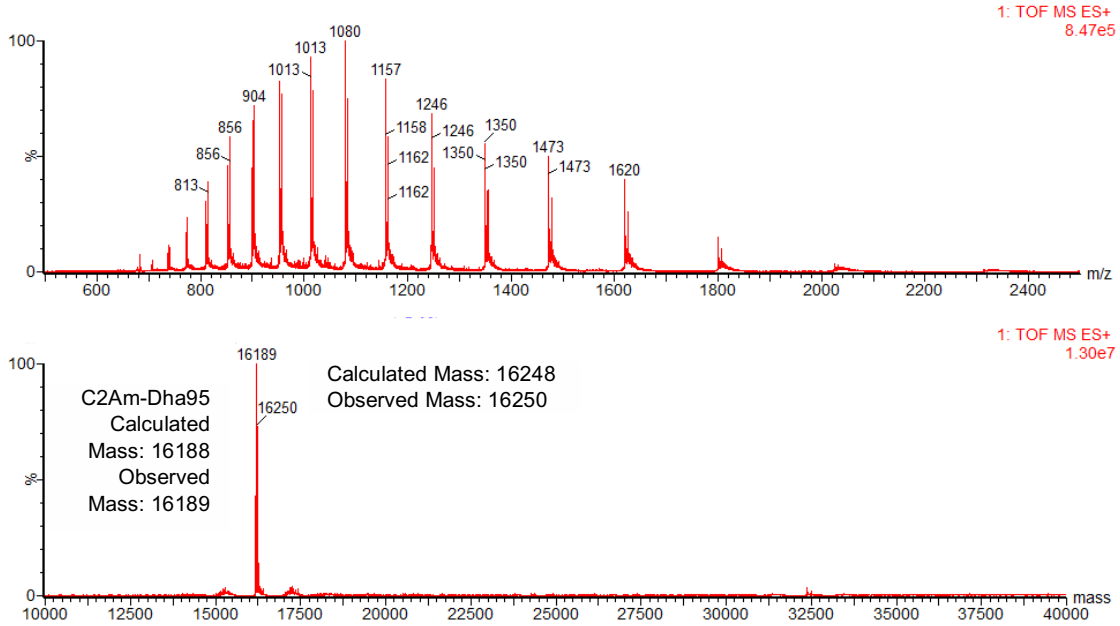

Figure S32. ESI–MS of the reaction of C2Am-Dha95 with ethanolamine (60.8 mM) after 24 h at 37 ºC.

Ethylene diamine

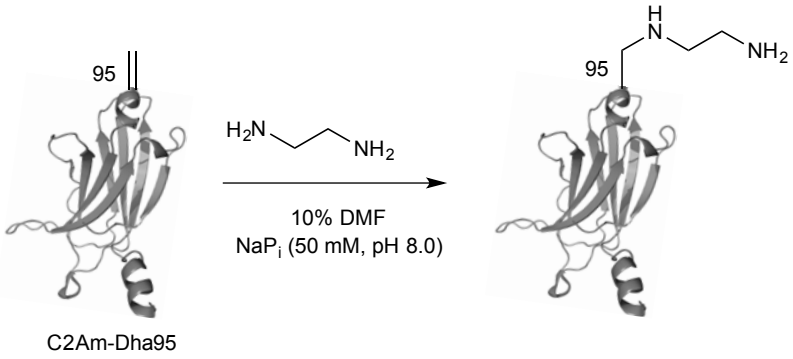

C2Am-Dha95

A 40 µL aliquot of C2Am-Dha95 (6.09 µM, 244 pmol) in 50 mM sodium phosphate buffer at pH 8.0 was thawed. Ethylene diamine (0.163 µL dissolved in 4 µL of DMF, 2.4 µmol) was added at 37 ºC and the resulting mixture vortexed for 30 seconds. The reaction progress was monitored by LC–MS with a time point taken after 24 h. Time points were taken by aliquoting 5 µL of the reaction mixture and diluting it with 5 µL of 50 mM sodium phosphate buffer at pH 8.0. 10 µL of this diluted sample was injected for LC–MS analysis. 60% conversion was observed after 24 h (calculated mass, 16248, observed mass, 16249).

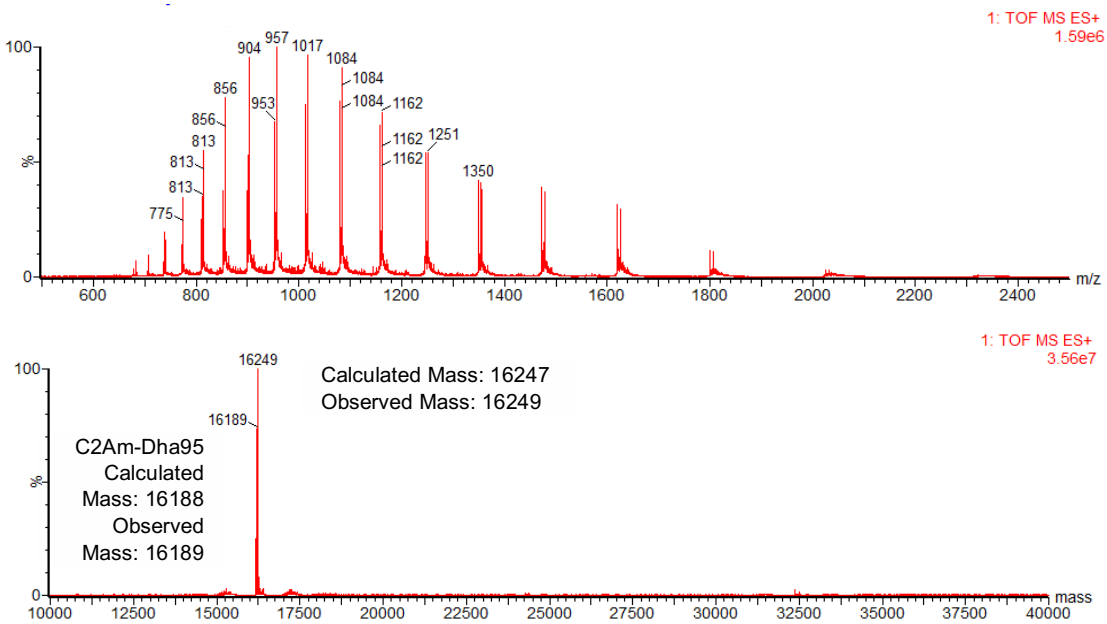

Figure S33. ESI–MS of the reaction of C2Am-Dha95 with ethylene diamine (61.1 mM) after 24 h at 37 ºC.

Tetraethylene glycol monoamine

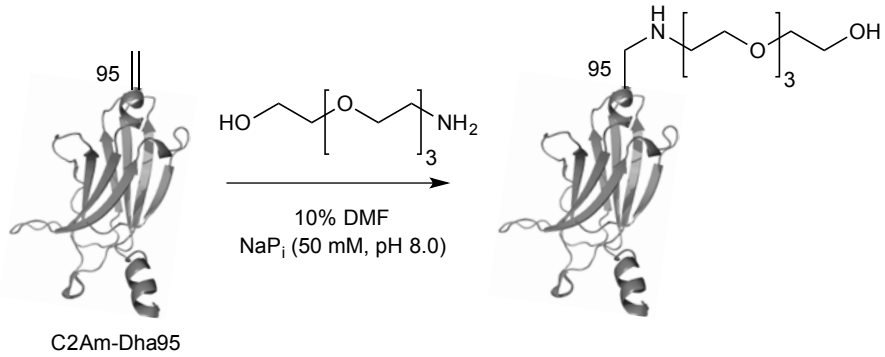

C2Am-Dha95

A 40 µL aliquot of C2Am-Dha95 (6.09 µM, 244 pmol) in 50 mM sodium phosphate buffer at pH 8.0 was thawed. Tetraethylene glycol (0.47 µL dissolved in 4 µL of DMF, 2.4 µmol) was added at 37 ºC and the resulting mixture vortexed for 30 seconds. The reaction progress was monitored by LC–MS with a time point taken after 24 h. Time points were taken by aliquoting 5 µL of the reaction mixture and diluting it with 5 µL of 50 mM sodium phosphate buffer at pH 8.0. 10 µL of this diluted sample was injected for LC–MS analysis. 40% conversion was observed after 24 h (calculated mass, 16381, observed mass, 16382).

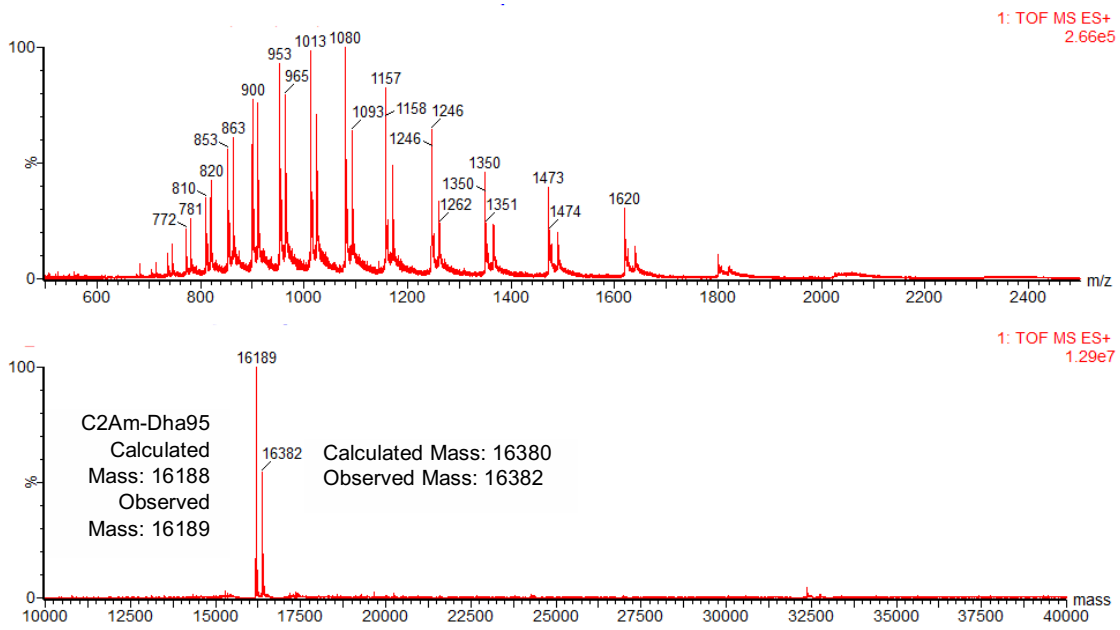

Figure S34. ESI–MS of the reaction of C2Am-Dha95 with tetraethylene glycol monoamine (60.9 mM) after 24 h at 37 ºC

N-Boc-1,6-hexanediamine

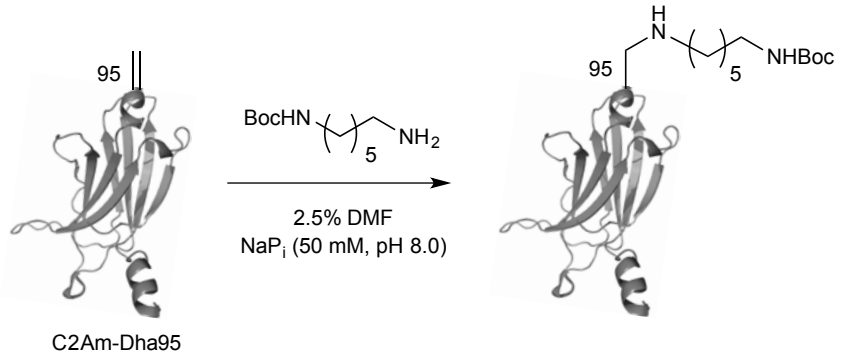

C2Am-Dha95

A 25 µL aliquot of C2Am-Dha95 (6.09 µM, 244 pmol) in 50 mM sodium phosphate buffer at pH 8.0 was thawed. *N*-Boc-1,6-hexanediamine (0.024 mg dissolved in 0.6 µL of DMF, 0.12 µmol) was added at room temperature and the resulting mixture vortexed for 30 seconds. After shaking for 3 h at room temperature, the temperature of the reaction mixture was raised to 37 ºC and was allowed to shake for 3 additional h. The reaction progress was monitored by LC–MS with time points taken after 3, 4 and 6 h. Time points were taken by aliquoting 2.5 µL of the reaction mixture and diluting it with 8 µL of 50 mM sodium phosphate buffer at pH 8.0. 10 µL of this diluted sample was injected. 65% conversion to the expected adduct was observed after 3 h at room temperature and 3 h at 37 ºC (calculated mass, 16404, observed mass, 16404).

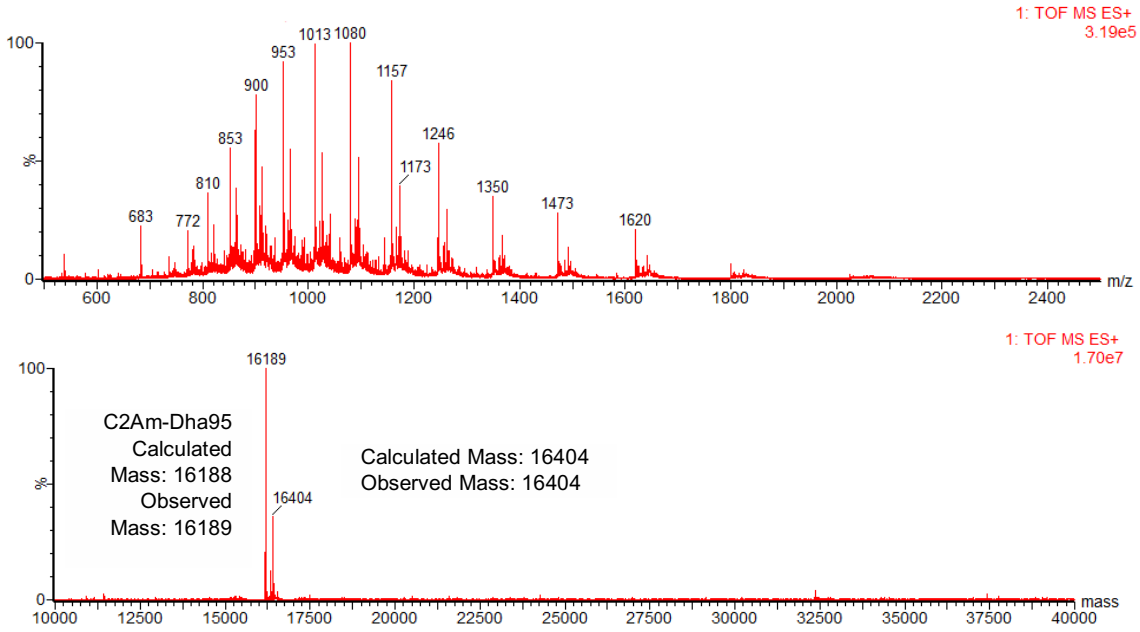

Figure S35. ESI–MS of the reaction of C2Am-Dha95 with *N*-Boc-1,6-hexanediamine (4.2 mM) after 3 h at room temperature.

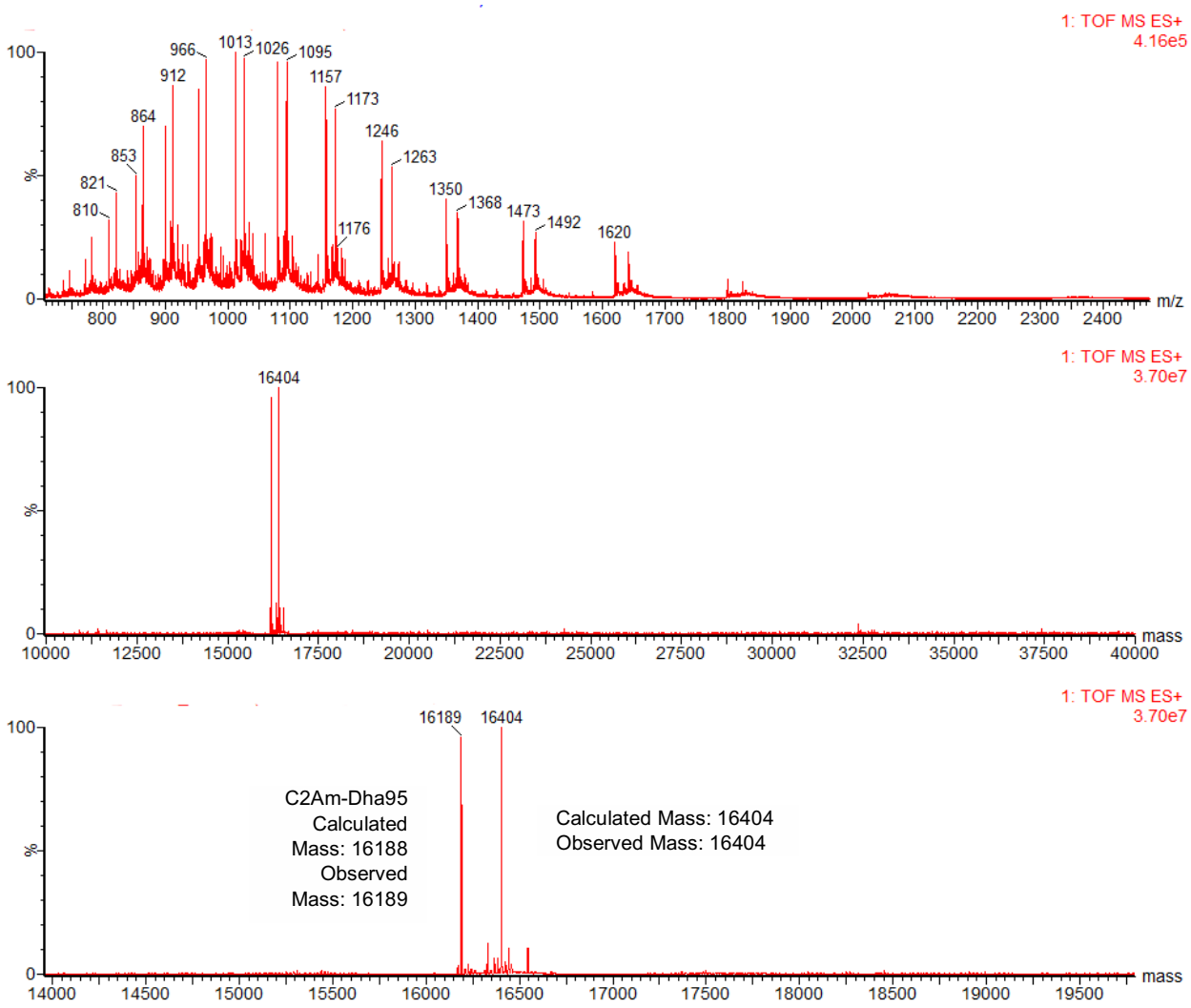

Figure S36. ESI–MS of the reaction of C2Am-Dha95 with *N*-Boc-1,6-hexanediamine (4.2 mM) after 3 h at room temperature and 1 h at 37 ºC.

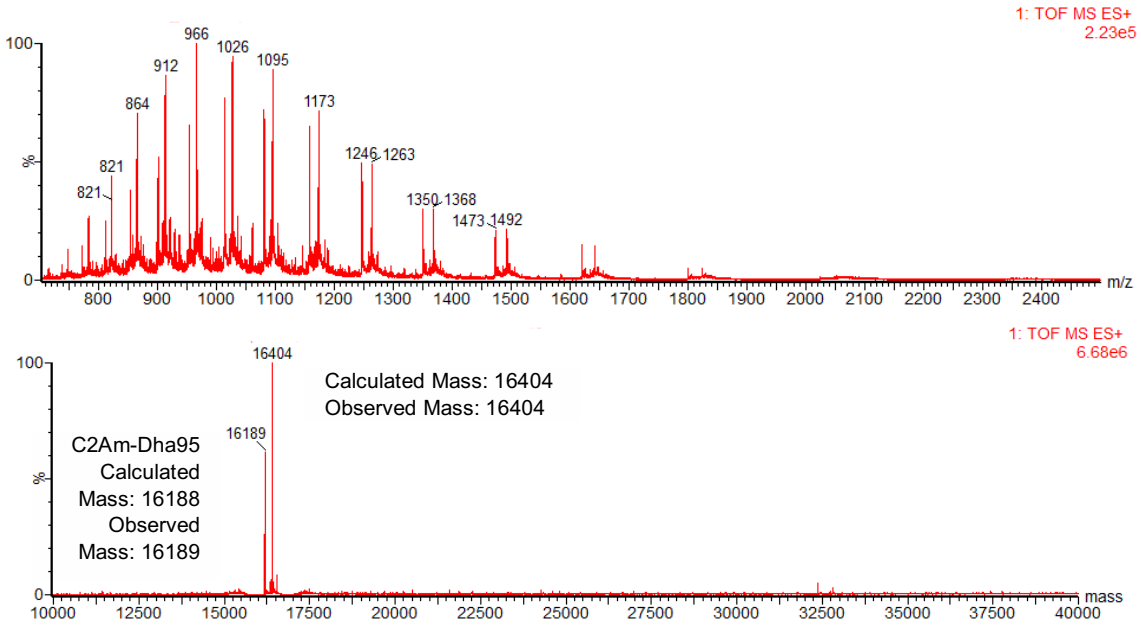

Figure S37. ESI–MS spectrum of the reaction of C2Am-Dha95 with *N*-Boc-1,6-hexanediamine (4.2 mM) after 3 h at room temperature and 3 h at 37 ºC.

4-Aminobutyl β-D-galactopyranoside 22

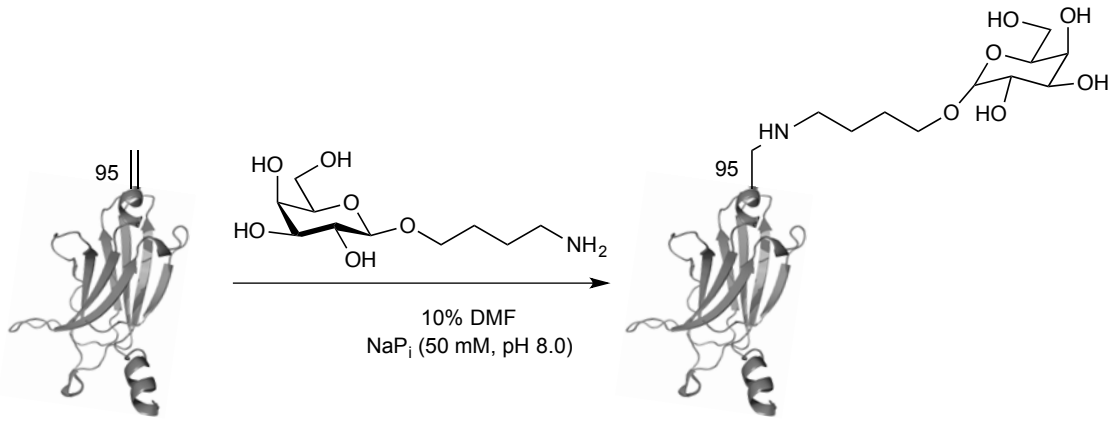

C2Am-Dha95

A 10 µL aliquot of C2Am-Dha95 (6.09 µM, 244 pmol) in 50 mM sodium phosphate buffer at pH 8.0 was thawed. 4-Aminobutyl β-D-galactopyranoside **22** (0.18 mg dissolved in 1.2 µL of DMF, 0.69 µmol) was added at 37 ºC and the resulting mixture vortexed for 30 seconds. After 30 h of additional shaking at room temperature, a 2.5 µL aliquot was analysed by LC–MS (2.5 µL aliquot diluted by 8 µL of 50 mM sodium phosphate buffer at pH 8.0) and complete conversion to the expected product was observed (calculated mass, 16439; observed mass, 16440).

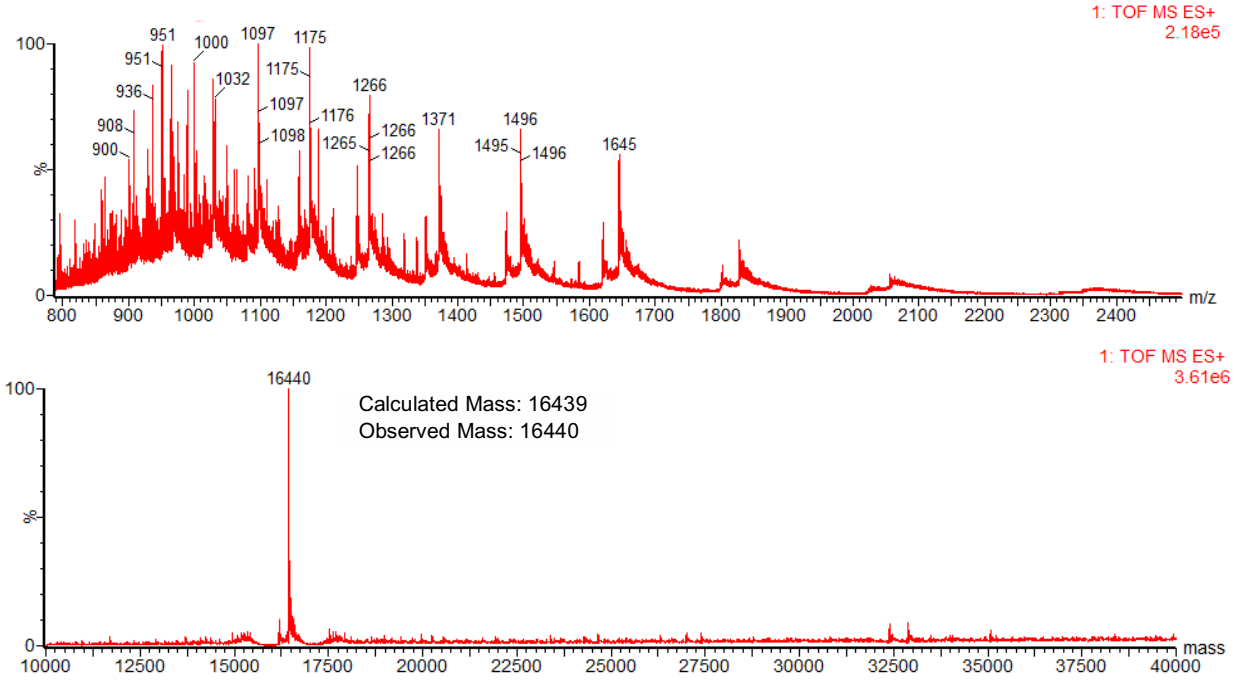

Figure S38. ESI–MS spectrum of the reaction of C2Am-Dha95 with **22** (61 mM) after 30 h at 37 ºC.

Piperidine 23

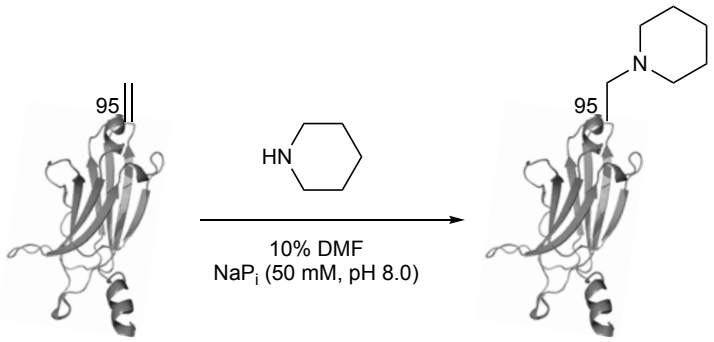

C2Am-Dha95

A 40 μL aliquot of C2Am–Dha95 (6.09 μM, 244 pmol) in 50 mM sodium phosphate buffer at pH 8.0 was thawed. Piperidine (0.30 μL of a 240 mM solution in DMF, 1.8 mM) was added at room temperature and the resulting mixture vortexed for 30 seconds. The reaction progress was monitored by LC–MS. After 2 h of additional shaking, small molecules were removed from the reaction mixture by loading the sample onto a Zeba Spin Desalting Column previously equilibrated with 50 mM sodium phosphate buffer at pH 8.0. The sample was eluted via centrifugation (2 min, 1500xg). A 5 μL aliquot was diluted with 5 μL of 50 mM sodium phosphate buffer at pH 8.0 and analysed by LC–MS. Complete conversion to the expected product was observed (calculated mass, 16272, observed mass, 16274).

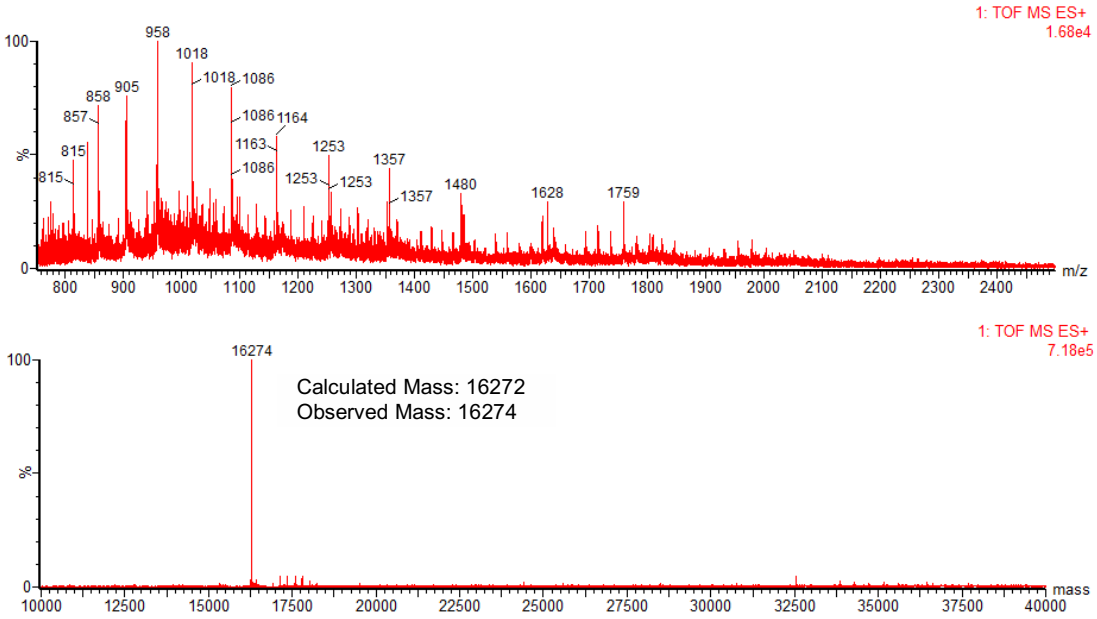

Figure S39. ESI–MS of the reaction of C2Am–Dha95 with piperidine **23** (1.8 mM) after 2 h at 37 ºC.

Stability of C2Am-Piperidine95 in human plasma

A 10 µL aliquot of C2Am-Dha95-Piperidine (20 µM, 200 pmol) in 50 mM sodium phosphate buffer at pH 8.0 was thawed. 1 µL of reconstituted human plasma (*Sigma Aldrich*) was added at room temperature and the resulting mixture vortexed for 30 seconds. The resulting reaction mixture was then shaken at 37 ºC overnight. After 1 and 24 h, a 2.5µL aliquot of each reaction mixture was analysed by LC–MS (2.5 µL aliquot diluted with 8 µL of 50 mM sodium phosphate buffer at pH 8.0). No significant degradation of the C2Am-Piperidine95 adduct was observed at 24 h.

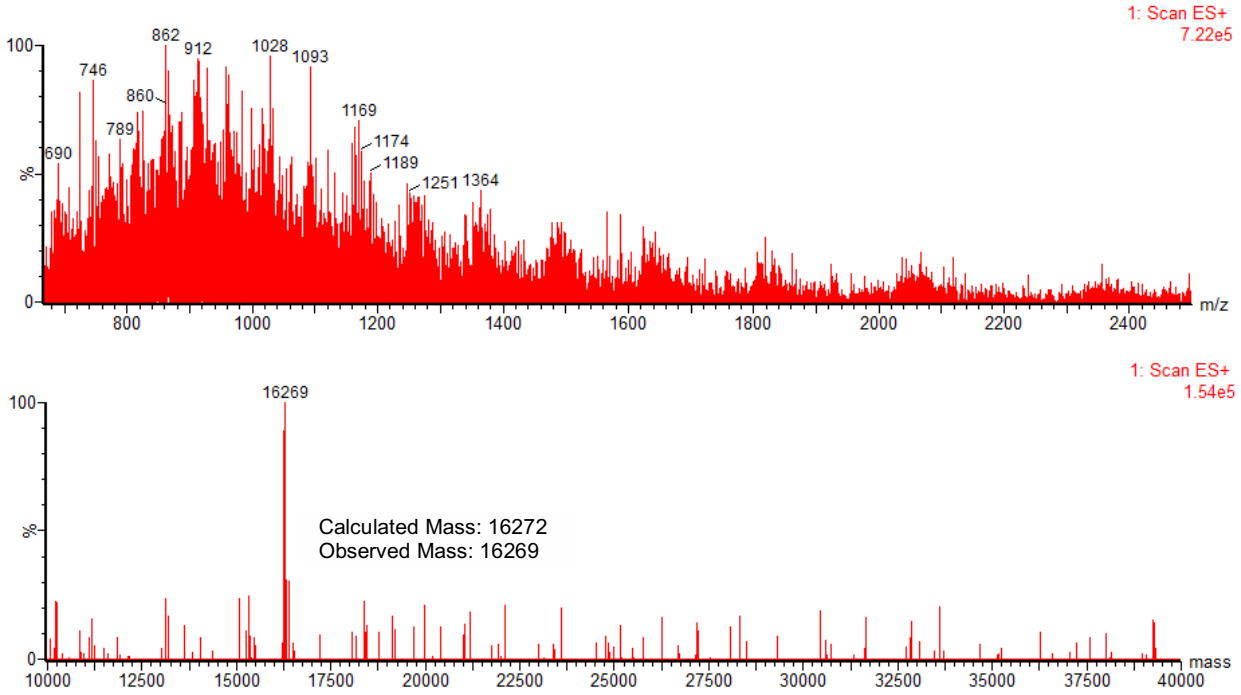

Figure S40. ESI–MS after incubating C2Am-Piperidine95 with human plasma for 24 h at 37 ºC.

Phenylhydroxylamine

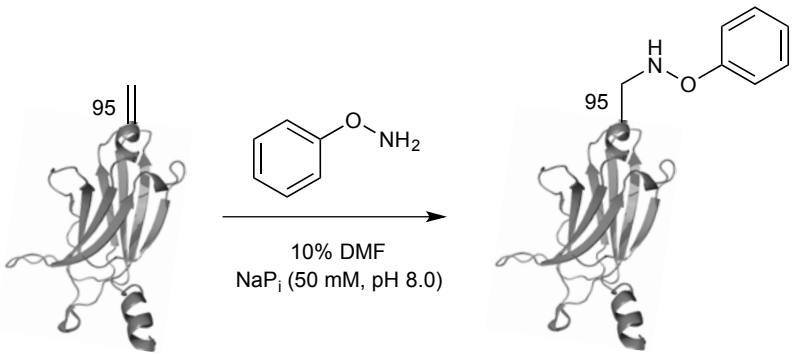

C2Am-Dha95

A 40 µL aliquot of C2Am-Dha95 (6.09 µM, 244 pmol) in 50 mM sodium phosphate buffer at pH 8.0 was thawed. *O*-Phenylhydroxylamine (0.26 mg dissolved in 4 µL of DMF, 2.4 µmol) was added at 37 ºC and the resulting mixture vortexed for 30 seconds. The reaction progress was monitored by LC–MS with a time point taken after 24 h. Time points were taken by aliquoting 5 µL of the reaction mixture and diluting it with 5 µL of 50 mM sodium phosphate buffer at pH 8.0. 10 µL of this diluted sample was injected for LC–MS analysis. >95% conversion was observed after 24 h (calculated mass, 16297, observed mass, 16295).

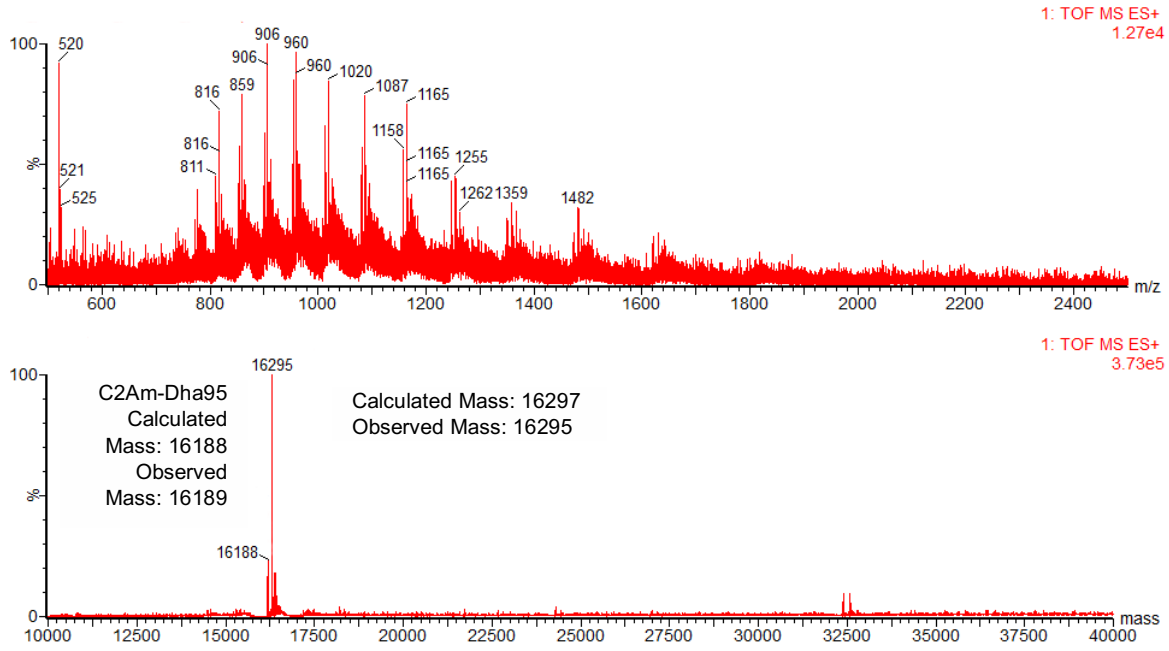

Figure S41. ESI–MS of the reaction of C2Am-Dha95 with phenylhydroxylamine (60.8 mM) after incubating for 24 h at 37 ºC.

Methyl hydrazine

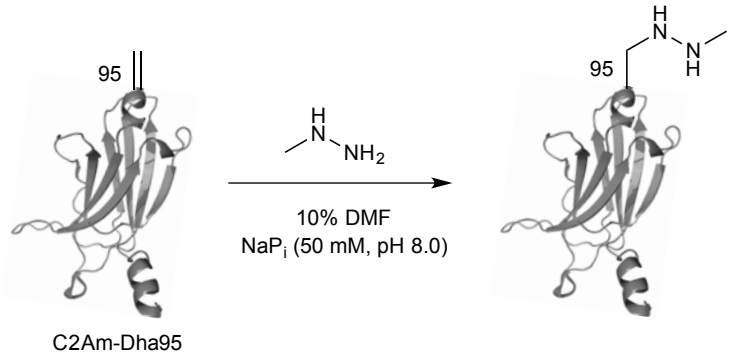

C2Am-Dha95

A 40 µL aliquot of C2Am-Dha95 (6.09 µM, 244 pmol) in 50 mM sodium phosphate buffer at pH 8.0 was thawed. Methyl hydrazine (0.13 µL dissolved in 4 µL of DMF, 2.4 µmol) was added at 37 ºC and the resulting mixture vortexed for 30 seconds. The reaction progress was monitored by LC–MS with a time point taken after 24 h. Time points were taken by aliquoting 5 µL of the reaction mixture and diluting it with 5 µL of 50 mM sodium phosphate buffer at pH 8.0. 10 µL of this diluted sample was injected for LC–MS analysis. >95% conversion was observed after 24 h (calculated mass, 16234, observed mass, 16235).

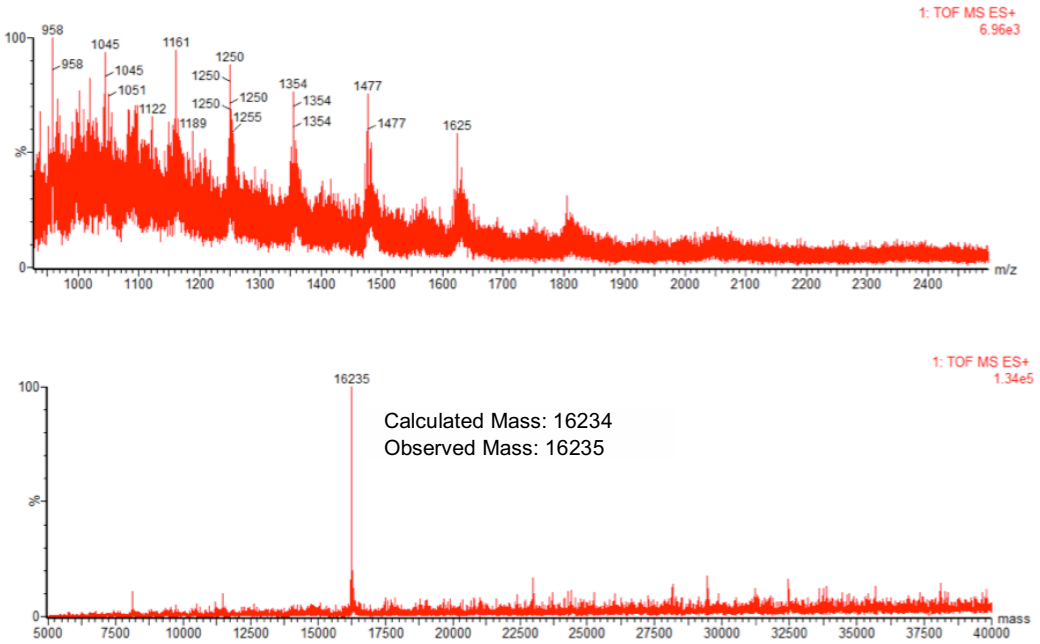

Figure S42. ESI–MS of the reaction of C2Am-Dha95 with methyl hydrazine (62.2 mM) after 24 h at 37 ºC.

Tetraethylene glycol benzylamine 26 addition to C2Am-Dha95

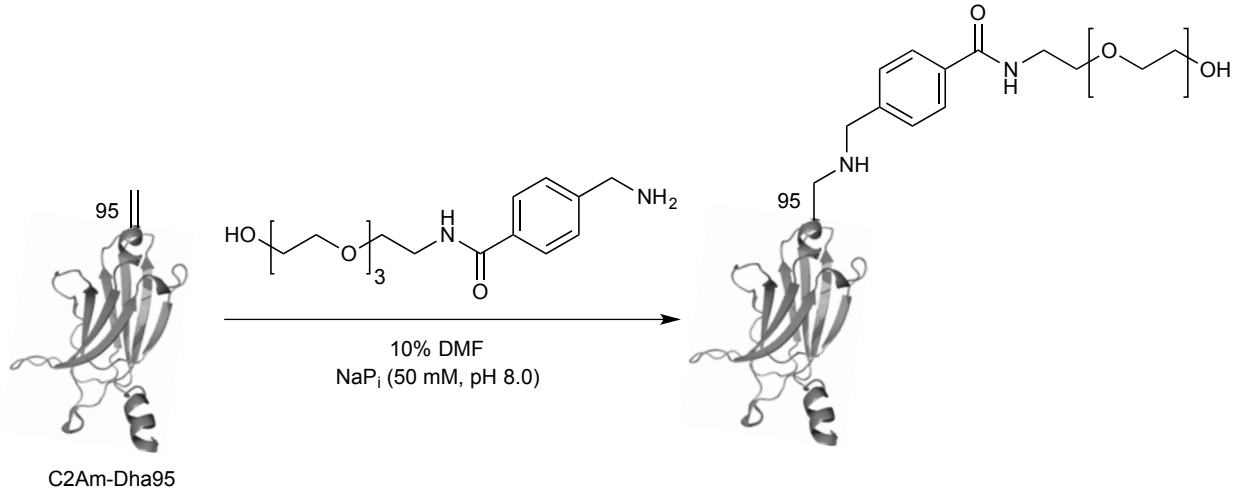

C2Am-Dha95

A 40 µL aliquot of C2Am-Dha95 (6.09 µM, 244 pmol) in 50 mM sodium phosphate buffer at pH 8.0 was thawed. Tetraethylene glycol benzylamine **26** (0.8 mg dissolved in 4 µL of DMF, 2.5 µmol) was added at 37 ºC and the resulting mixture vortexed for 30 seconds. Time points were taken by aliquoting 5 µL of the reaction mixture and diluting it with 5 µL of 50 mM sodium phosphate buffer at pH 8.0. 10 µL of this diluted sample was injected for LC–MS analysis. >95% conversion was observed after incubating for 48 h at 37 ºC (calculated mass, 16514, observed mass, 16515).

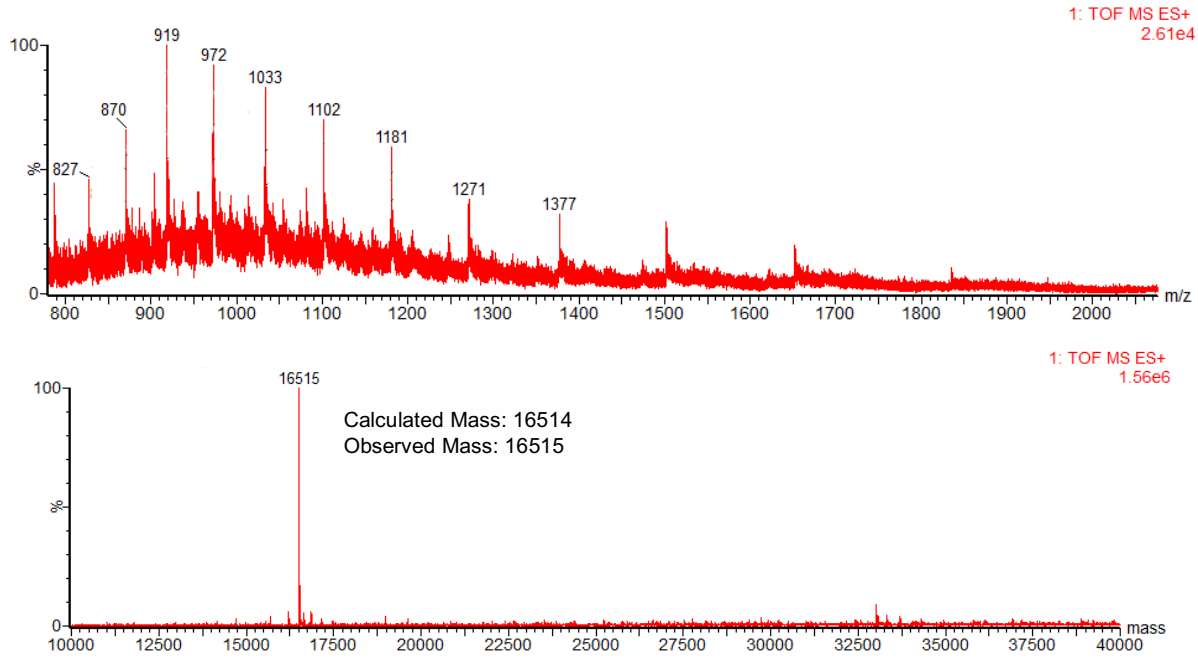

Figure S43. ESI–MS of the reaction of C2Am-Dha95 with **26** (62.5 mM) after 48 h at 37 ºC.

Fluorescein derivative 27 addition to C2Am-Dha95

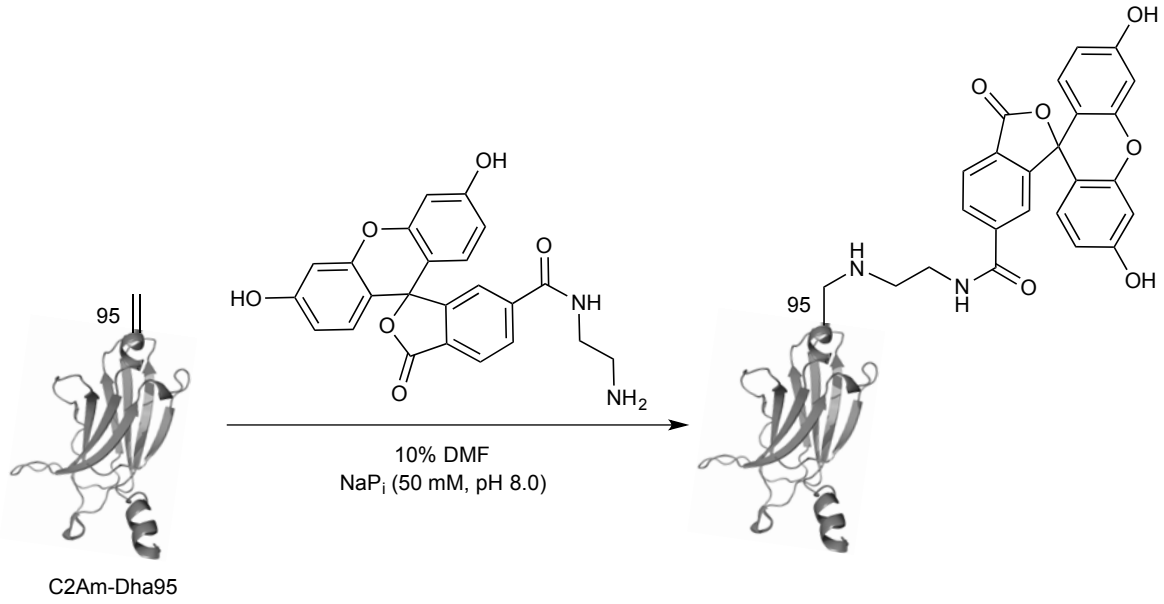

C2Am-Dha95

A 20 µL aliquot of C2Am-Dha95 (54.7 µM, 1.22 nmol) in 50 mM sodium phosphate buffer at pH 8.0 was thawed. Fluorescein derivative **27** (2.3 µL of 8.8 mg stock solution dissolved in 34 µL of DMF, 1.22 µmol) was added at 37 ºC and the resulting mixture vortexed for 30 seconds. After 48 h of additional shaking at 37 ºC, a 10 µL aliquot was desalted with a Zeba Spin Desalting Column and analysed by SDS-PAGE.

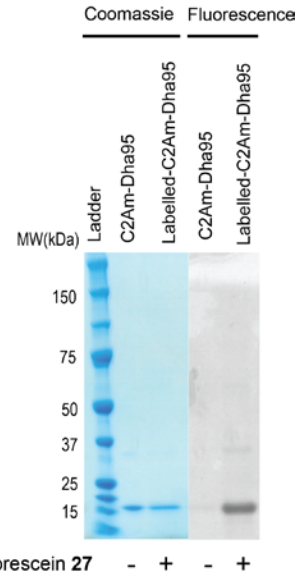

Figure S44. SDS-PAGE (MOPS running buffer) analysis of the reaction of C2Am-Dha95 with **27** (54.7 mM) after 48 h at 37 ºC.

Comparative experiment of addition of 2a and 28 to (C2Am-Cys95)$_2$

A 20 µL aliquot of C2Am-Cys95 (30.8 µM, 616.4 pmol) in 50 mM sodium phosphate buffer at pH 8.0 was thawed. The thawed protein was shaken open to the atmosphere for 1 h at 37 ºC to yield the disulfide product. The presence of the disulfide product (calculated mass, 32444, observed mass, 32444) was confirmed by analysing a 2.5 µL aliquot of the reaction mixture by LC–MS (2.5 µL aliquot diluted with 8 µL of 50 mM sodium phosphate buffer at pH 8.0). The reaction mixture was then split into two 10 µL aliquots. To one aliquot, benzylamine **2a** (0.25 µL dissolved in 0.5 µL DMF, 2.27 µmol) was added and the resulting mixture was stirred for 2 h at 37 ºC. To the second aliquot, β-mercaptoethanol **28** (0.03 µL, 0.45 µmol) was added and the resulting mixture was also stirred for 2 h at 37 ºC. After 2 h, a 2.5 µL aliquot of each reaction mixture was analysed by LC–MS (2.5 µL aliquot diluted with 8 µL of 50 mM sodium phosphate buffer at pH 8.0). The reaction mixture incubated with β-mercaptoethanol showed disappearance of the disulfide product (expected mass, 32444), consistent with the expectation that thiol nucleophiles disrupt disulfide bonds. However, the reaction mixture incubated with benzylamine **2a** showed no significant reaction with the disulfide bond product maintained (expected mass, 32444, observed mass, 32443), suggesting that the benzylamine **2a** nucleophile does not interfere with existing disulfide bonds.

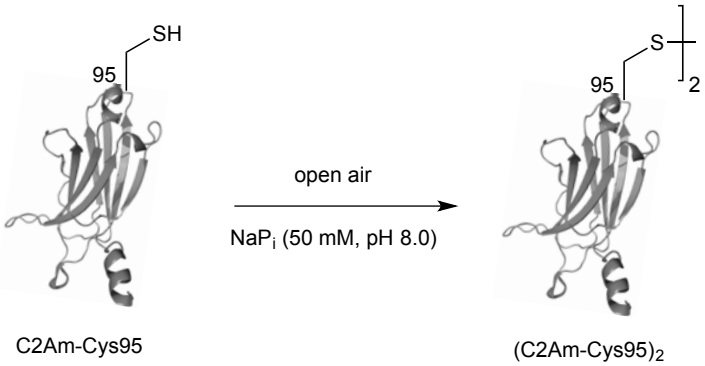

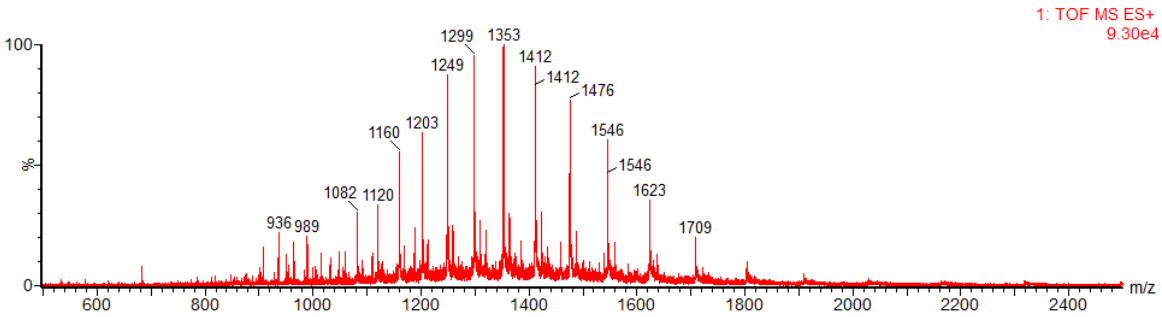

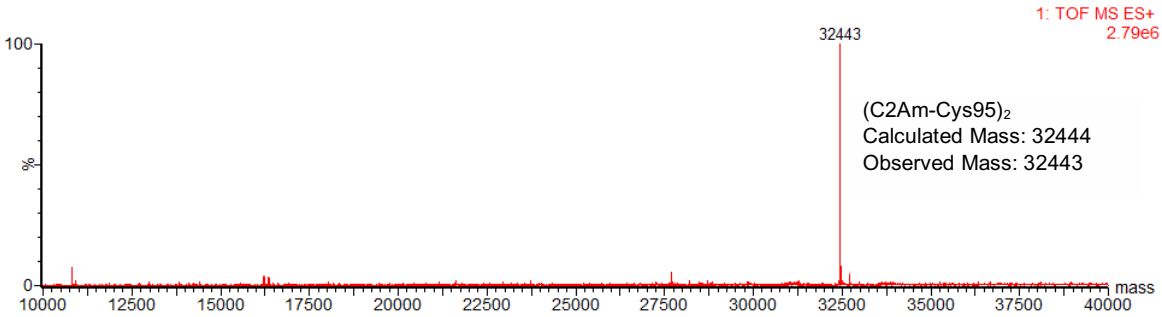

Figure S45. ESI–MS of C2Am-Cys95 after oxidising at open air for 1 h at 37 ºC.

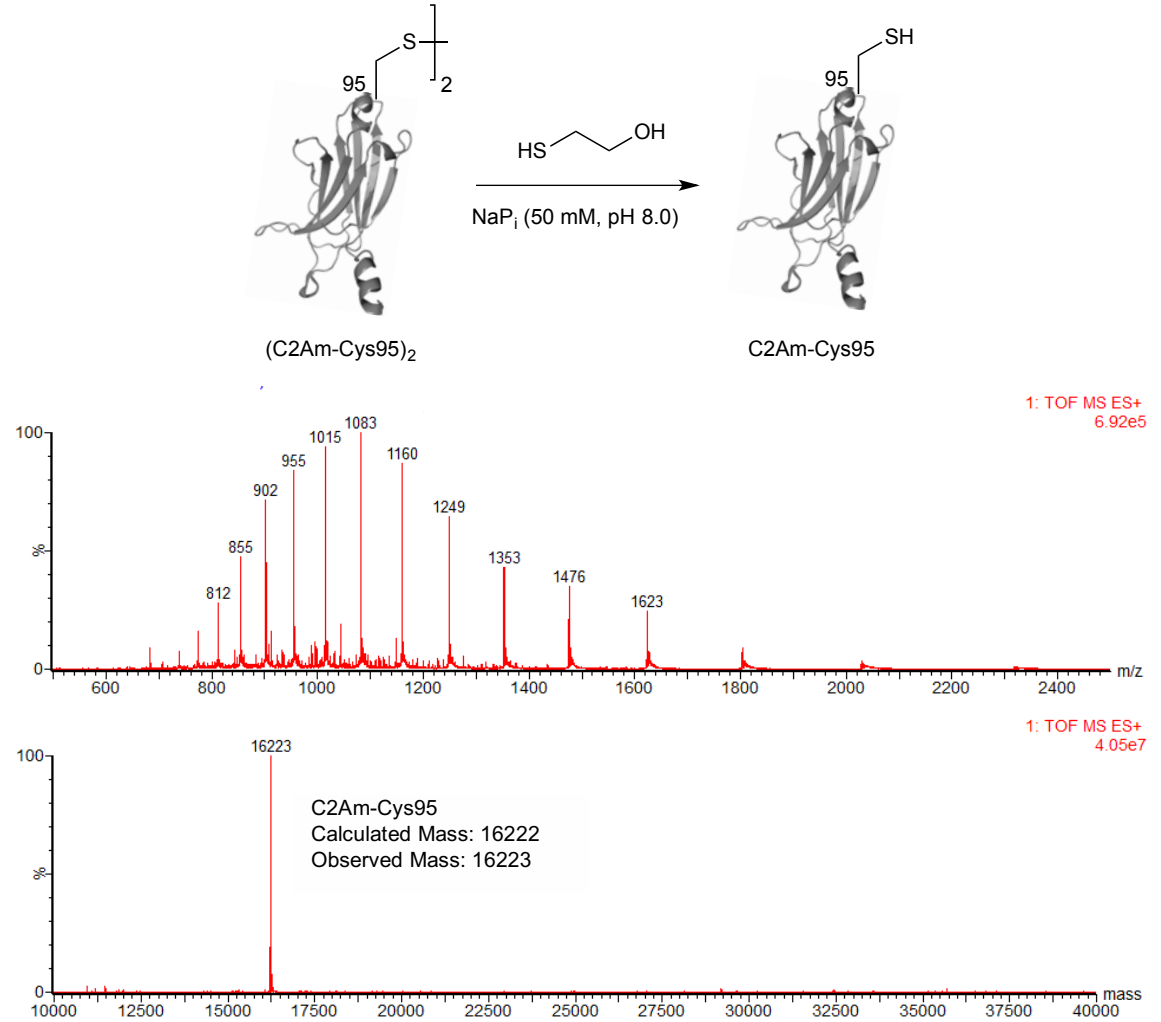

Figure S46. ESI–MS of the reaction of $(C2Am\text{-}Cys95)_2$ with β-mercaptoethanol (22.5 mM) after 2 h at 37 ºC.

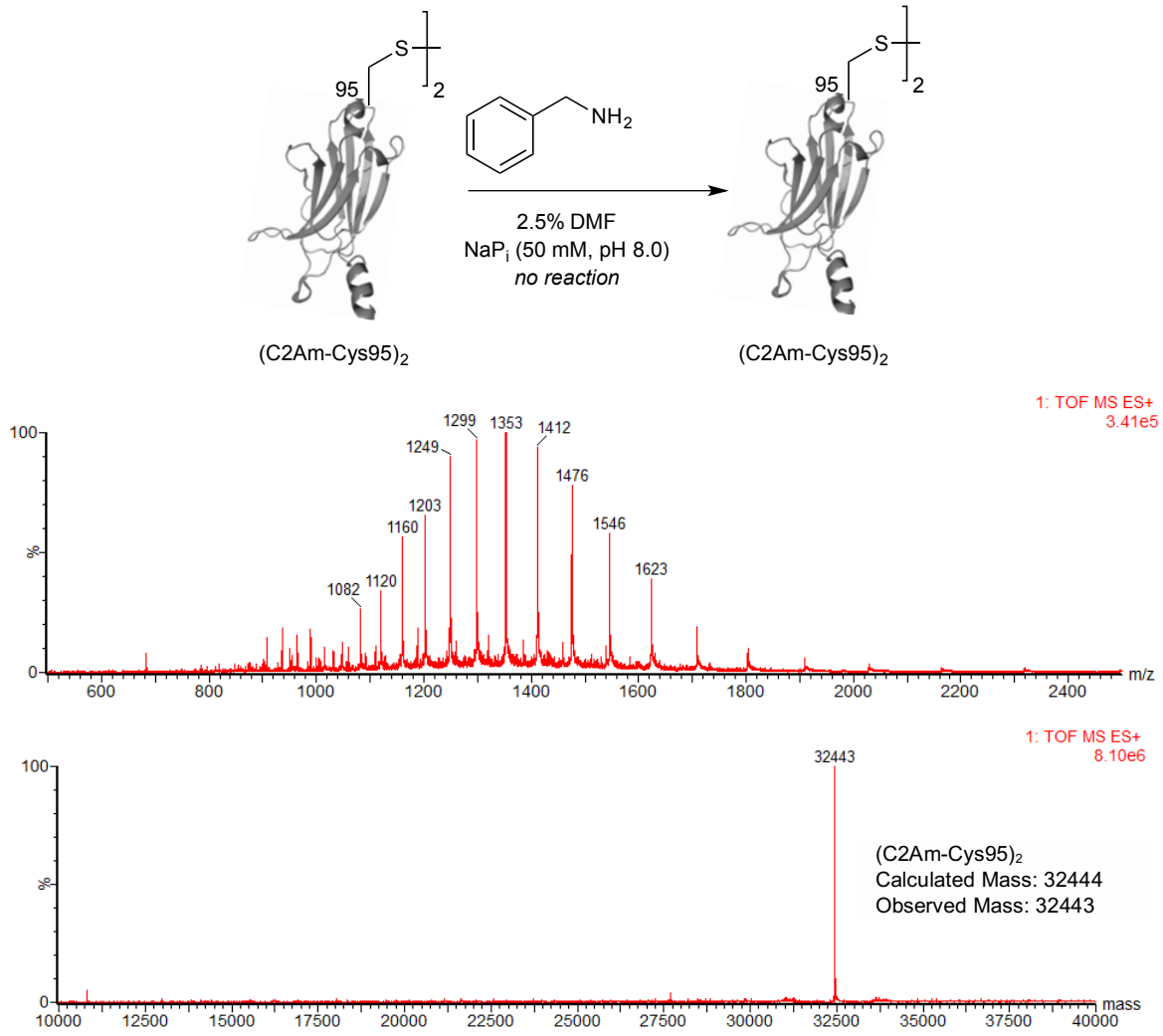

Figure S47. ESI–MS of the reaction of $(C2Am\text{-}Cys95)_2$ with benzylamine (56.6 mM) for 2 h at 37 ºC.

Stability of C2Am-NHBn95 in human plasma

A 10 µL aliquot of C2Am-NHBn95 (20.8 µM, 208.4 pmol) in 50 mM sodium phosphate buffer at pH 8.0 was thawed. 1 µL of reconstituted human plasma (*Sigma Aldrich*) was added at room temperature and the resulting mixture vortexed for 30 seconds. The resulting reaction mixture was then shaken at 37 ºC overnight. After 1 and 24 h, a 2.5 µL aliquot of each reaction mixture was analysed by LC–MS (2.5 µL aliquot diluted with 8 µL of 50 mM sodium phosphate buffer at pH 8.0). No significant degradation of the of the C2Am-NHBn95 adduct was observed at 1 or 24 h.

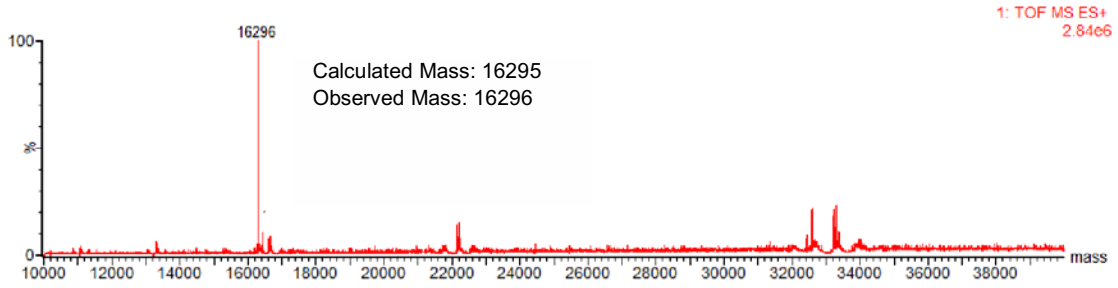

Figure S48. ESI–MS after incubating C2Am-NHBn95 with human plasma for 1 h at 37 ºC.

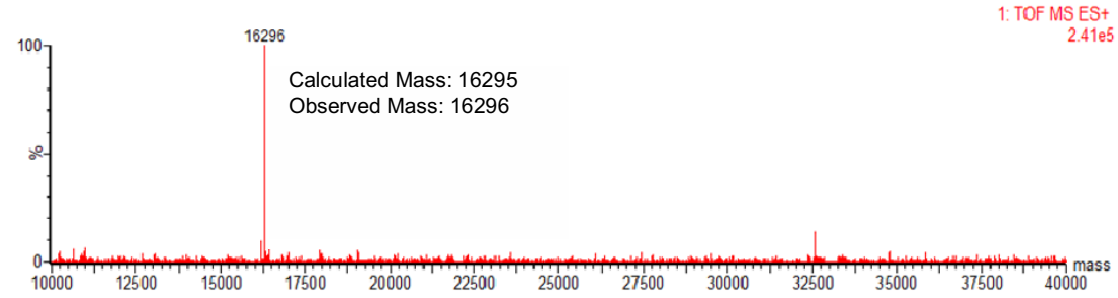

Figure S49. ESI–MS after incubating C2Am-NHBn95 with human plasma for 24 h at 37 ºC.

Stability of C2Am-NHBn95 in the presence of GSH (1 mM)

A 20 µL aliquot of C2Am-NHBn95 (20.8 µM, 416.7 pmol) in 50 mM sodium phosphate buffer at pH 8.0 was thawed. 1 µL of a 20 mM glutathione solution (6 mg glutathione dissolved in 1 mL of 50 mM sodium phosphate buffer at pH 8.0) was added at room temperature and the resulting mixture vortexed for 30 seconds. The resulting reaction mixture was then shaken at 37 ºC overnight. After 1 and 24 h, a 2.5 µL aliquot of each reaction mixture was analysed by LC–MS (2.5 µL aliquot diluted with 8 µL of 50 mM sodium phosphate buffer at pH 8.0). No significant degradation of the C2Am-NHBn95 adduct was observed at 1 or 24 h.

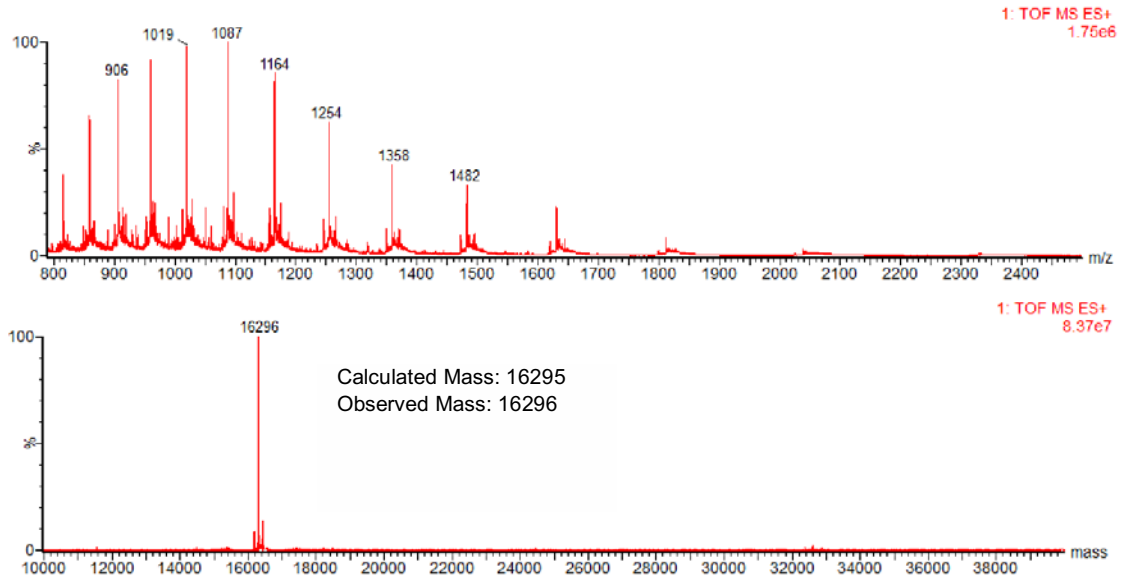

Figure S50. ESI–MS after incubating C2Am-NHBn95 with GSH (1 mM) for 1 h at 37 ºC.

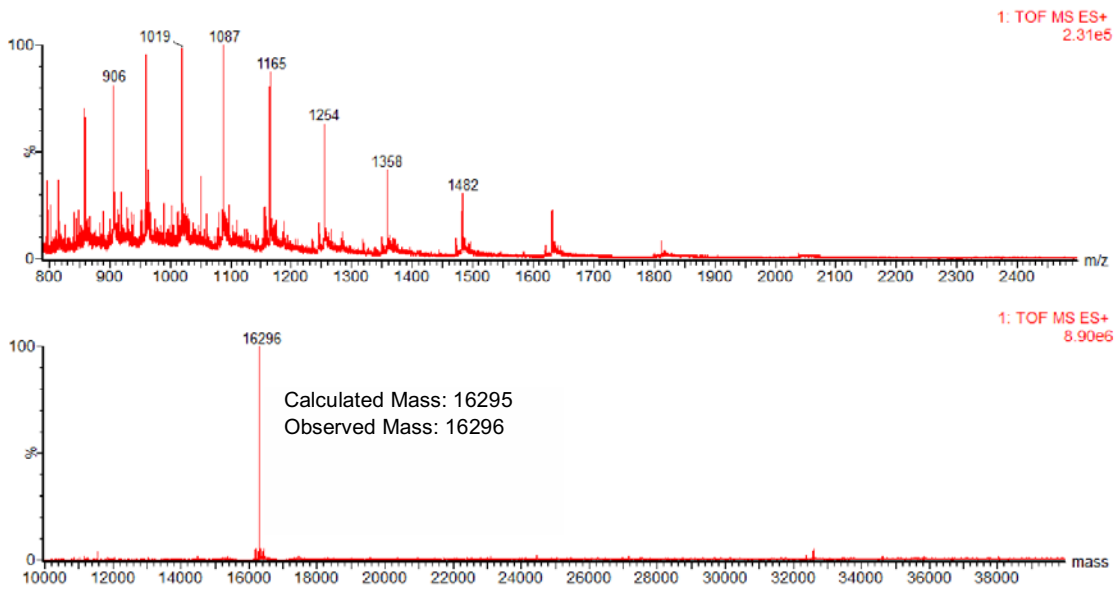

Figure S51. ESI–MS after incubating C2Am-NHBn95 with GSH (1 mM) for 24 h at 37 ºC.

Recombumin sequence (modified residue highlighted in bold and underlined):

DAHKSEVAHRFKDLGEENFKALVLIAFAQYLQQ**C**PFEDHVKLVNEVTEFAKTCVADES
AENCDKSLHTLFGDKLCTVATLRETYGEMADCCAKQEPERNECFLQHKDDNPNLPRL
VRPEVDVMCTAFHDNEETFLKKYLYEIARRHPYFYAPELLFFAKRYKAAFTECCQAAD
KAACLLPKLDELRDEGKASSAKQRLKCASLQKFGERAFKAWAVARLSQRFPKAEFAE
VSKLVTDLTKVHTECCHGDLLECADDRADLAKYICENQDSISSKLKECCEKPLLEKSHC
IAEVENDEMPADLPSLAADFVESKDVCKNYAEAKDVFLGMFLYEYARRHPDYSVVLLL
RLAKTYETTLEKCCAAADPHECYAKVFDEFKPLVEEPQNLIKQNCELFEQLGEYKFQN
ALLVRYTKKVPQVSTPTLVEVSRNLGKVGSKCCKHPEAKRMPCAEDYLSVVLNQLCVL
HEKTPVSDRVTKCCTESLVNRRPCFSALEVDETYVPKEFNAETFTFHADICTLSEKERQ
IKKQTALVELVKHKPKATKEQLKAVMDDFAAFVEKCCKADDKETCFAEEGKKLVAASQ
AALGL

Isotopically Averaged Molecular Weight = 66472.2; with 17 internal disulfides 66439 Da

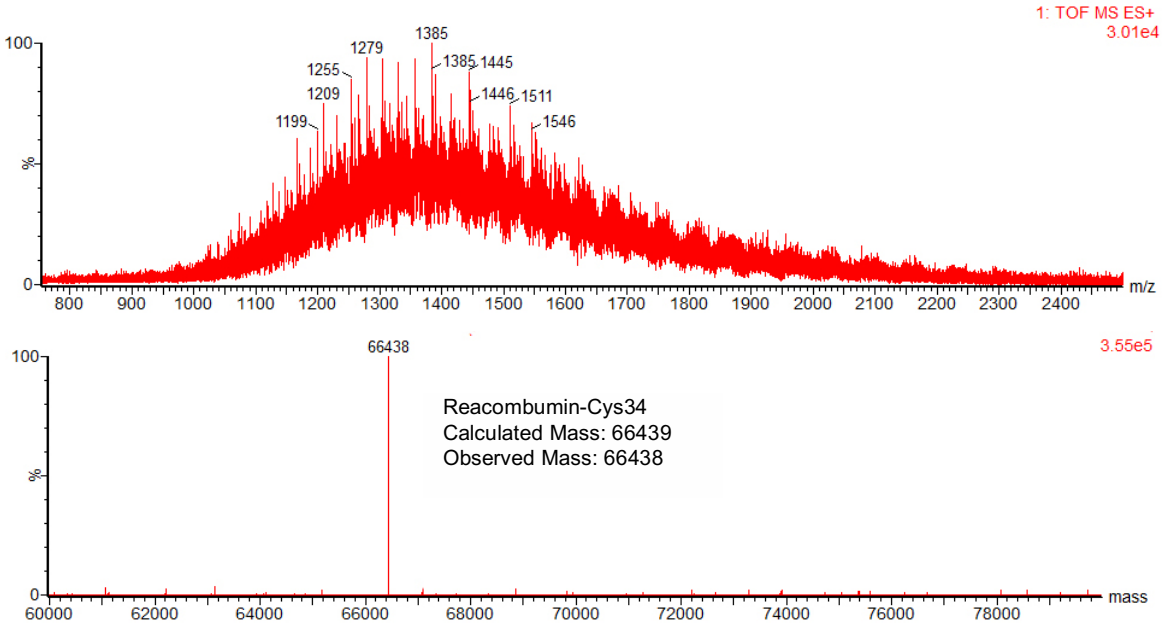

Figure S52. ESI–MS of Recombumin.

Control: Ellman's reagent addition to Recombumin-Cys34

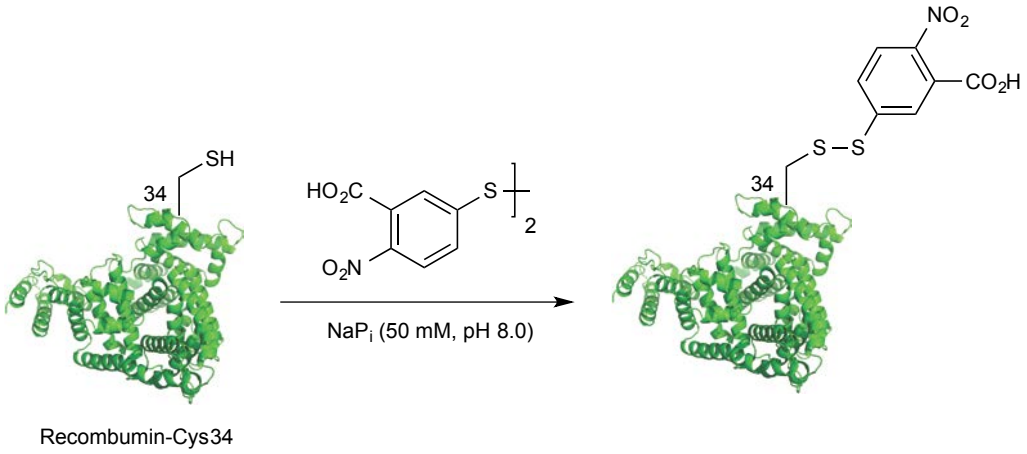

Recombumin-Cys34

A 40 µL aliquot of reduced Recombumin-Cys34 provided by Novozymes Biopharma, (15.1 µM, 602 pmol) was transferred to a 0.5 mL eppendorf tube. Ellman's reagent (0.12 mg dissolved in 10µL of sodium phosphate buffer at pH 8.0, 0.3 µmol) was added at room temperature and the resulting mixture vortexed for 30 seconds. After 30 min of additional shaking, a 5 µL aliquot was analysed by LC–MS (5 µL aliquot diluted by 5 µL of 50 mM sodium phosphate buffer at pH 8.0) and full conversion to Ellman's product (calculated mass, 16420; observed mass, 16419) was observed. The protein sample was stored at 4 ºC.

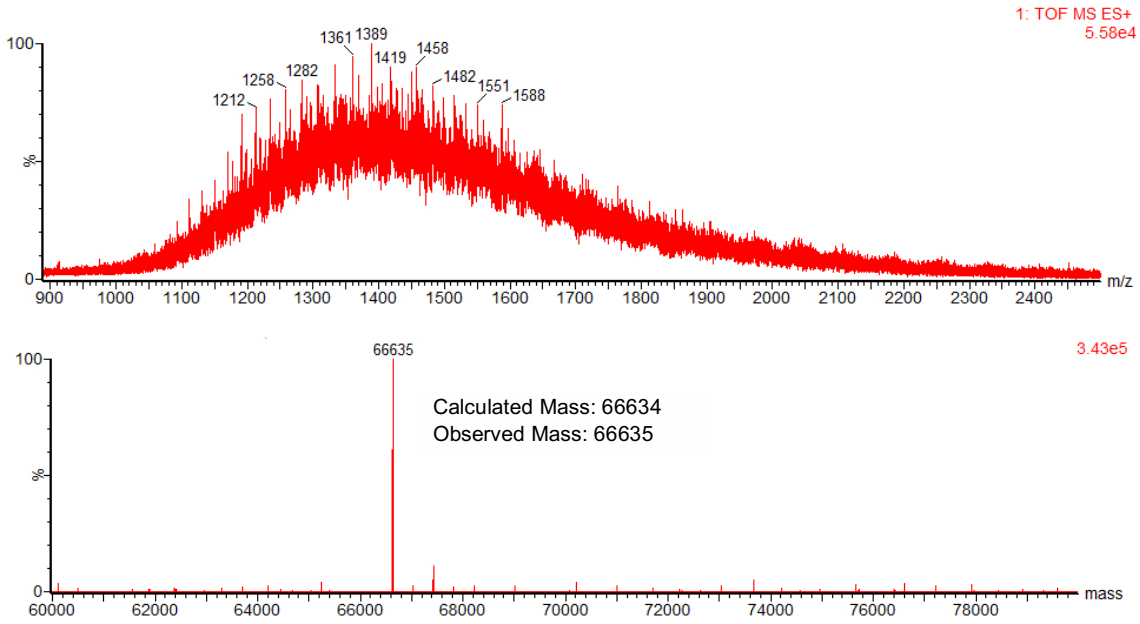

Figure S53. ESI–MS of the reaction of recombumin-Cys34 with Ellman's reagent after 1 h at 37 ºC.

Synthesis of Recombumin-Dha34

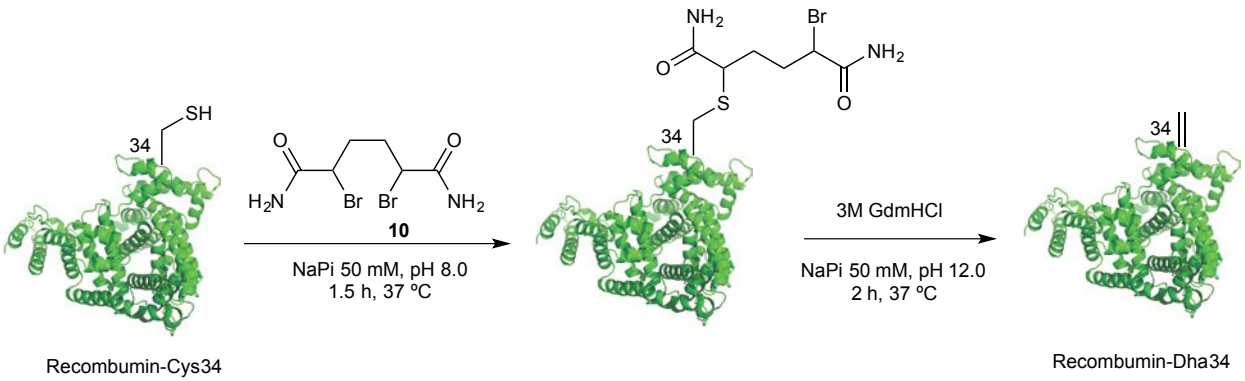

Recombumin-Cys34 Recombumin-Dha34

To a 100 µL aliquot of Recombumin-Cys34 provided by Novozymes Biopharma, (15.1 µM, 1.5 nmol), α,α′-di-bromo-adipyl(bis)amide **10** (679mg, 2.25 mmol) and DMF (10 µL) was added and the resulting mixture vortexed for 30 seconds and was shaken at 37 ºC. After 1.5 h, the reaction progress was monitored by LC–MS. Time points were taken by aliquoting 5 µL of the reaction mixture and diluting it with 5 µL of 50 mM sodium phosphate buffer at pH 8.0. 10 µL of this diluted sample was injected. Full conversion to the monoalkylated Recombinant Human Albumin (calculated mass, 66658; observed mass, 66661) was observed after 1.5 h. Small molecules were then removed from the reaction mixture and the buffer exchanged by loading the sample onto a Zeba Spin Desalting Column previously equilibrated with 50 mM sodium phosphate buffer at pH 12.0. The sample was eluted *via* centrifugation (2 min, 1500xg). To this solution, 3M GudHCl (28.5 mg, 0.3 mol) was added. The resulting mixture was vortexed for 30 seconds and shaken at 37 ºC. Time points were taken by aliquoting 5 µL of the reaction mixture and diluting it with 5µL of 50 mM sodium phosphate buffer at pH 12.0. 10 µL of this diluted sample was injected. Full conversion to Recombumin-Dha34 (calculated mass, 66402; observed mass, 66402) was observed after 2 h. The protein solution was then stored at 4 ºC.

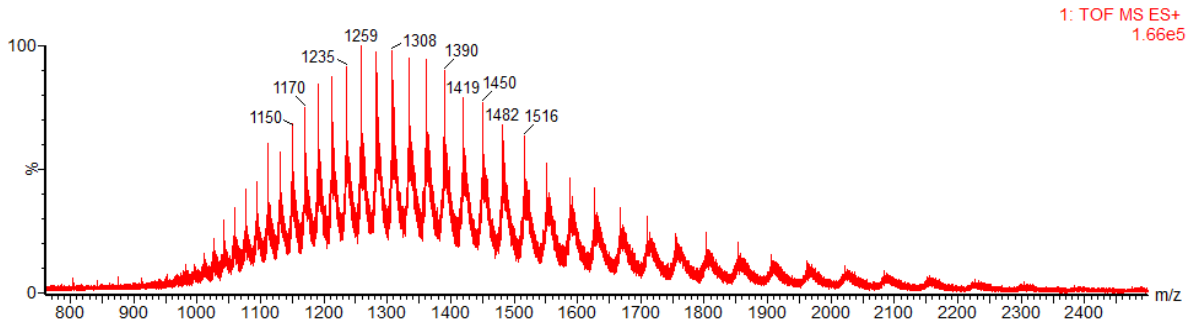

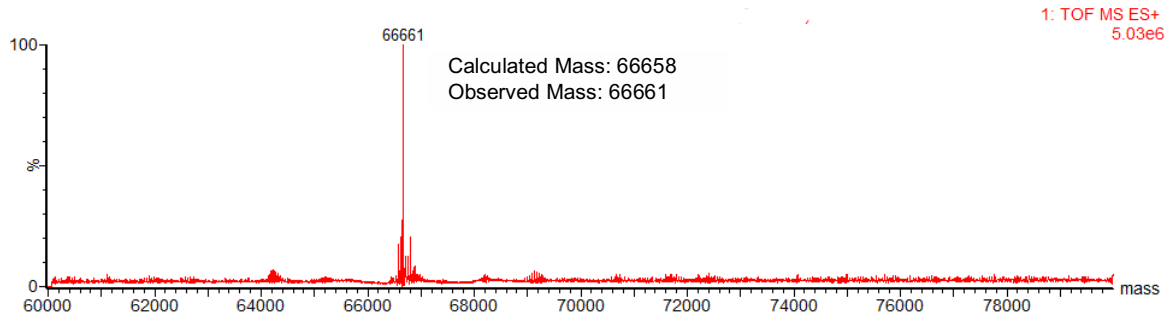

Figure S54. ESI–MS after 1.5 h in NaP_i buffer equilibrated to pH 8.0 at 37 ºC.

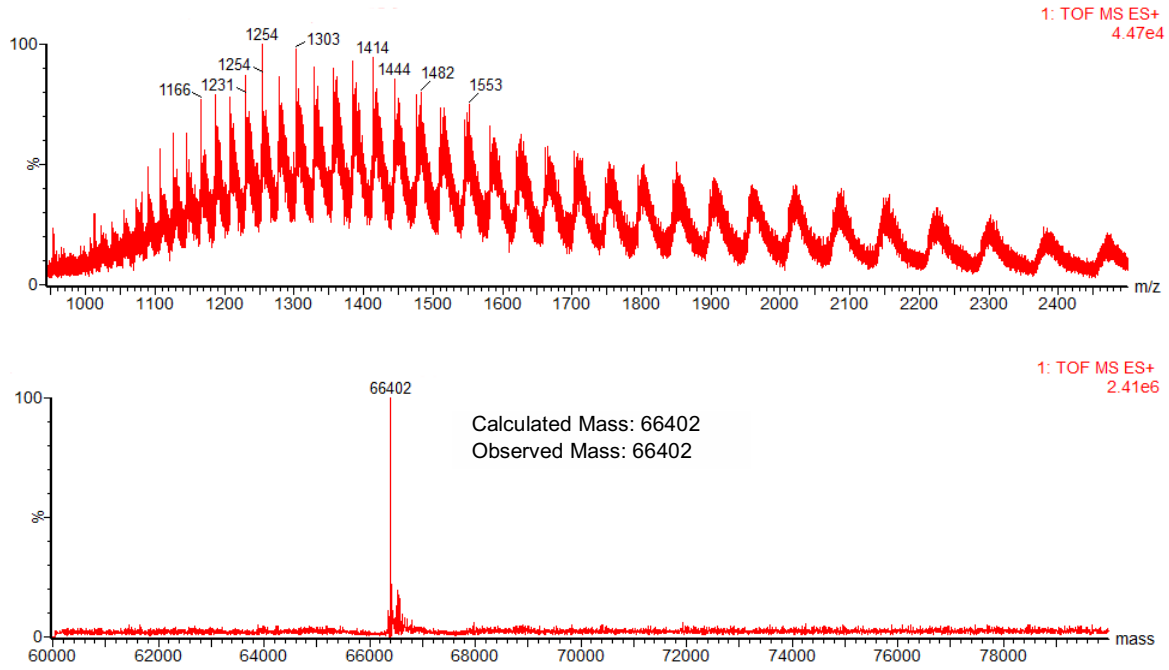

Figure S55. ESI–MS after 1.5 h in NaP_i buffer equilibrated to pH 8.0 at 37 ºC and 2 h in NaP_i buffer equilibrated to pH 12.0 at 37 ºC.

Benzylamine 2a addition to Recombumin-Dha34

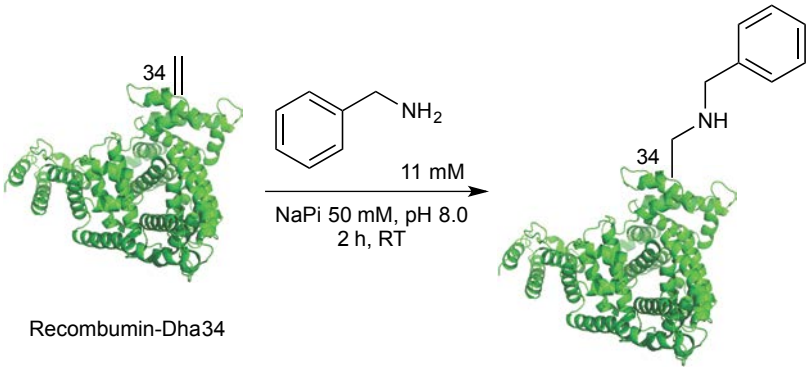

To a 20 µL aliquot of freshly synthesized Recombumin-Dha34 in 50 mM sodium phosphate buffer at pH 8.0, benzylamine (0.16 µL dissolved in 4 µL of DMF, 1.5 µmol) was added and the resulting mixture vortexed for 30 seconds. The reaction was then shaken for 1 h at 37 ºC. Time points were taken by aliquoting and injecting 10 µL of the reaction mixture. >95% conversion to the Recombumin-NHBn34 adduct was observed after 1 h (calculated mass, 66509, observed mass, 66512).

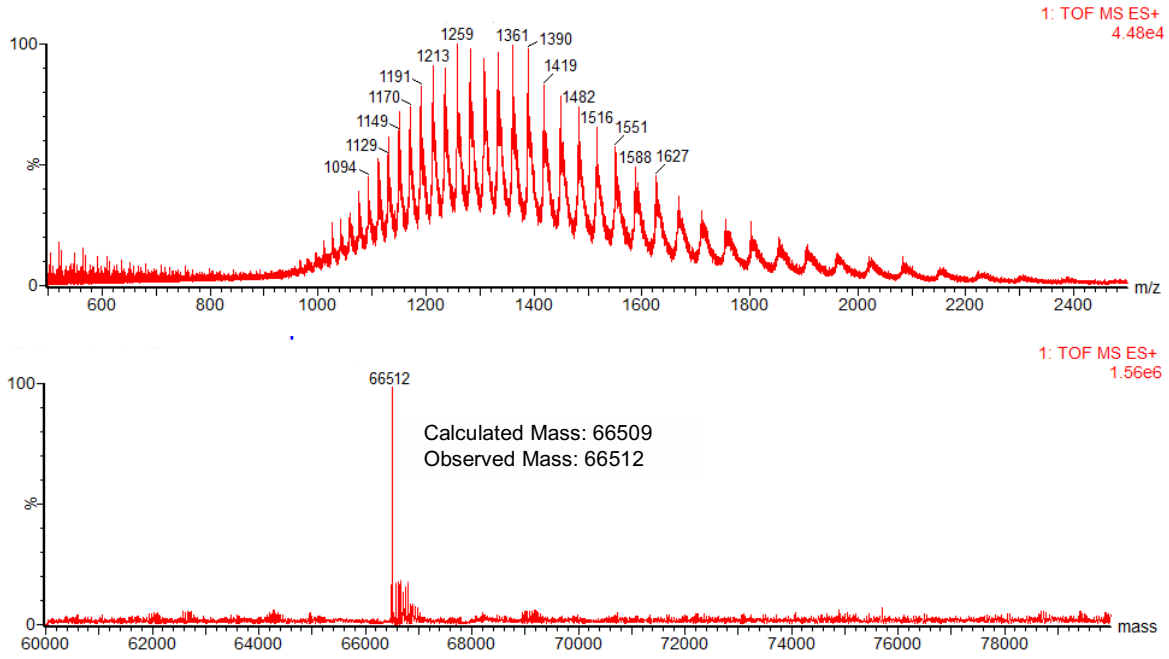

Figure S56. ESI–MS after 1 h in NaP_i buffer, pH 8.0 at 37 ºC.

11. Table S2. Biacore binding kinetics, affinity towards the human FcRn receptor.

Recombumin	On-rate, K_a (10^3/Ms)	Off-rate, K_d (10^{-3}/s)	Equilibrium constant, K_D (μM)
Recombumin-Cys34	6.58	54.07	8.22
Recombumin-NHBn34	4.23	55.70	13.17

12. Gel permeation UPLC analysis

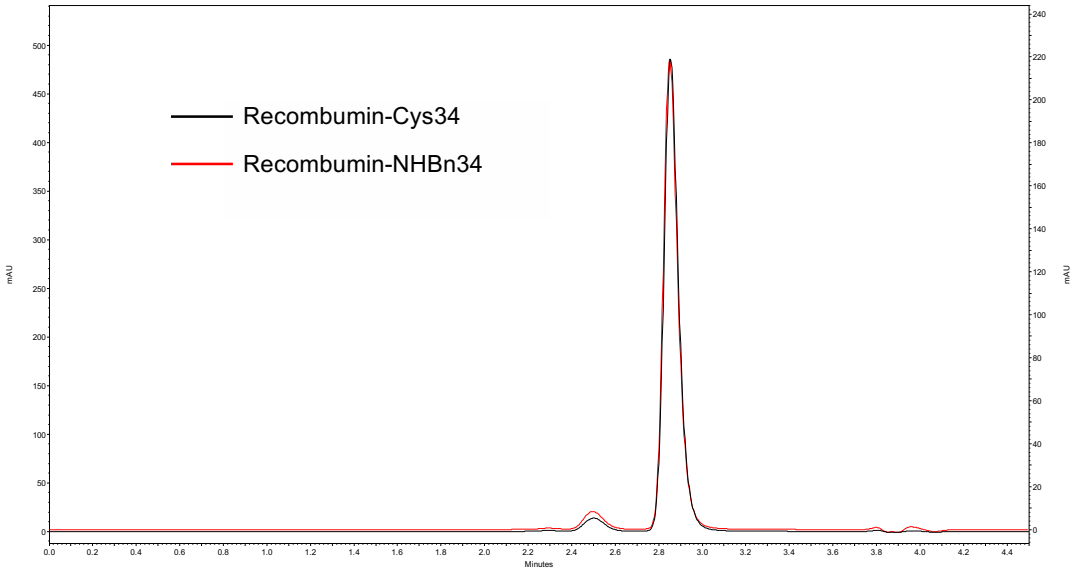

The concentration and percentage monomer of the Recombumin-NHBn34 sample was determined by Gel Permeation Ultra Performance Liquid Chromatography (UPLC). Protein concentration was determined using an Agilent 1260 Infinity LC system equipped with UV detection under OpenLAB CDS (EZChrom Edition) software control. Injections of 4 µL were made onto a 4.6 mm internal diameter x 150mm length ACQUITY UPLC Protein BEH SEC, 200Å, 1.7 µm column (Waters). Samples were chromatographed in 25 mM sodium phosphate, 100 mM sodium sulphate, 0.05% (w/v) sodium azide, pH 7.0 at 0.5 mL/min, with a run time of 4.5 minutes. Samples were quantified by UV detection at 280 nm, by peak height, relative to a Recombumin-Cys34 reference standard of known concentration (10 mg/mL).

Table S3. Gel permeation UPLC data, concentration and oligomer profile of Recombumin samples.

Recombumin	Monomer concentration (mg/mL)	Monomer percentage	Dimer percentage	Trimer percentage
Recombumin-Cys34 reference standard	9.8	95.9	3.8	0.3
Recombumin-NHBn34	4.4	94.6	5.0	0.4

13. LC–MS/MS analysis

The protein sample was enzymatically digested by trypsin overnight. All LC–MS/MS experiments were performed using a nanoAcquity UPLC (Waters Corp., Milford, MA) system and an LTQ Orbitrap Velos hybrid ion trap mass spectrometer (Thermo Scientific, Waltham, MA). Separation of peptides was performed by reverse-phase chromatography using a Waters reverse-phase nano column (BEH C18, 75 µm i.d. x 250 mm, 1.7 µm particle size) at flow rate of 300 nL min^{-1}. Peptides were initially loaded onto a pre-column (Waters UPLC Trap Symmetry C18, 180µm i.d. x 20mm, 5 µm particle size) from the nanoAcquity sample manager with 0.1% formic acid for 3 min at a flow rate of 10 µL min^{-1}. After this period, the column valve was switched to allow the elution of peptides from the pre-column onto the analytical column. Solvent A was water + 0.1% formic acid and solvent B was acetonitrile + 0.1% formic acid. The linear gradient employed was 5–40% B in 60 min.

The LC eluent was sprayed into the mass spectrometer by means of a New Objective nanospray source. All *m/z* values of eluting ions were measured in the Orbitrap Velos mass analyser, set at a resolution of 30000. Data dependent scans (Top 20) were employed to automatically isolate and generate fragment ions by collision-induced dissociation in the linear ion trap, resulting in the generation of MS/MS spectra. Ions with charge states of 2+ and above were selected for fragmentation. Post-run, the data was processed using Protein Discoverer (version 1.3., ThermoFisher). Briefly, all MS/MS data were converted to mgf files and these were submitted to the Mascot search algorithm (Matrix Science, London UK) and searched against a custom database containing the C2A domain of Synaptotagmin-I and applying variable modifications of oxidation (M), deamination (NQ) and a custom modification of either benzylamine **2a** (C) (Figure S57) or methyl hydrazine **25** (Figure S58), using a peptide tolerance of 25 ppm (MS) and 0.8Da (MS/MS). Peptide identifications were accepted if they could be established at greater than 95.0% probability.

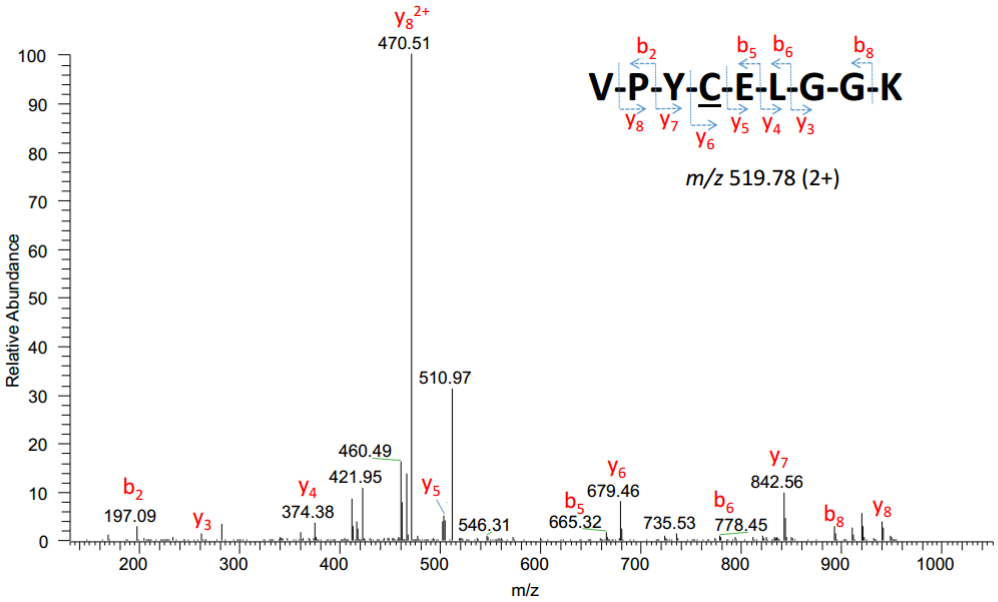

Figure S57. MS/MS spectrum of the *m/z* 529.78 doubly charged ion of the tryptic peptide VPYCELGGK, containing the **dehydroalanine/benzylamine** modification at the original cysteine residue. The generated fragment ions are consistent with the mass of the modification.

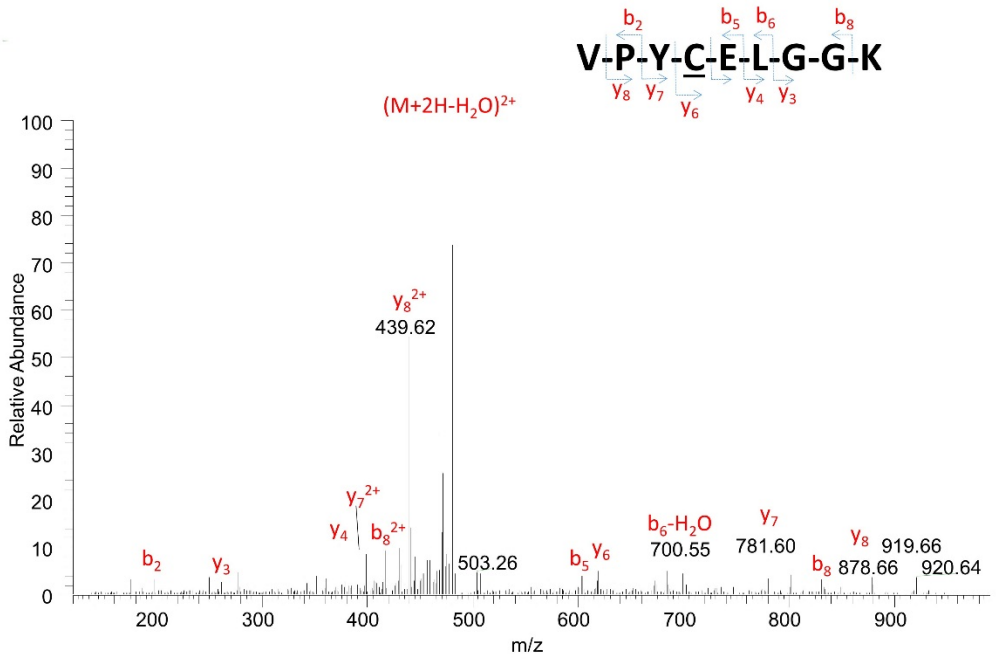

Figure S58. MS/MS spectrum of the doubly charged ion of the tryptic peptide VPYCELGGK, containing the **dehydroalanine/hydrazine** modification at the original cysteine residue. The generated fragment ions are consistent with the mass of the modification.

14. Labelling of C2Am-NHBn95 with NHS-ester AlexaFluor 647

Fluorescent conjugates of both the unmodified and benzylamine conjugated C2A Domain of Synaptotagmin-I were synthesised for flow cytometry. Both the unmodified and benzylamine modified proteins were labelled with NHS Ester AlexaFluor 647 (Life Technologies) to non-specifically label these proteins with this lysine-reactive fluorescent dye. Fluorescence of the proteins was confirmed by gel electrophoresis. Utilising the fluorescent conjugates described above, flow cytometry was performed on EL4 cells (murine T-cell lymphoma) treated with a chemotherapeutic agent (10mM etoposide) to stimulate apoptosis. Cell viability was confirmed by dye exclusion (ViCell). These cells were then treated with the AlexaFluor 647 labelled C2A Domain of Synaptotagmin-I conjugates and examined for fluorescence by FACS sorting as previously described in the literature.[11] 20,000 events were sampled and run in triplicate. Cell gating was based upon the cell's apoptotic status as determined by UV autofluorescence derived from NADH pool in the cell that is depleted upon apoptosis and a cell death marker (Sytox green from Life Technologies).

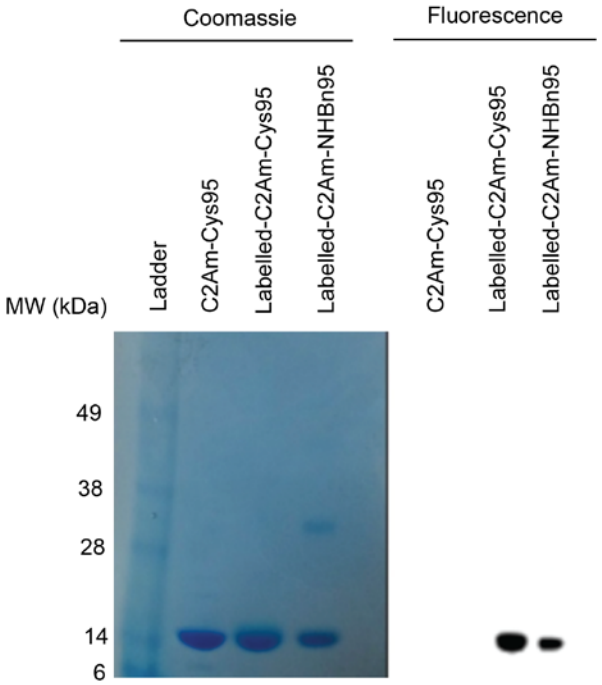

Figure S59. Fluorescent labelling of benzylamine **2a** modified protein and unmodified protein with AlexaFluor647 NHS Ester (Life Technologies). Gel electrophoresis was performed confirming labelling of both unmodified and benzylamine-modified protein.

15. Construction of an ADC using aza-Michael addition at Dha

15.1 Reduction/re-oxidation procedure for Thiomab LC-V205C

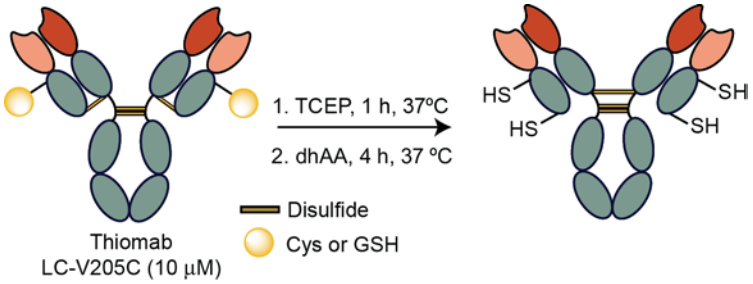

Thiomab LC-V205C (15 μL, 400 nmol) disulfide bonds were reduced by mild reduction in 50 mM sodium phosphate buffer at pH 8.0 (23 μL) at 37 ºC by the addition of thirty-fold molar excess reducing agent tris(2-carboxyethyl)phosphine (TCEP, 3 μL, 4,000 μM) for 1 h. Small molecules were removed from the reaction mixture by loading the sample onto a Zeba Spin Desalting Column previously equilibrated with 50 mM sodium phosphate buffer at pH 8.0. The sample was eluted via centrifugation (2 min, 1500xg). To re-form the interchain disulfide bonds, the reduced Thiomab was incubated for 4 h at 37 ºC with dehydroascorbic acid at a ten-fold molar excess. After, a 5 µL aliquot was analysed by LC–MS (5 µL aliquot diluted by 5 µL of 50 mM sodium phosphate buffer at pH 8.0).

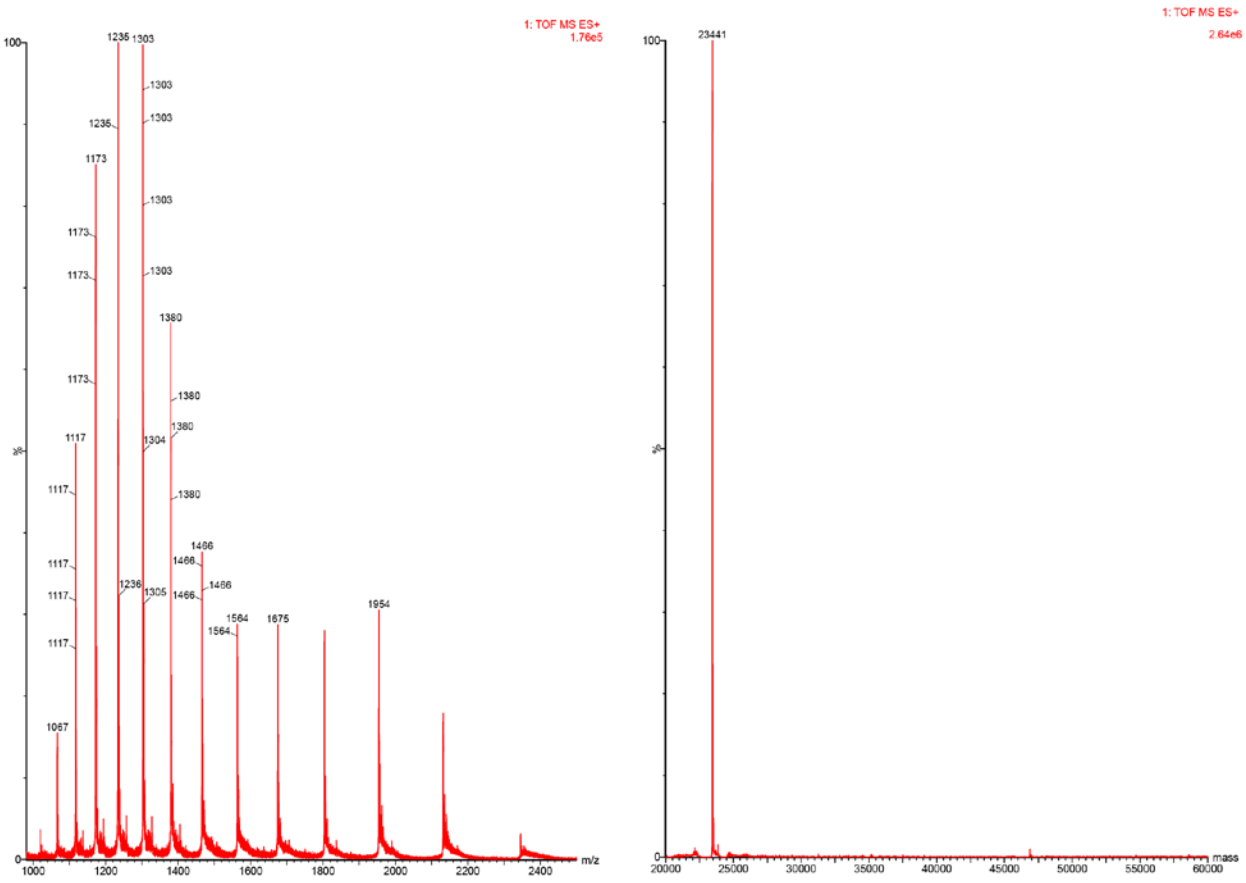

Figure S60. ESI–MS of the light-chain after reduction/re-oxidation of Thiomab LC-V205C.

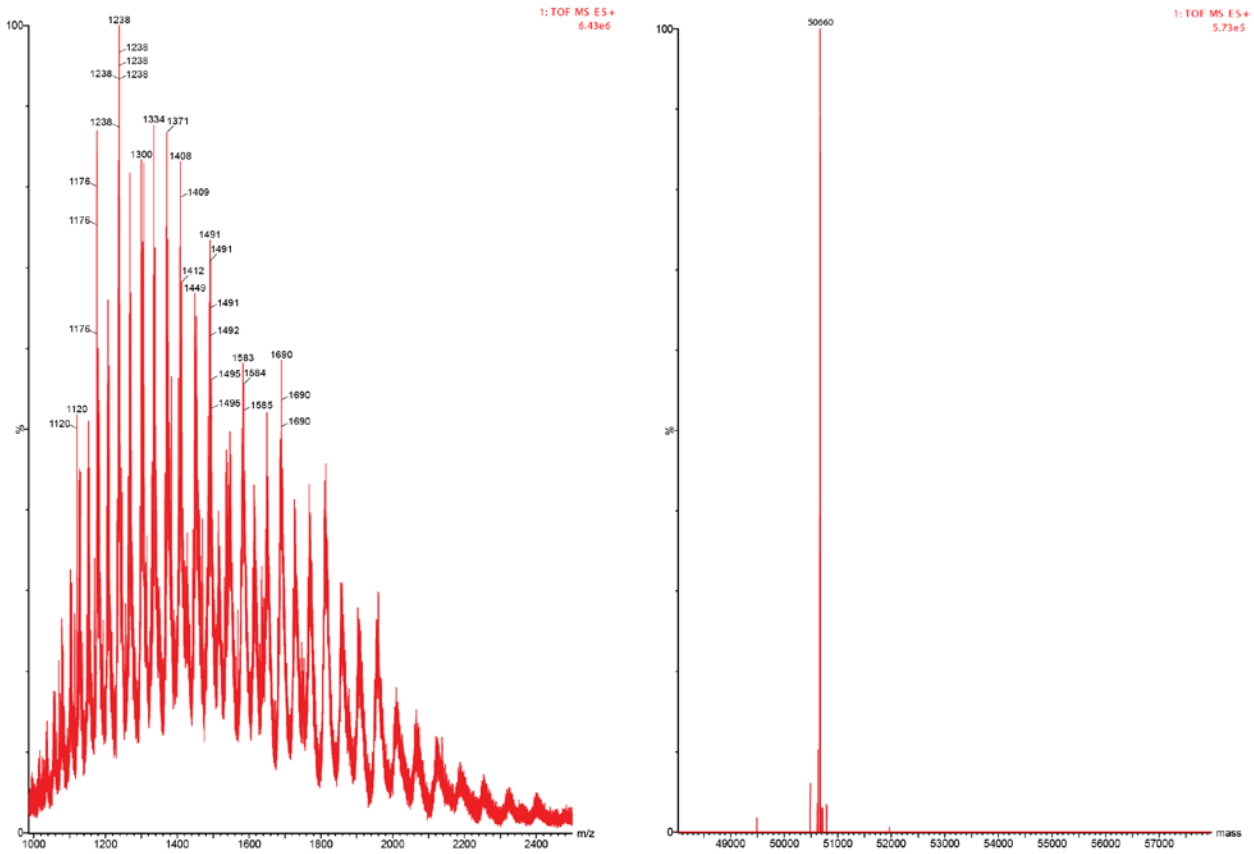

Figure S61. ESI–MS of the heavy-chain after reduction/re-oxidation of Thiomab LC-V205C.

15.2 Installation of Dha into Thiomab LC-V205C

Reaction of Thiomab LC-V205C with α,α'-dibromo-adipyl(bis)amide 10

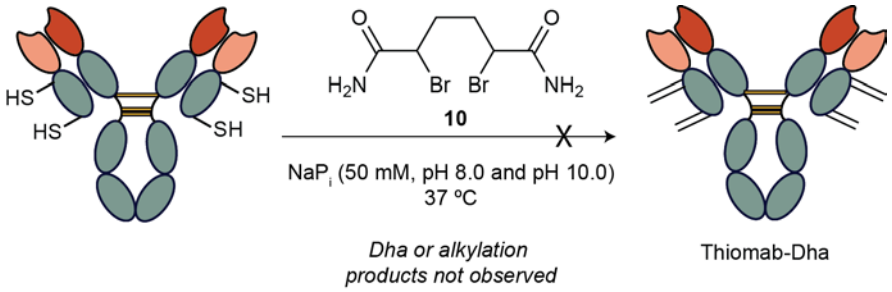

To a 100 μL aliquot of reduced/re-oxidized Thiomab (10.0 μM, 1.0 nmol), a freshly prepared solution of α,α'-dibromo-adipyl(bis)amide **10** (1.0 μL of 500.0 mM solution, 0.5 μmol) in DMF was added and the resulting mixture was vortexed for 30 seconds and then was shaken at 21 ºC. The reaction progress was monitored by LC–MS with time points taken after 3 and 24 h. Time point was taken by aliquoting 5 μL of the reaction mixture and diluting it with 5 μL of 50 mM sodium phosphate buffer at pH 8.0. Small molecules were removed from the reaction mixture by loading the sample onto a Zeba Spin Desalting Column previously equilibrated with 50 mM sodium phosphate buffer at pH 8.0. The sample was eluted via centrifugation (2 min, 1500xg). 10 μL of this diluted sample was injected. Conversion to Thiomab–Dha or any of the possible alkylation products was not observed after 24 h. The same profile, i.e. no reaction, was observed when Thiomab was reacted with 100 equiv. of *O*-Mesitylsulfonylhydroxylamine (MSH).[14]

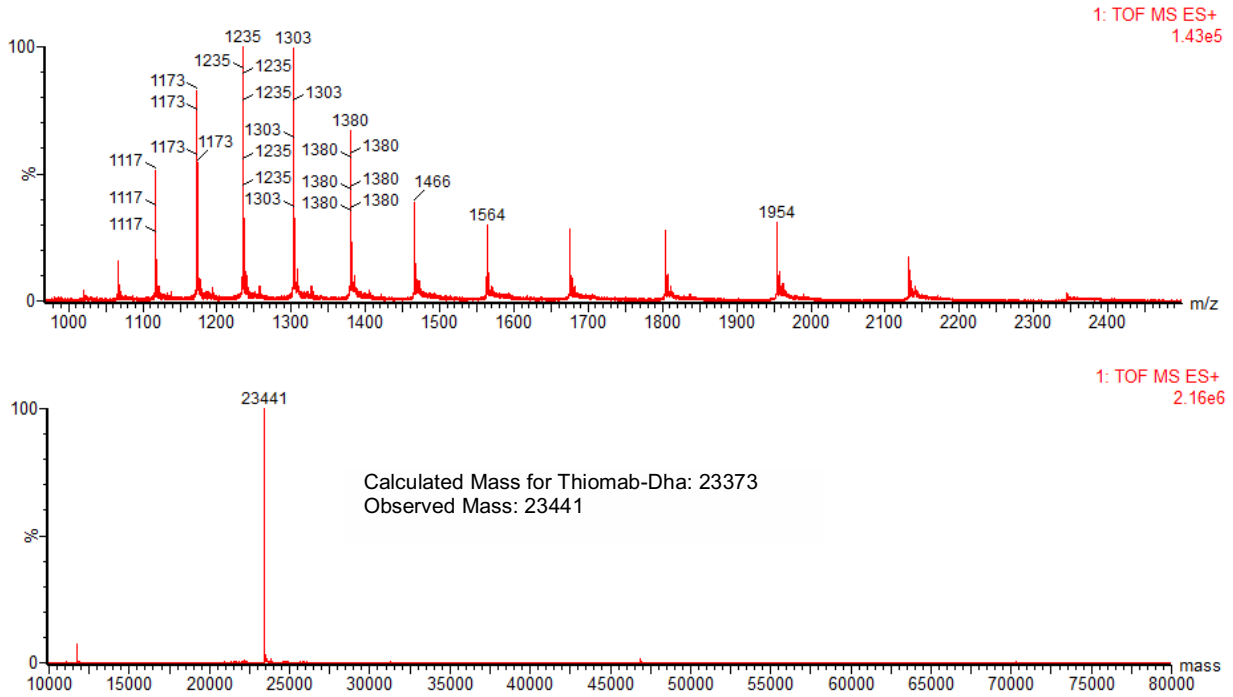

Figure S62. ESI–MS of the light-chain after reaction of reduced/re-oxidized Thiomab LC-V205C with α,α'-dibromo-adipyl(bis)amide **10** (5.0 mM) at pH 8.0, after 24 h at 37 ºC. No reaction observed. An identical spectrum was obtained when Thiomab LC-V205C was reacted with MSH.

Reaction of Thiomab LC-V205C with methyl 2,5-dibromopentanoate 29

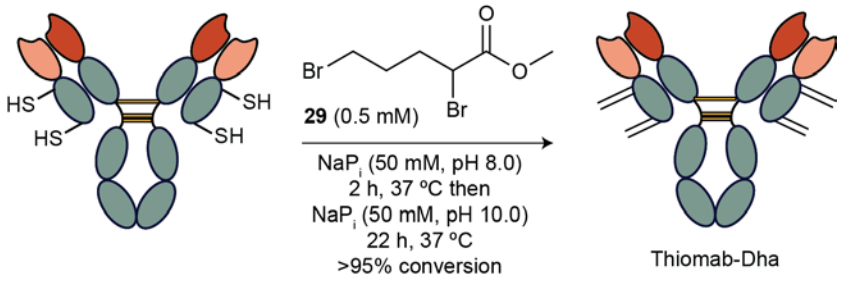

To a 100 μL aliquot of reduced/re-oxidized Thiomab LC-V205C (10.0 μM, 1.0 nmol), a freshly prepared solution of methyl 2,5-dibromopentanoate (1.0 μL of 50.0 mM solution, 0.05 μmol) was added and the resulting mixture was vortexed for 30 seconds and then was shaken at 37 ºC. The reaction progress was monitored by LC–MS. After 2 h, small molecules were removed from the reaction mixture by a buffer exchange column Viva

500 (10 KDa). The sample was eluted via centrifugation (5 min, 1500xg) using 50 mM sodium phosphate buffer at pH 10.0 to dilute the sample. After 24 h, small molecules were removed from the reaction mixture by loading the sample onto a Zeba Spin Desalting Column previously equilibrated with 50 mM sodium phosphate buffer at pH 8.0. The sample was eluted via centrifugation (2 min, 1500xg). Time points were taken by aliquoting 5 μL of the reaction mixture and diluting it with 5 μL of 50 mM sodium phosphate buffer. 10 μL of this diluted sample was injected. Complete conversion to a single product with a mass corresponding to the formation of two Dha in the light-chain was observed after 24 h (calculated mass light chain bearing two Dha, 23373, observed mass, 23376). The heavy-chain remained intact after the modification (calculated mass heavy chain, 50660, observed mass, 50660).

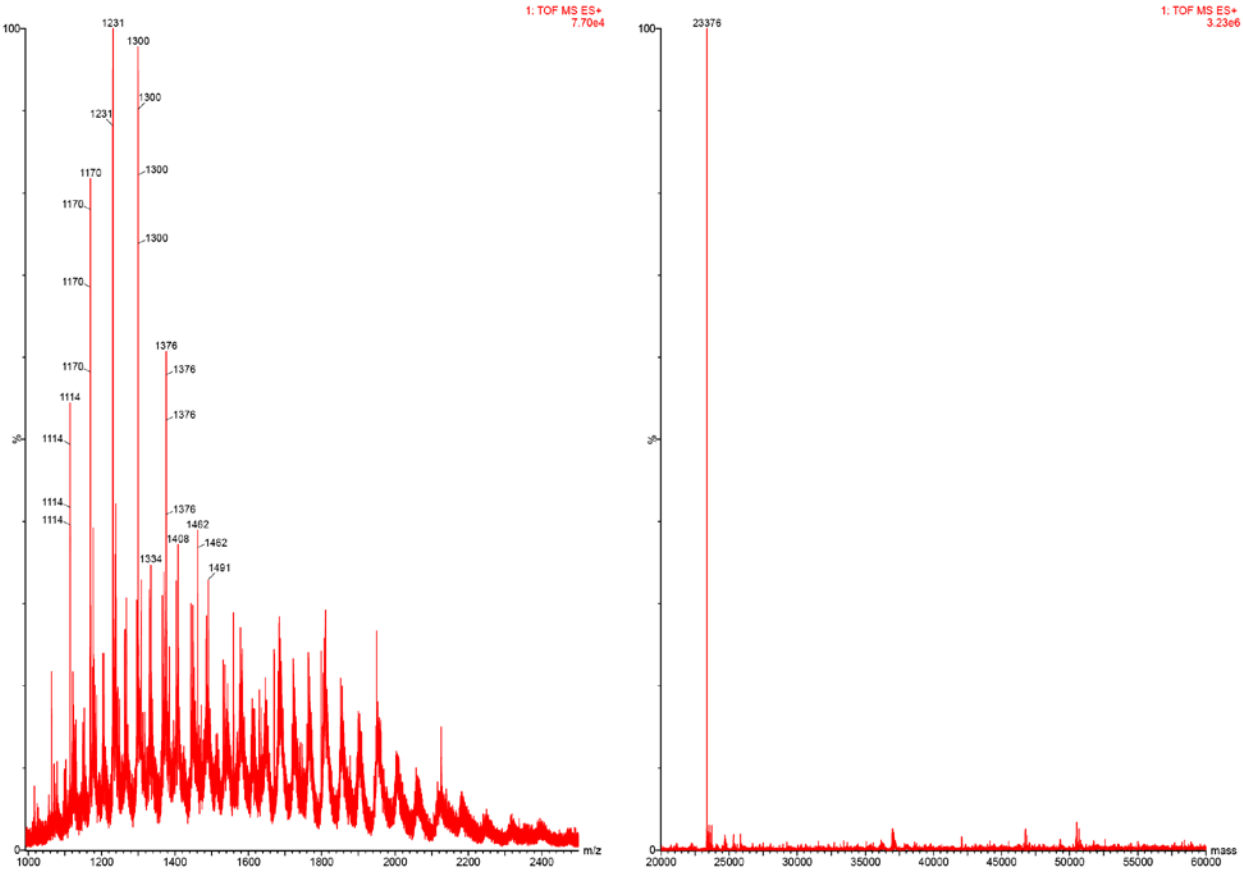

Figure S63. ESI–MS of the light-chain after reaction of reduced/re-oxidized Thiomab with methyl 2,5-dibromopentanoate (0.5 mM) at pH 8.0 for 2 h and then at pH 10.0 for an additional 22 h period at 37 ºC.

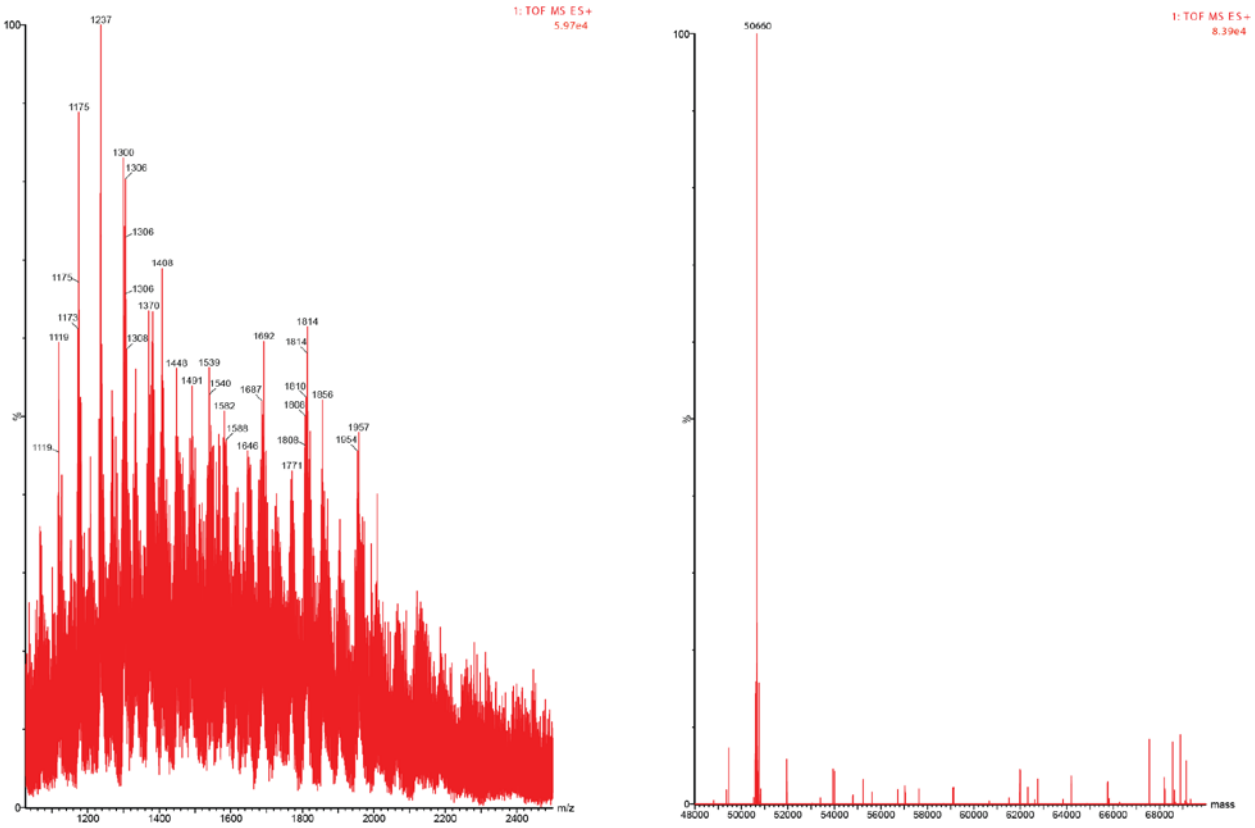

Figure S64. ESI–MS of the heavy-chain after reaction of reduced/re-oxidized Thiomab with methyl 2,5-dibromopentanoate **29** (0.5 mM) at pH 8.0 for 2 h and then at pH 10.0 for a period of 22 h at 37 ºC.

Control: Reaction of Thiomab LC-V205C with 5,5′-dithiobis(2-nitrobenzoic acid) (Ellman's reagent)

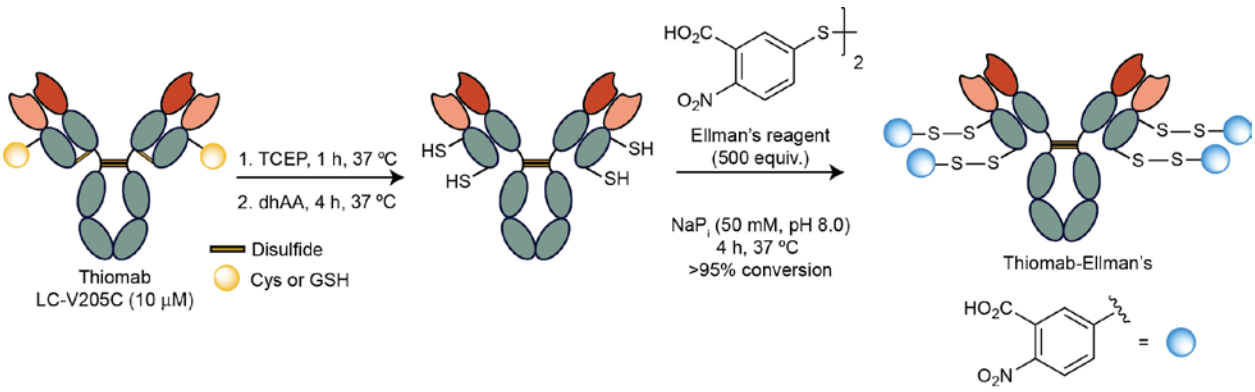

A 40 µL aliquot of Thiomab LC-V205C (10 µM) was transferred to a 0.5 mL eppendorf tube. An aliquot of 0.8 µL (500 equiv.) of a stock suspension of 5,5′-dithiobis(2-nitrobenzoic acid) (0.500 mM) was added and the resulting mixture vortexed for 10 seconds. After 4 h of additional mixing, at 37 ºC, small molecules were removed from the reaction mixture by loading the sample into a Zeba Spin Desalting Column previously equilibrated with NaPi (50 mM, pH 8.0). The sample was eluted via centrifugation (2 min, 1000xg). A 10 µL aliquot was analysed by LC–MS and complete conversion to a conjugate bearing two modifications in the light chain was observed (calculated mass, 23834 Da, observed mass, 23838 Da). Mass alterations were not observed in the heavy-chain (data not shown).

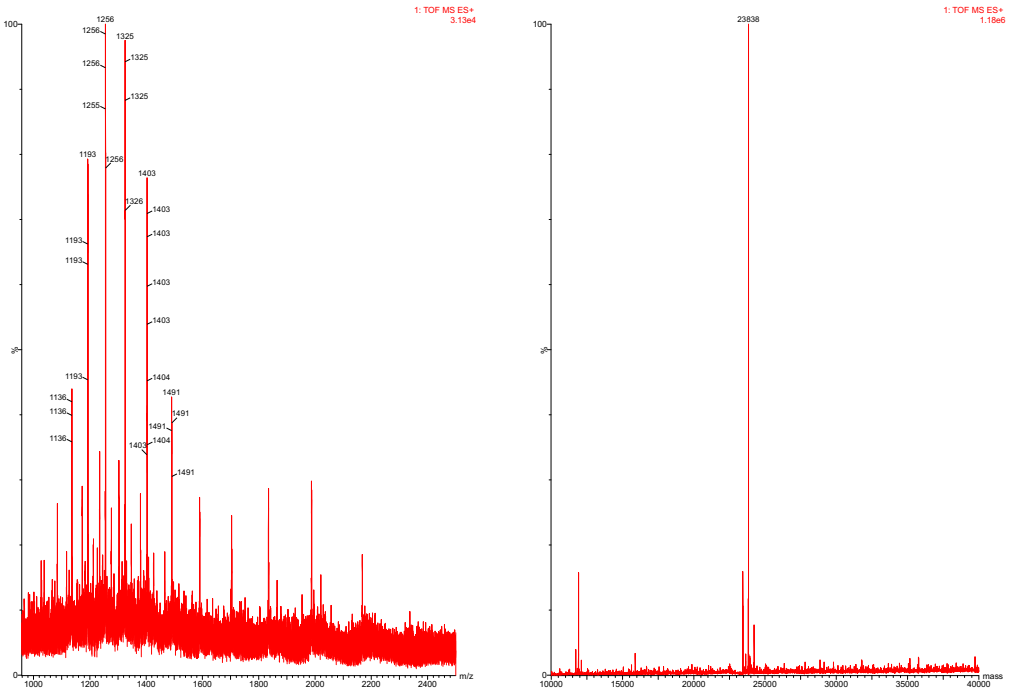

Figure S65. Combined ion series and deconvoluted mass spectrum of the reaction of Thiomab LC-V205C with 5,5′-dithiobis(2-nitrobenzoic acid) (Ellman's reagent 500 equiv.) after 4 h at 37 ºC.

15.3 Antigen binding properties of Thiomab-Dha

Biotinylation of antibodies. Non-modified Thiomab and Thiomab-Dha were conjugated to a biotin linker (Biotin-(PEG)4-N-hydroxysuccinimide, Thermofisher Scientific) in order to carry out Bio-layer Interferometry (BLI) experiments using Streptavidin (SA) Biosensors. A solution of EZ-Link NHS-(PEG)4-Biotin (20 μL, 200 mM in PBS, pH 7.4) was added to the corresponding antibody (20 μL, 20 mM in PBS, pH 7.4) and was shacked at room temperature for 30 min. The crude reaction mixture was buffer exchanged (3x) with PBS pH 7.4 to remove the excess of biotin-linker, obtaining a biotin-to-antibody ratio of ~1 to 2 (determined using the Pierce™ Biotin Quantitation Kit, ThermoFisher Scientific).

Bio-layer interferometry. Binding assays were performed on an Octet Red Instrument (fortéBIO). Ligand immobilization, binding reactions, regeneration and neutralizations were conducted in wells of black polypropylene 96-well microplates. Thiomab and Thiomab-Dha were immobilized on Streptavidin (SA) Biosensors in PBS pH 7.4 with 0.1% BSA and 0.02% tween at 30 ºC. Binding analysis were carried out at 25 ºC, 1,000 r.p.m. in PBS pH 7.4 with 0.1% BSA and 0.02% tween. Association time was 600 s, followed by 2,200 s of dissociation, using different concentrations (200, 66.6, 22.2, 7.4 and 2.47 nM) of ErbB2/Her2 Recombinant Protein Antigen to obtain the association curve. Glycine pH 2.0 was used as a regeneration buffer. Data were analysed using Data Analysis (fortéBIO), with Savitzky-Golay filtering. Binding was fitted to a 2:1 Heterogeneous ligand model, steady state analysis was performed to obtain the binding kinetics constants (KD).

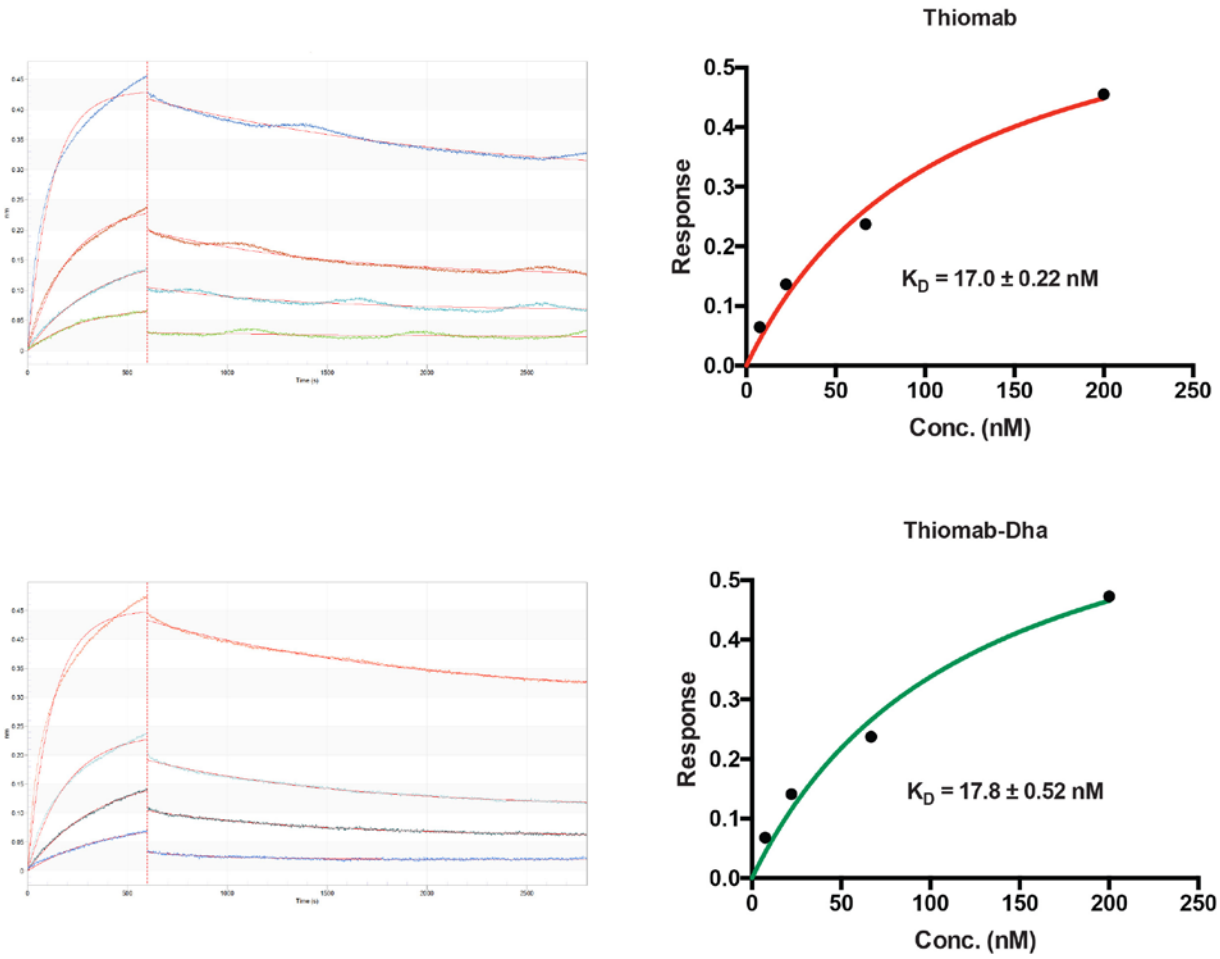

Figure S66. Bio-Layer Interferometry (BLI) curves and fitting curves obtained for Thiomab and Thiomab-**30** with Her2 receptor, together with the K_D constants derived from BLI experiments.

15.4 Aza-Michael addition of piperidine 23 to Thiomab–Dha

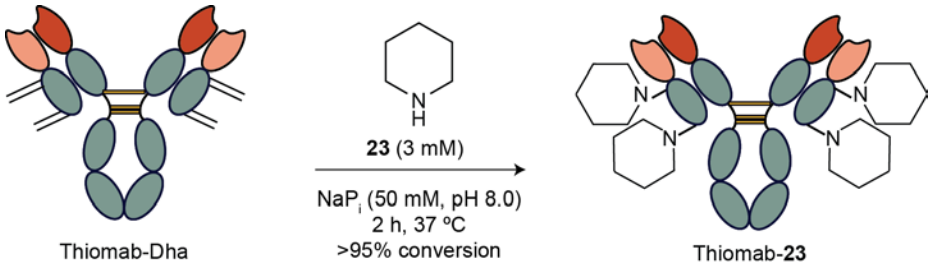

A 40 μL aliquot of Thiomab-Dha (10 μM, 399 pmol) in 50 mM sodium phosphate buffer at pH 8.0-11.0 was thawed. Piperidine **23** (1.2 μL of a 100 mM solution in DMF) was added at 37 ºC and the resulting mixture vortexed for 30 seconds. The reaction progress was monitored by LC–MS. After additional mixing for 2 h at 37 ºC, small molecules were removed from the reaction mixture by loading the sample onto a Zeba Spin Desalting Column previously equilibrated with 50 mM sodium phosphate buffer at pH 8.0. The sample was eluted via centrifugation (2 min, 1500xg). An aliquot of 5 μL of the purified protein was diluted with 5 μL of 50 mM sodium phosphate buffer at pH 8.0. 10 μL of this diluted sample was injected. Complete conversion was observed to the tertiary amine-linked conjugate was observed (calculated mass light chain, 23541, observed mass, 23545). Mass alterations were not observed in the heavy-chain (data not shown).

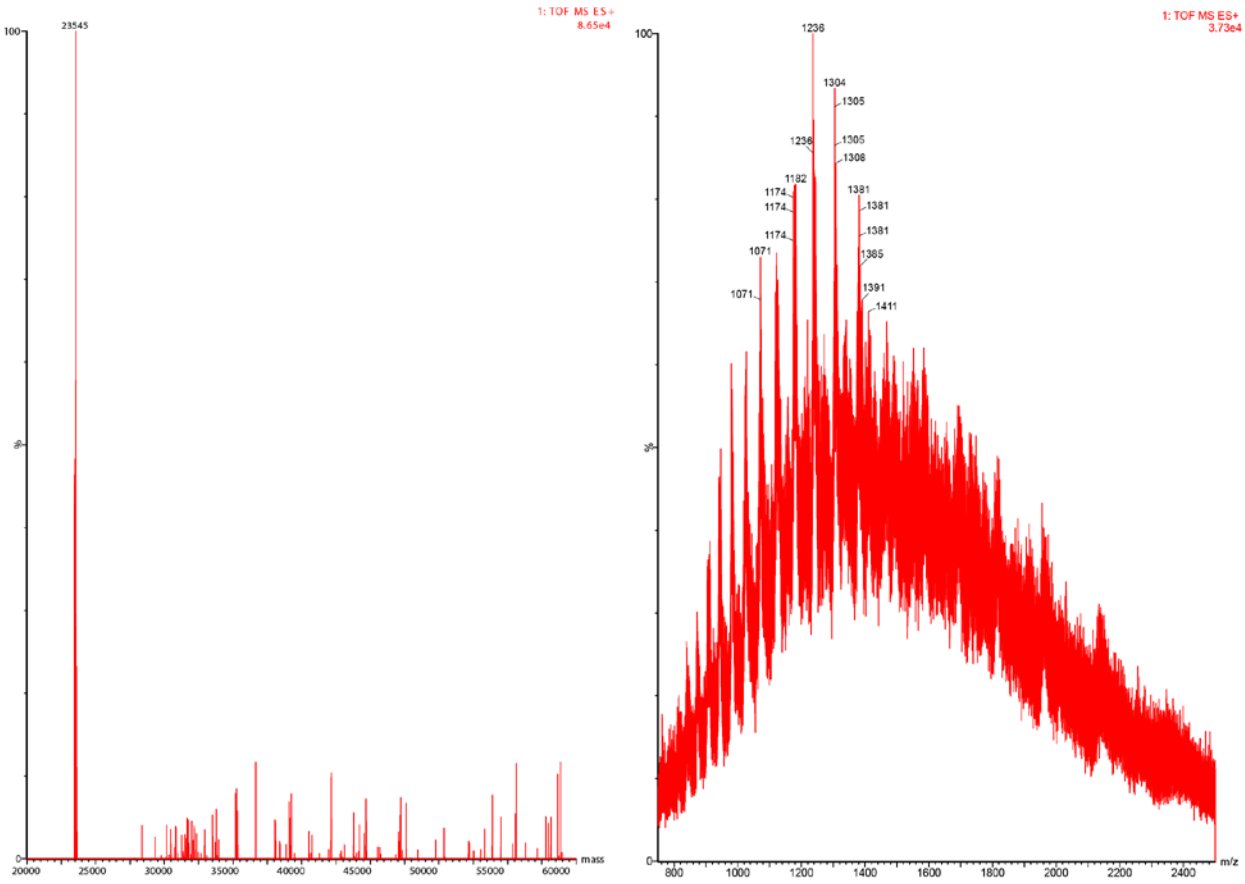

Figure S67. ESI–MS of the light-chain after the reaction of Thiomab–Dha with piperidine **23** (3 mM) after 2 h, at pH 8.0, 37 ºC.

15.5 Aza-Michael addition of crizotinib 30 to Thiomab–Dha

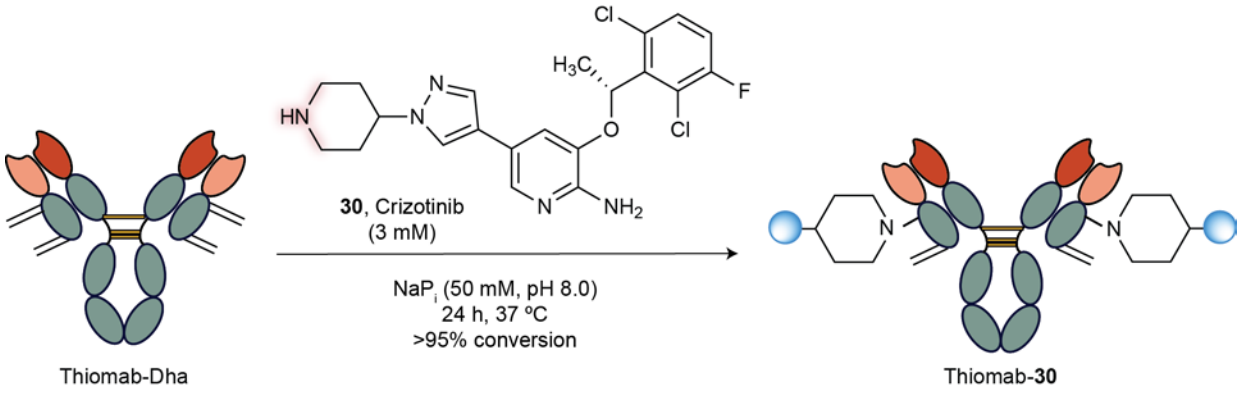

A 40 μL aliquot of Thiomab–Dha (10 μM, 399 pmol) in 50 mM sodium phosphate buffer at pH 8.0-11.0 was thawed. Crizotinib (0.54 μL of a 222 mM solution in DMF) was added at 37 ºC and the resulting mixture vortexed for 30 seconds. The reaction progress was monitored by LC–MS with time points taken after 2, 4 and 24 h at 37 ºC. Small molecules were removed from the reaction mixture by loading the sample onto a Zeba Spin Desalting Column previously equilibrated with 50 mM sodium phosphate buffer at pH 8.0. The sample was eluted via centrifugation (2 min, 1500xg). When the reaction was scaled up for in vitro studies, this procedure was repeated 3 times to optimize the efficiency of the method. These columns are described to have at least 95% retention (removal) of salts and other small molecules (<1000 MW). Time points were taken by aliquoting 5 μL of the reaction mixture and diluting it with 5 μL of 50 mM sodium phosphate buffer at pH 8.0. 10 μL of this diluted sample was injected. Complete conversion was observed after 24 h (calculated mass light chain, 23822, observed mass, 23826). Mass alterations were not observed in the heavy-chain.

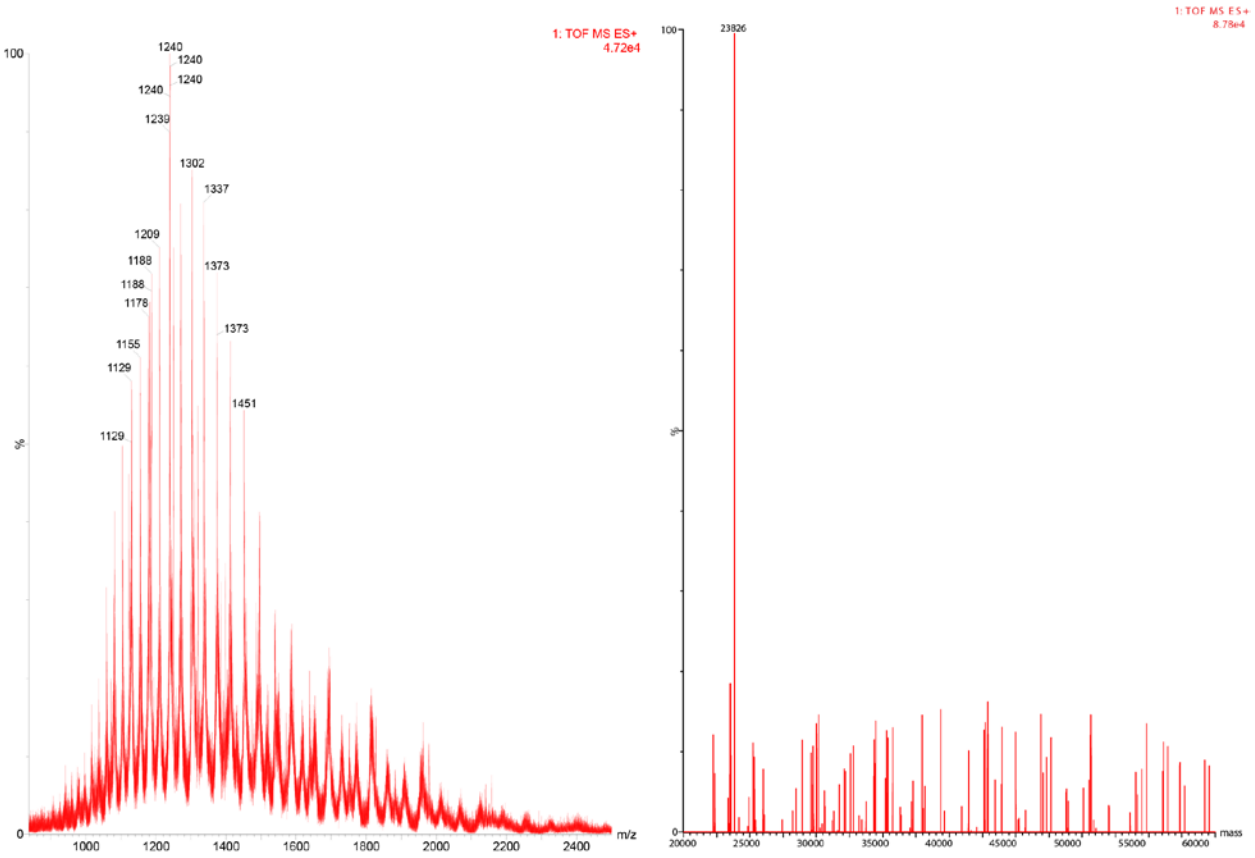

Figure S68. ESI–MS of the light-chain after reaction of Thiomab-Dha with crizotinib (3 mM) after 24 h, at pH 8.0, 37 ºC.

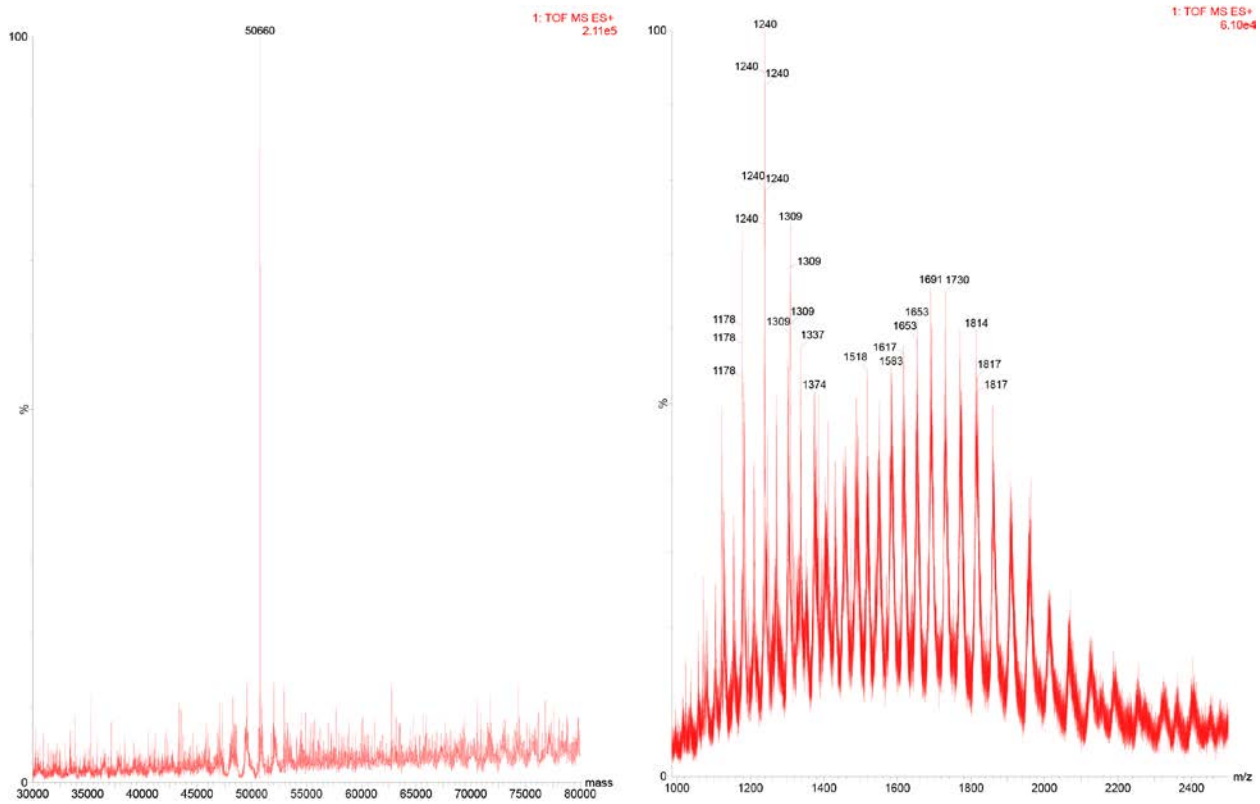

Figure S69. ESI–MS of the heavy-chain after reaction of Thiomab-Dha with crizotinib **30** (3 mM) after 24 h, at pH 8.0, 37 ºC.

15.6 Molecular Dynamics (MD) simulations

The structure of Thiomab was obtained from the protein data bank web site (PDB id: 5d6c). Parameters for Dha were generated with the antechamber module of Amber16,[15] using the general Amber force field (GAFF),[16] with partial charges set to fit the electrostatic potential generated with HF/6-31G(d) by RESP.[17] The charges are calculated according to the Merz-Singh-Kollman scheme using Gaussian 09[6] (http://gaussian.com/g09citation/). Each protein was immersed in a water box with a 10 Å buffer of TIP3P[18] water molecules. The system was neutralized by adding explicit counter ions (Cl^-). All subsequent simulations were performed using the ff14SB force field, which is an evolution of the Stony Brook modification of the Amber 99 force field force field (ff99SB).[19] A two-stage geometry optimization approach was performed. The first stage minimizes only the positions of solvent molecules and ions, and the second stage is an unrestrained minimization of all the atoms in the simulation cell. The systems were then gently heated by incrementing the temperature from 0 to 300 K under a constant pressure of 1 atm and periodic boundary conditions. Harmonic restraints of 30 $kcal \cdot mol^{-1}$ were applied to the solute, and the Andersen temperature coupling scheme[20] was used to control and equalize the temperature. The time step was kept at 1 fs during the heating stages, allowing potential inhomogeneities to self-adjust. Water molecules are treated with the SHAKE algorithm such that the angle between the hydrogen atoms is kept fixed. Long-range electrostatic effects are modelled using the particle-mesh-Ewald method.[21] An 8 Å cutoff was applied to Lennard-Jones and electrostatic interactions. Each system was equilibrated for 2 ns with a 2 fs time step at a constant volume and temperature of 300 K. Production trajectories were then run for additional 100 ns under the same simulation conditions.

Solvent Accessible Surface Area (SASA) for Dha residues were calculated using the keyword 'SURF' in *cpptraj*.[22]

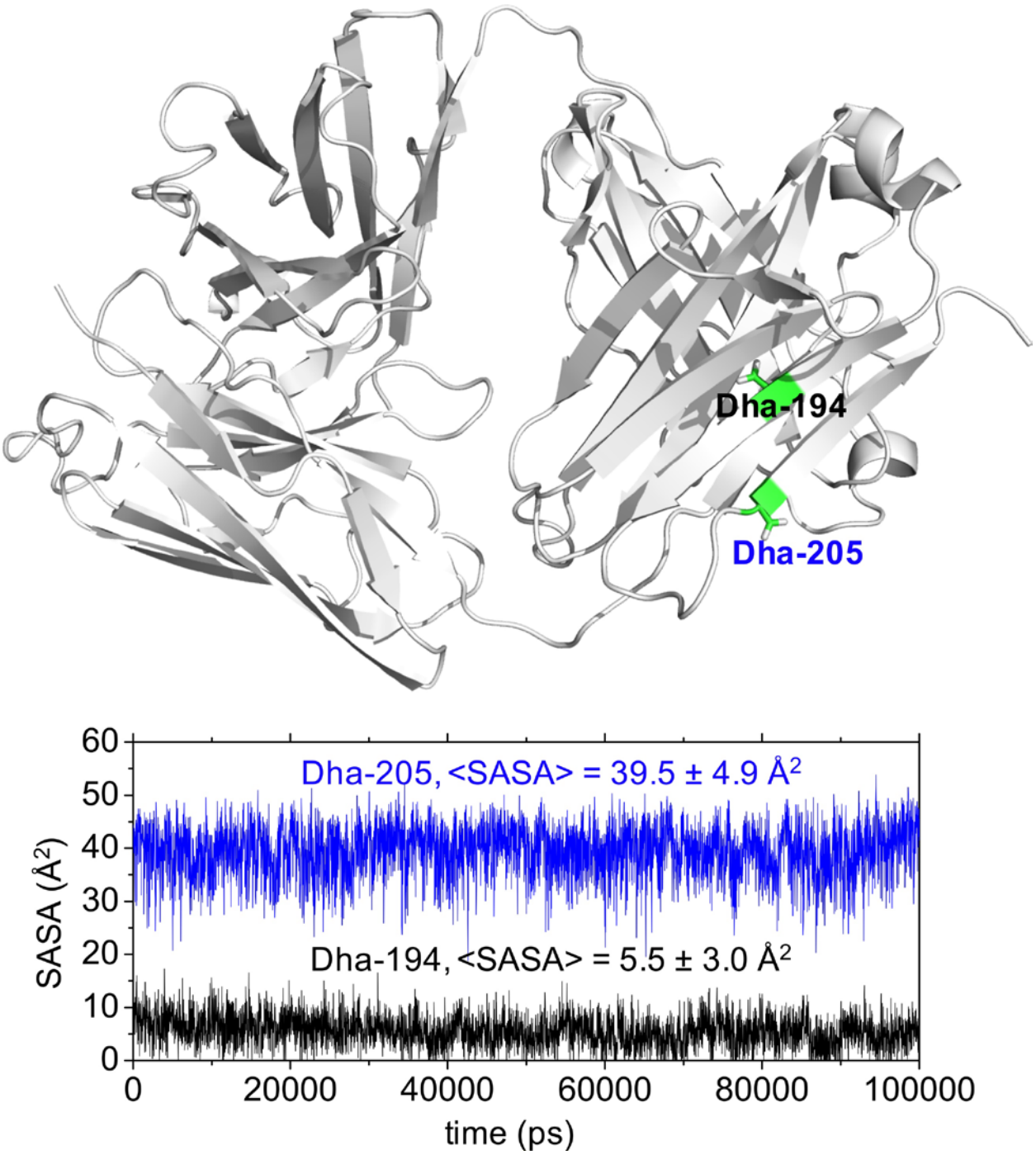

Figure S70. Solvent Accessible Surface Area (SASA) calculated through 100 ns MD simulations in explicit water for antibody Thiomab (PDB id: 5d6c). Presumably, the greater SASA value obtained for residue Dha-205 in comparison to the inner Dha-194 indicates that the Thiomab-**30** reacts selectivity with solvent expose Dha-205. The averaged SASA values are also shown.

15.7 Reaction of 2-aminopyridine with C2Am-Dha95 (control experiment)

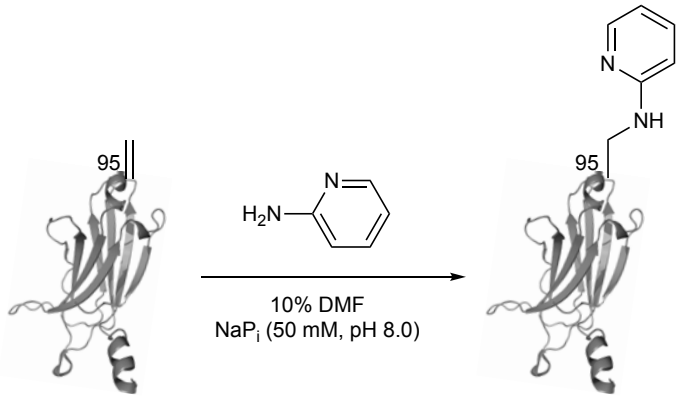

C2Am-Dha95

no reaction observed

A 40 μL aliquot of C2Am-Dha95 (10 μM, 399 pmol) in 50 mM sodium phosphate buffer at pH 8.0 was thawed. 2-Aminopyridine (4 μL of a 1000 mM solution in DMF) was added at room temperature and the resulting mixture vortexed for 30 seconds. Time points were taken by aliquoting 5 μL of the reaction mixture and diluting it with 5 μL of 50 mM sodium phosphate buffer at pH 8.0. Small molecules were removed from the reaction mixture by loading the sample onto a Zeba Spin Desalting Column previously equilibrated with 50 mM sodium phosphate buffer at pH 8.0. The sample was eluted via centrifugation (2 min, 1500xg). 10 μL of this diluted sample was injected for LC–MS analysis. No conversion to any product was observed after 24 h (calculated mass, 16280 Da, observed mass, 16188 Da).

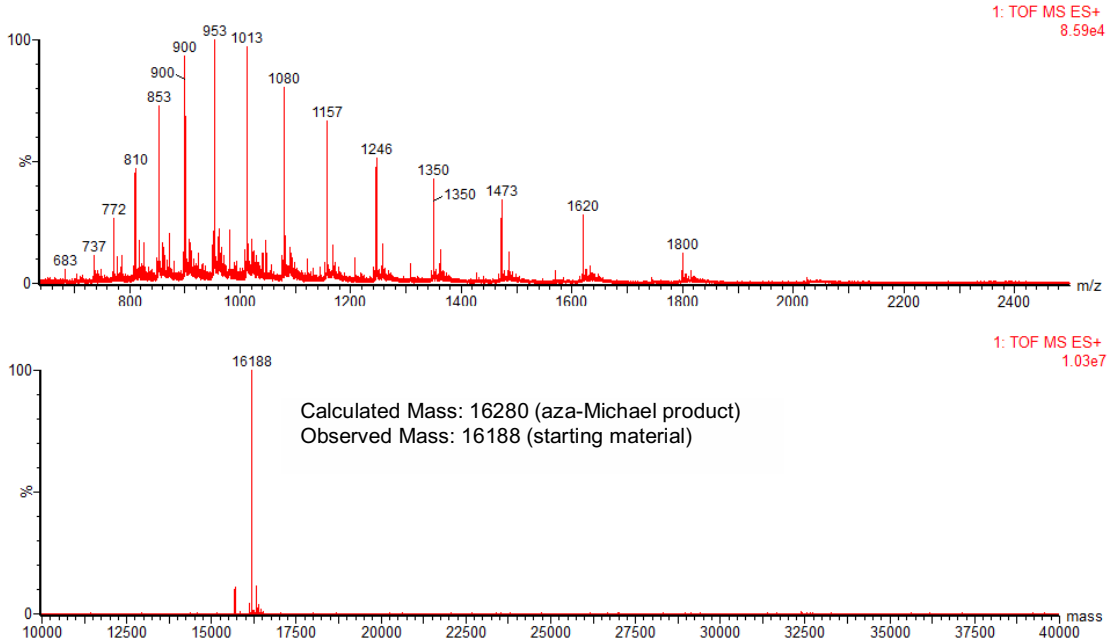

Figure S71. ESI–MS of the reaction of C2Am-Dha95 with 2-aminopyridine (100 mM) after 24 h at 37 ºC.

16. Chemoinformatics

Table S4. The DrugBank v5 database containing approved and investigational drugs was searched for the presence of piperidine moieties with RDKit, using the respective SMARTS pattern ("C1CCCCN1"). Compounds with anticancer and anti-infective activities were manually extracted.

Structure	Code	Drug target	Activity
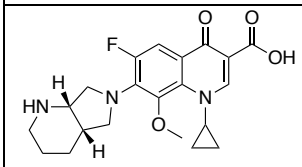 Moxifloxacin	DB00218	DNA gyrase	Anti-infective
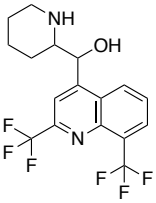 Mefloquine	DB00358	Fe(II)-protoporphyrin IX	Anti-infective
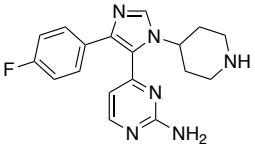 SB220025	DB04338	p38 MAPK	Anticancer
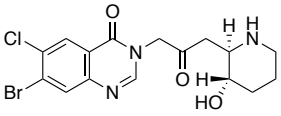 Halofuginone	DB04866	MMP2, Collagen alpha-1(I)	Anti-metastatic
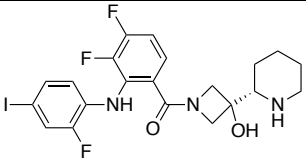 Cobimetinib	DB05239	MAP2K1, MEK2	Anticancer
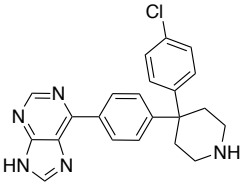	DB07856	PKBbeta, PKA, GSK4beta,	Anticancer

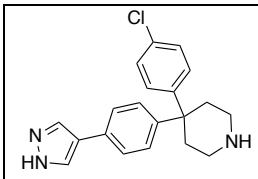	DB07859	PKBbeta	Anticancer
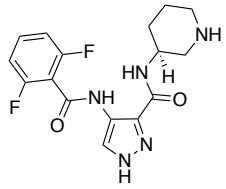	DB08141	CDK2	Anticancer
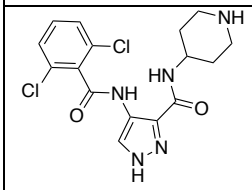	DB08142	CDK2	Anticancer
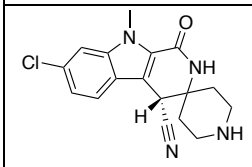	DB08166	Pim-1	Anticancer
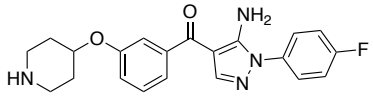	DB08423	MAPK14	Anticancer
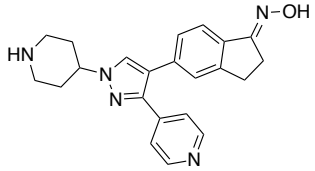	DB08553	B-raf	Anticancer
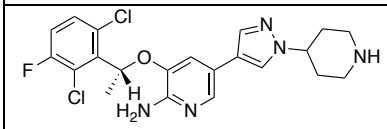 Crizotinib	DB08865	ALK	Anticancer
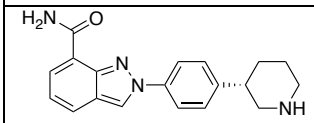 Niraparib	DB11793	PARP	Anticancer
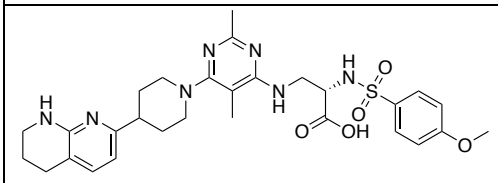	DB12297	n.a.	Anticancer

GLPG-0187			
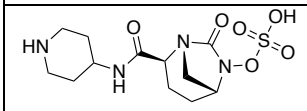 Relebactam	DB12377	Beta-lactamase	Anti-infective
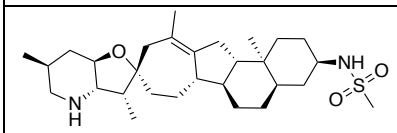 Patidegib	DB12655	Smo	Anticancer

17. Biological testing of Thiomab-30

Cell culture. Three cell lines were used for the *in vitro* studies, namely HepG2 (a human hepatoma cell line), HEK 293T (embryonic kidney cell line) and SKBR3 cells (human breast adenocarcinoma cell line). The cells were maintained in a humidified incubator at 37 ºC under 5% CO2 and grown using 1x D-MEM (Dulbecco's modified Eagle medium) with Sodium Pyruvate and without L-Glutamine (Invitrogen, Life Technologies) supplemented with 10% heat-inactivated fetal bovine serum (FBS) (Gibco, Life Technologies), 1x MEM NEAA (Gibco, Life Technologies) ,1x GlutaMAX (Gibco, Life Technologies), 200 units/mL penicillin and 200 µg/mL streptomycin (Gibco, Life Technologies) and 10 mM HEPES (Gibco, Life Technologies).

Cell viability assay and IC50 calculation. 10,000 SKBR3 cells/well were seeded in 96 well-plates and were treated with crizotinib, Thiomab or Thiomab-**30** 24 h after the seeding, to allow the cells to stabilize. The cells were incubated with several concentrations of crizotinib (0.5, 1, 2.5, 5, 10, 15, 25, 50, 75, 100 µM), Thiomab (0.5, 1, 2.5, 5, 8 µM) and Thiomab-**30** (0.5, 1, 2.5, 5, 8 µM) for 24 h. After this incubation period, the culture medium was removed and the cells were incubated with CellTiter-Blue (Promega) for 90 min at 37 ºC. The viability of the cells was evaluated by measuring the Emission Intensity in RFUs – relative fluorescent units – with an Infinite M200 plate reader. The IC50 was calculated using GraphPad Prism5 software.

Cell viability with medium wash out. SKBR3 and HepG2 cells were seeded in 96 well-plates (10,000 cells/well) and treated with Thiomab-**30** 24 h after the seeding, to allow the cells to stabilize. The cells were then incubated with 1 µM of Thiomab-**30** for 1 h. After this incubation period, the culture medium was removed and fresh medium was added to the cells. 24 h after treatment, the culture medium was removed and the cells were incubated with CellTiter-Blue (Promega) for 90 min at 37 ºC. The viability of the cells was evaluated by measuring the Emission Intensity in RFUs – relative fluorescent units – with an Infinite M200 plate reader.

Thiomab-30 binding affinity determined by flow cytometry analysis. The binding affinity of the ADC Thiomab-**30** was determined by Flow Cytometry analysis. For this purpose, SKRB3 cells (with high expression of HER2 receptor) and HEK 293T cells (with low expression of HER2 receptor) were plated in 96 well plates (100,000 cells per well) and incubated with 10 µL of 1µM Thiomab-**30** at room temperature. After 1 h of incubation, cells were washed with medium and were incubated with 50 µL/well of Goat anti-Mouse IgG (H+L) Superclonal Alexa Fluor 647 (10

µg/mL) secondary antibody from ThermoScientific, for 1 h. After this incubation period, the cells were washed by adding 100 µL of 10%FBS in PBS pH 7.4 to the cells and centrifuged for 5 min at 400xg.The supernatant was then removed, the cells were re-suspended in 400 µL of 10%FBS in PBS pH 7.4 and transferred to flow cytometry tubes. Acquisition was done using a BD LSR Fortessa set up with a 640 nm laser and a 670/14 nm band-pass filter (combination used for APC detection). Data analysis was done with FlowJo (version 6.3.4, FlowJo) software. Data represents mean ± s.d. of 3 biological replicates and only single-cell events are shown.

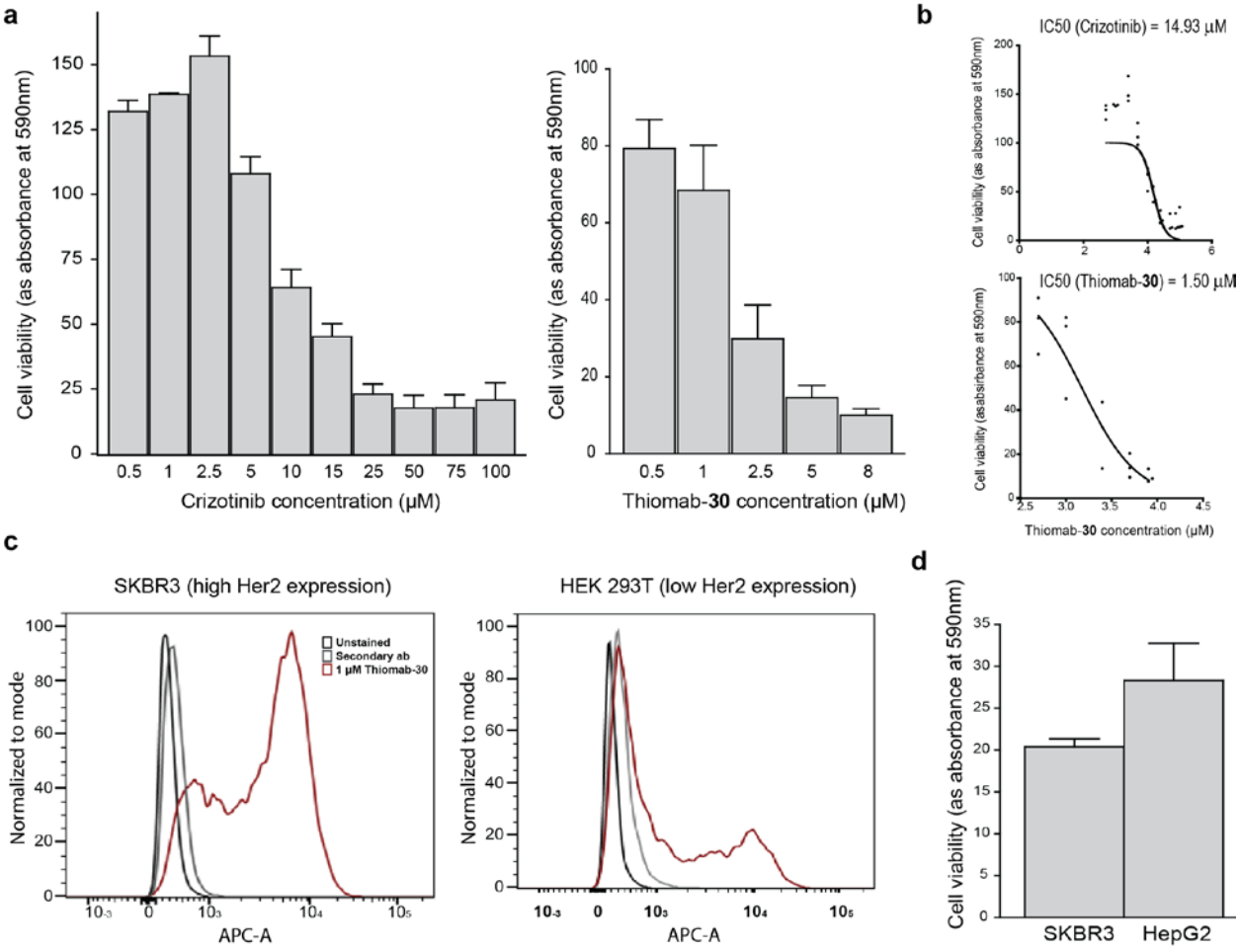

Figure S72. Thiomab-**30** *in vitro* cellular assays. **a.** SKBR3 cells viability after treatment with crizotinib or Thiomab-**30** for 24 h. Results are shown as percentage of control (medium + vehicle – PBS) and correspond to 3 biological replicates (mean + s.d.). **b.** IC50 of crizotinib and Thiomab-**30** in SKBR3 cells. **c.** Thiomab-**30** binding affinity to SKBR3 and HEK 293T cells measured by flow cytometry. **d.** Cell viability of SKBR3 cells in comparison to HepG2 cells after 1 h incubation with1 µM Thiomab-**30** followed by medium wash out (analysis performed after 24 h). The results

correspond to 3 biological replicates and are shown as percentage of control (mean + s.d.). Differences were tested with a Mann-Whitney test that indicated no significant differences.

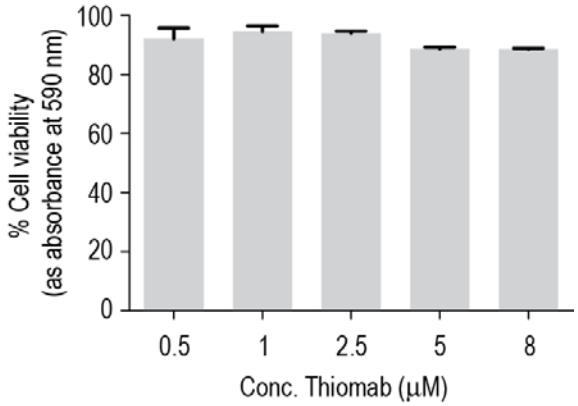

Figure S73. SKBR3 cells viability after treatment with naked Thiomab for 48 h. Results are shown as percentage of control (medium + vehicle – PBS) and correspond to 3 biological replicates (mean ± s.d.).

18. References

(1) Cinelli, M. A.; Cordero, B.; Dexheimer, T. S.; Pommier, Y.; Cushman, M. *Bioorg. Med. Chem.* **2009**, *17*, 7145–7155.

(2) Davis, B. G.; Lloyd, R. C.; Jones, J. B. *J. Org. Chem.* **1998**, *63*, 9614–9615.

(3) Chalker, J. M.; Gunnoo, S. B.; Boutureira, O.; Gerstberger, S. C.; Fernandez-Gonzalez, M.; Bernardes, G. J. L.; Griffin, L.; Hailu, H.; Schofield, C. J.; Davis, B. G. *Chem. Sci.* **2011**, *2*, 1666–1676.

(4) Lin, Y. A.; Boutureira, O.; Lercher, L.; Bhushan, B.; Paton, R. S.; Davis, B. G. *J. Am. Chem. Soc.* **2013**, *135*, 12156–12159.

(5) Zhao, Y.; Truhlar, D. *Theor. Chem. Acc.* **2008**, *120*, 215–241.

(6) Frisch, M. J.; Trucks, G. W.; Schlegel, H. B.; Scuseria, G. E.; Robb, M. A.; Cheeseman, J. R.; Scalmani, G.; Barone, V.; Mennucci, B.; Petersson, G. A.; Nakatsuji, H.; Caricato, M.; Li, X.; Hratchian, H. P.; Izmaylov, A. F.; Bloino, J.; Zheng, G.; Sonnenberg, J. L.; Hada, M.; Ehara, M.; Toyota, K.; Fukuda, R.; Hasegawa, J.; Ishida, M.; Nakajima, T.; Honda, Y.; Kitao, O.; Nakai, H.; Vreven, T.; Montgomery, Jr., J. A.; Peralta, J. E.; Ogliaro, F.; Bearpark, M.; Heyd, J. J.; Brothers, E.; Kudin, K. N.; Staroverov, V. N.; Kobayashi, R.; Normand, J.; Raghavachari, K.; Rendell, A.; Burant, J. C.; Iyengar, S. S.; Tomasi, J.; Cossi, M.; Rega, N.; Millam, J. M.; Klene, M.; Knox, J. E.; Cross, J. B.; Bakken, V.; Adamo, C.; Jaramillo, J.; Gomperts, R.; Stratmann, R. E.; Yazyev, O.; Austin, A. J.; Cammi, R.; Pomelli, C.; Ochterski, J. W.; Martin, R. L.; Morokuma, K.; Zakrzewski, V. G.; Voth, G. A.; Salvador, P.; Dannenberg, J. J.; Dapprich, S.; Daniels, A. D.; Farkas, Ö.; Foresman, J. B.; Ortiz, J. V.; Cioslowski, J.; Fox, D. J. *Gaussian 09* (Gaussian, Inc., Wallingford CT, 2009).

(7) Ribeiro, R. F.; Marenich, A. V.; Cramer, C. J.; Truhlar, D. G. *J. Phys. Chem. B* **2011**, *115*, 14556–14562.

(8) Gonzalez, C.; Schlegel, H. B. *J. Phys. Chem.* **1990**, *94*, 5523–5527.

(9) Scalmani, G.; Frisch, M. J. *J. Chem. Phys.* **2010**, *132*, 114110.

(10) Cramer, C. J. *Essentials of Computational Chemistry: Theories and Models, 2nd Edition*; Wiley, 2004.

(11) Alam, I. S.; Neves, A. A.; Witney, T. H.; Boren, J.; Brindle, K. M. *Bioconjug. Chem.* **2010**, *21*, 884–891.

(12) Jin, M.; Smith, C.; Hsieh, H.-Y.; Gibson, D. F.; Tait, J. F. *J. Biol. Chem.* **2004**, *279*, 40351–40357.

(13) Coxon, K. M.; Duggan, J.; Cordeiro, M. F.; Moss, S. E. In *Cancer Cell Culture: Methods and Protocols*; Cree, A. I., Ed.; Humana Press: Totowa, NJ, 2011, p 293-308.

(14) Bernardes, G. J. L.; Chalker, J. M.; Errey, J. C.; Davis, B. G. *J. Am. Chem. Soc.* **2008**, *130*, 5052–5053.

(15) Case, D. A.; Betz, R. M.; Cerutti, D. S.; Cheatham, III, T. E.; Darden, T. A.; Duke, R. E.; Giese, T. J.; Gohlke, H.; Goetz, A. W.; Homeyer, N.; Izadi, S.; Janowski, P.; Kaus, J.; Kovalenko, A.; Lee, T. S.; LeGrand, S.; Li, P.; Lin, C.; Luchko, T.; Luo, R.; Madej, B.; Mermelstein, D.; Merz, K. M.; Monard, G.; Nguyen, H.; Nguyen ,H. T.; Omelyan, I.; Onufriev, A.; Roe, D. R.; Roitberg, A.; Sagui, C.; Simmerling, C. L.; Botello-Smith, W. M.; Swails, J.; Walker, R. C.; Wang, J.; Wolf, R. M.; Wu, X.; Xiao, L.; Kollman, P. A. *AMBER 2016* (University of California, San Francisco, 2016).

(16) Wang, J.; Wolf, R. M.; Caldwell, J. W.; Kollman, P. A.; Case, D. A. *J. Comput. Chem.* **2004**, *25*, 1157–1174.

(17) Bayly, C. I.; Cieplak, P.; Cornell, W.; Kollman, P. A. *J. Phys. Chem.* **1993**, *97*, 10269–10280.

(18) Jorgensen, W. L.; Chandrasekhar, J.; Madura, J. D.; Impey, R. W.; Klein, M. L. *J. Chem. Phys.* **1993**, *79*, 926–935.

(19) Hornak, V.; Abel, R.; Okur, A.; Strockbine, B.; Roitberg, A.; Simmerling, C. *Proteins* **2006**, *65*, 712–725.

(20) Andrea, T. A.; Swope, W. C.; Andersen, H. C. *J. Chem. Phys.* **1993**, *79*, 4576–4584.

(21) Darden, T.; York, D.; Pedersen, L. *J. Chem. Phys.* **1993**, *98*, 1008910092.

(22) Roe, D. R.; Cheatham III, T. E. *J. Chem. Theory Comput.* **2013**, *9* 3084–3095.